

**UNIVERSITY OF MINES AND TECHNOLOGY (UMaT),  
TARKWA**

**FACULTY OF MINING AND MINERALS TECHNOLOGY  
DEPARTMENT OF MINERALS ENGINEERING**

**A THESIS REPORT ENTITLED**

**PROCESSING OF GANGRA IRON ORE USING END-OF-LIFE  
TYRES AS REDUCTANT-A CASE STUDY**

**BY**

**MAGNUS KAMAKER MENDEE**

**SUBMITTED IN PARTIAL FULFILLMENT OF THE REQUIREMENT  
FOR THE AWARD OF THE DEGREE OF MASTER OF SCIENCE IN  
MINERALS ENGINEERING**



**THESIS SUPERVISORS**

-----  
**ASSOC PROF JAMES RANSFORD DANKWAH**

-----  
**DR GEORGE MENSAH TETTEH**

**TARKWA, GHANA  
NOVEMBER 2023**

## DECLARATION

I, Magnus Kamaker Mendee, declare that this thesis is my work and is being submitted for the degree of Master of Science at the University of Mines and Technology (UMaT), Tarkwa, Ghana. It has not been submitted for any degree or examination in any other University.

.....

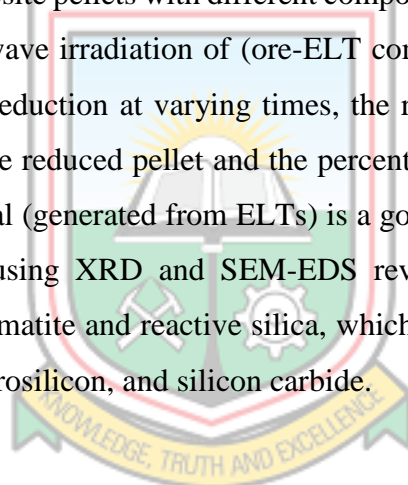
(Signature of candidate)

..... day of ..... (year) .....



## ABSTRACT

ArcelorMittal Liberia is actively mining the Mount Gangra iron ore deposit. Mt Gangra is primarily underlain with Precambrian rocks, including Banded Iron Formation (BIF) with significant ore reserves. Lowgrade and transition ores are found in Gangra. By removing the silica, these ores can be beneficiated to high-grade iron metals. The oxide's iron content ranges from 50%Fe<58%, fresh rock 20%Fe<35%, transition high-grade from 42%Fe<50%, and transition low-grade from 35%Fe<42%. Previous DSO mining methods have resulted in an enormous lowgrade and transition stockpiles. End-of-Life Tyres (ELTs) generated by haulage trucks are stockpiled and there is no recycling strategy in place in Liberia. Hence, this study aims to beneficiate the lowgrade and transition iron ores using ELTs as reductants. Utilising iron oxide mined from Mount Gangra, the recycling of ELTs was investigated. The carbonaceous material was combined with iron oxide, binder, and water to create composite pellets with different compositions (70 wt% ore, 75 wt% ore), ELT, and binder. Microwave irradiation of (ore-ELT composite pellets) was used for the reduction studies. After reduction at varying times, the reduced material was weighed to ascertain the weight of the reduced pellet and the percent weight lost. The results indicate that carbonaceous material (generated from ELTs) is a good reductant for the formation of iron metal. The study, using XRD and SEM-EDS reveals that Gangra lowgrade and transition ores contain hematite and reactive silica, which react with carbon from ELTs to produce metallic iron, ferrosilicon, and silicon carbide.



## DEDICATION

This thesis work is dedicated to my Sponsor Company ArcelorMittal Liberia Limited for supporting me to achieve my career goals. Secondly, I thank my hard-working parents, wife, professors, and friends, who stood by me amidst the difficult situation during my academic sojourn at the University of Mines and Technology (UMaT).



## ACKNOWLEDGEMENT

My heartfelt appreciation goes to my thesis Supervisor Assoc Prof James Ransford Dankwah, and my Co-Supervisor Dr George Mensah Tetteh, who inspired me during my study at the University of Mines, and Technology (UMaT). Their unwavering guidance was the pillar and driving energy of my motivation during this report writing. I am happy that I got the opportunity to work with them professionally and personally. Professors, I salute you for your dedication, steadfastness, and resoluteness in making my academic journey throughout these many years. Your assured suggestions during this period have always improved my work.

I thank every faculty of the Department of Minerals Engineering, School of Postgraduate Studies, University of Mines and Technology (UMaT), for the knowledge, encouragement, and inspiration given to me throughout my master's degree.

Lastly, special gratitude is also worth mentioning to ArcelorMittal Liberia Limited for giving me the necessary support concerning my laboratory work.

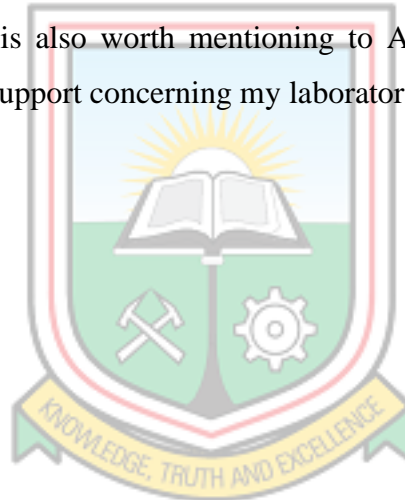
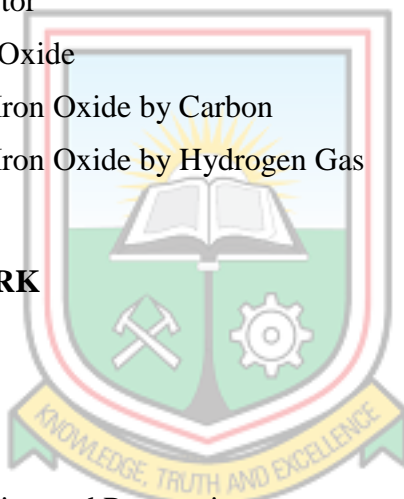


# TABLE OF CONTENTS

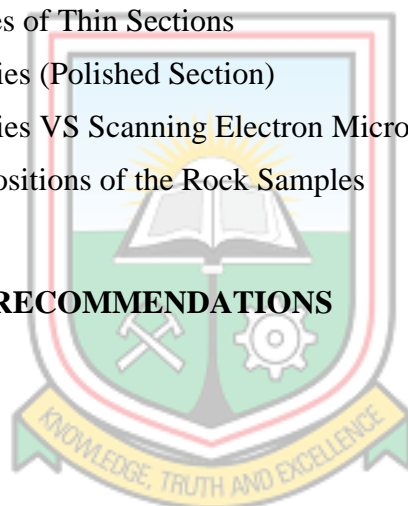
| CONTENTS  | PAGE        |
|---|-------------|
| <b>DECLARATION</b>  | <b>i</b>    |
| <b>ABSTRACT</b>   | <b>ii</b>   |
| <b>DEDICATION</b>   | <b>iii</b>  |
| <b>ACKNOWLEDGEMENT</b>  | <b>iv</b>   |
| <b>TABLE OF CONTENTS</b>  | <b>v</b>    |
| <b>LIST OF FIGURES</b>  | <b>viii</b> |
| <b>LIST OF TABLES</b>   | <b>xi</b>   |
| <b>ABBREVIATIONS</b>  | <b>xiii</b> |
| <b>CHAPTER 1</b>  | <b>1</b>    |
| <b>INTRODUCTION</b>   | <b>1</b>    |
| 1.1 Statement of the Problem                                    | 1           |
| 1.2 Objectives of Research                                      | 3           |
| 1.3 Method Used   | 3           |
| 1.4 Facilities Used   | 3           |
| 1.5 Organisation of the Report                                  | 3           |
| <b>CHAPTER 2</b>  | <b>4</b>    |
| <b>LITERATURE REVIEW</b>  | <b>4</b>    |
| 2.1 Introduction  | 4           |
| 2.2 Iron Ore  | 7           |
| 2.3 Iron Ore Deposits Formation                                 | 9           |
| 2.3.1 Iron Ore Formation Processes                              | 10          |
| 2.3.2 Mineral Types found in Iron Ore                           | 12          |
| 2.4 Types of Iron Minerals                                      | 14          |
| 2.5 Gangue Minerals   | 15          |
| 2.6 Reviews of Ore Geology of Liberia                           | 15          |
| 2.6.1 Geology of the Study Area                                 | 15          |
| 2.6.2 Liberia's Iron Ore Mining History                         | 17          |
| 2.7 ArcelorMittal Liberia Proposed Iron Ore Beneficiation Plant | 18          |
| 2.7.1 Process Description                                       | 18          |



| <b>CONTENTS</b>  | <b>PAGE</b> |
|--|-------------|
| 2.8 Iron Production  | 21          |
| 2.8.1 Blast Furnace  | 21          |
| 2.8.2 Process of Direct Reduction  | 23          |
| 2.9 Steel Production   | 29          |
| 2.9.1 Basic Oxygen Furnace   | 33          |
| 2.9.2 Electric Arc Furnace (EAF)   | 33          |
| 2.10 Pelletising   | 35          |
| 2.10.1 Pelletising Binder  | 37          |
| 2.11 Microwave Technology  | 37          |
| 2.12 End-of-Life Tyres (ELTs)  | 38          |
| 2.13 Pyrolysis of End-of-life Tyres (ELTs)   | 40          |
| Tyres Pyrolysis Reactor  | 41          |
| 2.14 Reduction of Iron Oxide   | 43          |
| 2.14.1 Reduction of Iron Oxide by Carbon   | 44          |
| 2.14.2 Reduction of Iron Oxide by Hydrogen Gas                                       | 45          |
| <b>CHAPTER 3</b>   | <b>47</b>   |
| <b>EXPERIMENTAL WORK</b>   | <b>47</b>   |
| 3.1 Material Used  | 47          |
| 3.2 Apparatus Used   | 47          |
| 3.3 Methods Used   | 48          |
| 3.3.1 Iron Ore Sampling and Preparation  | 48          |
| 3.3.2 Iron Ore Preparation   | 48          |
| 3.3.3 Pellets Formation  | 49          |
| 3.3.4 Microwave Reduction  | 51          |
| 3.3.5 Magnetic Separation  | 51          |
| 3.4 Samples Analysis   | 51          |
| 3.4.1 X-Ray Fluorescence Analysis  | 52          |
| 3.4.2 Scanning Electron Microscopy-Energy Dispersive Spectroscopy (SEM-EDS) Analysis | 52          |
| 3.4.3 X-ray Diffraction (XRD)  | 53          |
| 3.5 Petrographic Studies   | 54          |



| <b>CONTENTS</b>   | <b>PAGE</b> |
|---|-------------|
| <b>CHAPTER 4</b>  | <b>55</b>   |
| <b>RESULTS AND DISCUSSION</b>   | <b>55</b>   |
| 4.1 Nature of Mount Gangra Iron Ores  | 55          |
| 4.2 SEM-EDS Results of Mt. Gangra Lowgrade (Pulverised) Ore for Region 1  | 56          |
| 4.3 SEM-EDS Results of Mt. Gangra Transition (Pulverised Ore)   | 60          |
| 4.4 SEM-EDS Results of Gangra Lowgrade Iron Ore (Reduced)   | 63          |
| 4.5 SEM-EDS Results of Gangra Transition Ore (Reduced)  | 67          |
| 4.6 X-ray Diffraction Results for Low-grade and Transition Ore (Pulverised)   | 73          |
| 4.7 X-ray Diffraction (XRD) Results of Gangra Transition and Lowgrade Ores (Reduced)  | 74          |
| 4.8 Formation of Iron Metal (Reduction Studies)   | 77          |
| 4.9 Petrographic Studies of Thin Sections   | 78          |
| 4.10 Petrographic Studies (Polished Section)  | 82          |
| 4.11 Petrographic Studies VS Scanning Electron Microscopy   | 83          |
| 4.12 Geological Compositions of the Rock Samples  | 84          |
| <b>CHAPTER 5</b>  | <b>85</b>   |
| <b>CONCLUSIONS AND RECOMMENDATIONS</b>  | <b>85</b>   |
| 5.1 Conclusions   | 85          |
| 5.2 Recommendations   | 86          |
| <b>REFERENCES</b>   | <b>87</b>   |
| <b>APPENDICES</b>   | <b>95</b>   |
| APPENDIX A PHOTOMICROGRAPHS OF POLISHED SECTION SHOWING GANGRA FRESH ROCK, OXIDE, TRANSITION LOW-GRADE, AND TRANSITION HIGH-GRADE | 95          |
| APPENDIX B TABLE OF VALUES FOR MICROWAVE REDUCTION OF GANGRA LOWGRADE ORE   | 97          |
| APPENDIX C TABLE OF VALUES FOR MICROWAVE REDUCTION OF GANGRA LOWGRADE ORE   | 98          |
| APPENDIX D MOUNT GANGRA LOWGRADE STOCKPILES   | 99          |
| <b>INDEX</b>  | <b>100</b>  |





## LIST OF FIGURES

| <b>Figure</b> | <b>Title</b>   | <b>Page</b> |
|---------------|--|-------------|
| 1.1           | Drone Image of Gangra Lowgrade Stockpiles: (a) Permanent Low-grade Dump (b) Valley Dump (Source: Author's Construct, 2023) | 2           |
| 1.2           | Stockpile of End-of-Life Tyres along the Mt. Gangra Haul Road (Source: Author's Construct' 2023)                           | 2           |
| 2.1           | Map of Mount Beeton, Gangra, and Yuelliton from the Old Nimba Mine (Source: Anon, 2010)                                    | 5           |
| 2.2           | Map of Liberia showing ArcelorMittal Concession Area (Source: Amikiya 2014)  | 6           |
| 2.3           | Drone Image of Gangra Mine (Source: Author's Construct, 2023)  | 6           |
| 2.4           | Drone Images of (a) Gangra Pit -2 (b) Gangra Pit 3- Top (Source: Author's Construct, 2023)                                 | 7           |
| 2.5           | Total Production of Crude Steel (Thousand Tonnes) World and Top five Steel Producers (Source: Sani, 2022)                  | 8           |
| 2.6           | Overview of Iron Ore Trade Together with Main Players (Sani, 2022)   | 9           |
| 2.7           | Market Share of Iron from 2000-2019 (Sani, 2022)   | 9           |
| 2.8           | Mt. Gangra High-Grade Direct Shipping Ore (DSO) (Source: Author's Construct, 2023)   | 13          |
| 2.9           | Types of Iron Ore Minerals (Source: Anon., 2020)   | 15          |
| 2.10          | Distribution Map of the Principal Iron Ore Deposits in Liberia (Gunn <i>et al.</i> , 2018)                                 | 17          |
| 2.11          | ArcelorMittal Liberia Proposed Process Block Diagram (Amikiya, 2014)   | 19          |
| 2.12          | Blast Furnace (Dankwah, 2022)  | 22          |
| 2.13          | Temperature Zones of a Blast Furnace (Dankwah, 2022)   | 23          |
| 2.14          | Worldwide Direct Reduced Iron Production by Process in 2019 (Anon., 2019)  | 24          |
| 2.15          | MIDREX/FASTMET Plants in the World (Akihiro and Mitamoto, 2010)  | 25          |
| 2.16          | Appearance of (a) Direct Reduced Iron and (b) Hot Briquetted Iron (Masaaki <i>et al.</i> , 2010)                           | 26          |
| 2.17          | World's MIDREX Plants (Masaaki <i>et al.</i> , 2010)   | 26          |
| 2.18          | MIDREX Process Flowsheet (Masaaki <i>et al.</i> , 2010).   | 27          |
| 2.19          | Operational Region of Ironmaking Processes (Kikuchi <i>et al.</i> , 2010)  | 28          |

| <b>Figure</b> | <b>Title</b>   | <b>Page</b> |
|---------------|--|-------------|
| 2.20          | Chain of the steelmaking process; routes for producing oxygen steel along the blast furnace (BF) and basic oxygen furnace (BOF); routes for producing electric steel along the electric arc furnace (EAF) (Odenthal, 2017) | 30          |
| 2.21          | Iron and Steelmaking Processes Flowsheet (Yildirim and Prezei, 2011)   | 32          |
| 2.22          | Schematic Representation of the Electric-Arc-Furnace Steelmaking and Ladle Refining Process (Yildirim, and Prezzi, 2011)   | 35          |
| 2.23          | Three (3) Basic Stages of the Pelletising Process (Mourao, 2022)   | 36          |
| 2.24          | Process Flowsheet of Producing Iron Ore Pellets in Factories (Zheo <i>et al.</i> , 2022a)  | 37          |
| 2.25          | Microwave in Operation (Aakyiir and Dankwah, 2017)   | 38          |
| 2.26          | Typical Tyre Structure (Source: Xiao <i>et al.</i> , 2022)   | 39          |
| 2.27          | Schematic representation of the ELTs pyrolysis and ensuing products (Costa <i>et al.</i> , 2022)   | 41          |
| 2.28          | Pyrolysis process flowsheet (Jahirul <i>et al.</i> , 2021)   | 41          |
| 2.29          | (a) Pulverised Carbonaceous Material (b) Liquid Fuel Obtained From (ELTs) (c) Pyrolysis Reactors (Source: Author's Construct, 2023)  | 42          |
| 3.1           | (a) Unpulverised Iron Ore (b) Pulverised Iron Ore (Source: Author's Construct, 2023)   | 49          |
| 3.2           | Pellet Composition Comprising of (a) Iron Ore (b) Baking Flour (c) Carbonaceous Char (Source: Author's Construct, 2023)  | 50          |
| 3.3           | (a) Newly Formed Pellets (b) Dried Pellets (Source: Author's Construct, 2023)  | 50          |
| 3.4           | (a) Gangra Oxide (b) Gangra Fresh Rock (c) Gangra Transition High-grade (d) Gangra Transition Lowgrade   | 54          |
| 4.1           | SEM Micrograph of Gangra Lowgrade Ore (Pulverised) at Region 1 (GLG-2567)  | 57          |
| 4.2           | SEM Micrograph of Gangra Lowgrade Pulverised Ore in Region 2 (2568)  | 58          |
| 4.3           | SEM Micrograph of Gangra Lowgrade Ore (Pulverised) for Region 3 (GLG-2569)   | 59          |
| 4.4           | SEM Micrograph of Gangra Pulverised Transition Ore for Region 1(2572)  | 61          |
| 4.5           | SEM Micrograph of Gangra Pulverised Transition Ore at Region 3.  | 62          |
| 4.6           | SEM Micrograph of Gangra (Reduced) Lowgrade Ore at Region 1 (M1-2751)  | 63          |
| 4.7           | SEM Micrograph of Gangra Lowgrade Reduce Ore for Region 2 (M1-2752)  | 64          |
| 4.8           | SEM Micrograph of Gangra Lowgrade Ore (Reduced) for Region 3 (M1-2753)   | 66          |
| 4.9           | SEM Micrograph of Gangra Transition Ore (Reduced) at Region 1 (C1-2745)  | 67          |

| <b>Figure</b> | <b>Title</b>   | <b>Page</b> |
|---------------|--|-------------|
| 4.10          | SEM Micrograph of Gangra Transition Ore (Reduced) for Region 2 (C1-2746)   | 68          |
| 4.11          | SEM Micrograph of Gangra Transition Ore (Reduced) at Region 3 (C1-2747)  | 69          |
| 4.12          | SEM Micrograph of Gangra Transition (Reduced) at Region 4 (E1-2748)  | 70          |
| 4.13          | SEM Micrograph of Gangra Transition Ore (Pulverised) for Region 5 (E1-2749)  | 71          |
| 4.14          | SEM Micrograph of Gangra Transition Ore (Reduced) at Region 6 (E1-2750)  | 72          |
| 4.15          | XRD Spectrum of Gangra Lowgrade Ore (Pulverised)   | 73          |
| 4.16          | XRD Spectrum of Gangra Transition Ore (Pulverised)   | 74          |
| 4.17          | XRD Spectrum of Gangra Transition Ore (Reduced) (a) Sample B2 and (b) Sample C2  | 75          |
| 4.18          | XRD Micrograph of Gangra Lowgrade Ore (Reduced) (a) Sample Z1, and (b) Sample Z2   | 76          |
| 4.19          | Iron Metal Produced after Microwave Reduction (a) Carbon Pellets (b) Fire Clay Crucible (c) Mixture of Iron Ore with Carbon (d) Reduced Iron Ore                   | 77          |
| 4.20          | Photomicrograph of Thin Sections under PPL (a) and XPL (b) of Fresh Rock (opq = Opaque Minerals; Qtz = quartz; and Grt = Garnet)                                   | 79          |
| 4.21          | Photomicrograph of Thin Sections under PPL (c) and XPL (d) of Gangra Transition High-grade (opq = Opaque Minerals; qtz = quartz; pyr = Pyroxene; and Ep = Epidote) | 80          |
| 4.22          | Photomicrograph of Thin Sections under PPL (e) and XPL (f) of Gangra Transition Low-grade (opq = Opaque Minerals; qtz = quartz; and Garnet)                        | 81          |
| 4.23          | Photomicrograph of Thin Sections under PPL (g) and XPL (h) of Gangra Oxide (opq = Opaque Minerals; qtz = quartz; and Garnet)                                       | 81          |

## LIST OF TABLES

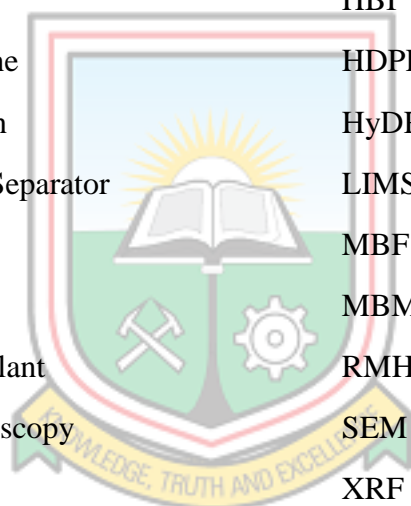
| <b>Table</b> | <b>Title</b>   | <b>Page</b> |
|--------------|--|-------------|
| 2.1          | Geological Mechanisms of Iron Formation (Source: Amikiya, 2014)                                    | 10          |
| 2.2          | Crude Steel Production by Region (Source: Anon., 2010)   | 11          |
| 2.3          | Ten Steel Producing Countries (Source: Anon., 2023)  | 12          |
| 2.4          | Properties of Major Iron Minerals (Amikiya, 2014)  | 12          |
| 2.5          | Specifications for the Proposed Magnetic Separation Plant's Final Products (Source: Amikiya, 2014) | 18          |
| 2.6          | Alternative Ironmaking Processes (Modified after Ramakgala and Danha, 2019)                        | 24          |
| 2.7          | Specific Composition Values for the ITmK3 Process (Source: Gulhane, 2017)                          | 28          |
| 2.8          | Leading Steel Producers and Projected Market Share for 2019 (Source: Anon, 2020)                   | 31          |
| 2.9          | Proximate Analysis of End-of-Life Tyres (Source: Abotar <i>et al.</i> , 2020)                      | 42          |
| 3.1          | Iron Ore Grade Specification (Source: Author' Construct, 2023)                                     | 52          |
| 4.1          | Chemical Composition by XRF of the Mt. Gangra Iron Ores (Anon, 2022)                               | 56          |
| 4.2          | EDS Chemical Analysis of Gangra Lowgrade Ore (Pulverised) at Region 1 (GLG-2567)                   | 57          |
| 4.3          | EDS Chemical analysis of Gangra Lowgrade Pulverised Ore for Region 2 (GLG-2568)                    | 59          |
| 4.4          | EDS Chemical Analysis of Gangra Lowgrade Pulverised Ore for Region 3 (GLG-2569)                    | 60          |
| 4.5          | EDS Chemical Analysis of Gangra Transition Pulverised Ore for Region 1 (GLT-2572)                  | 61          |
| 4.6          | EDS Chemical Composition of Gangra Transition Ore (Pulverised) for Region 3 (GLG-2574)             | 62          |
| 4.7          | EDS Chemical Analysis of Gangra Lowgrade Reduced Ore at Region 1 (M1-2751)                         | 64          |
| 4.8          | EDS Chemical Analysis of Gangra Lowgrade (Reduced) Ore for Region 2 (M1-2752)                      | 65          |
| 4.9          | EDS Chemical Analysis of Gangra Lowgrade Reduced Ore at Region 3 (M1-2753)                         | 66          |
| 4.10         | EDS Chemical Analysis of Gangra Transition Ore (Reduced) at Region 1(C1-2745)                      | 68          |

| <b>Table</b> | <b>Title</b>  | <b>Page</b> |
|--------------|---|-------------|
| 4.11         | EDS Chemical Analysis of Gangra Transition Ore (Reduced) at Region 2 (C1-2746)  | 69          |
| 4.12         | EDS Chemical Analysis of Gangra Transition Ore (Reduced) at Region 3 (C1-2747)  | 70          |
| 4.13         | EDS Chemical Analysis of Gangra Transition (Reduced) Ore at Region 4 (E1-2748)  | 71          |
| 4.14         | EDS Chemical Analysis of Gangra Transition Ore (Reduced) for Region 5 (E1-2749] | 72          |
| 4.15         | EDS Chemical Analysis of Gangra Transition Ore (Reduced) at Region 6 (E1-2750)  | 73          |
| 4.16         | Modal Composition of the Rocks in Thin Section                                  | 82          |
| 4.17         | Modal Composition of Rocks in Polished Section                                  | 83          |



## ABBREVIATIONS

|                                  |       |
|----------------------------------|-------|
| Blast Furnace                    | BF    |
| Banded Iron Formation            | BIF   |
| Basic Oxygen Furnace             | BOF   |
| Direct Reduction                 | DR    |
| Direct Reduced Iron              | DRI   |
| Direct Shipping Ore              | DSO   |
| Electron Dispersed Spectroscopy  | EDS   |
| Electric Arc Furnace             | EAF   |
| End-of-Life Tyres                | ELTs  |
| Hot Briquetted Iron              | HBI   |
| High-Density Polyethylene        | HDPE  |
| Hydrogen Direct Reaction         | HyDR  |
| Low-Intensity Magnetic Separator | LIMS  |
| Mini Blast Furnace               | MBF   |
| Mini Blast Material              | MBM   |
| Raw Material Handling Plant      | RMHHP |
| Screening Electron Microscopy    | SEM   |
| X-ray Fluorescence               | XRF   |
| X-ray Diffraction                | XRD   |



# CHAPTER 1

## INTRODUCTION

### 1.1 Statement of the Problem

The advent of vehicles has made life easier for mankind; unfortunately, the automobile's industrial revolution has resulted in the generation of waste car tires (End-of-Life Tyres, ELTs) (Dankwah *et al.*, 2012; Abotar *et al.*, 2020). Unlike in advanced nations, used car tyres are disposed into the environment in Africa, culminating in the landfilling of ELTs (Dankwah *et al.*, 2012; Dankwah *et al.*, 2013; Abotar *et al.*, 2020). Landfilling of ELT(s) serve as a habitat for mosquitoes and reptiles (snakes and frog). This poses a serious risk to the health of men resulting in the spread of malaria (Dankwah *et al.*, 2012; Abotar *et al.*, 2020).

Again, findings from other literature confirm that stockpiling of end-of-life tyres might create a fire outbreak when catalysed by a lightning strike (Dankwah *et al.*, 2012; Dankwah *et al.*, 2013; Abotar *et al.*, 2020). In general, about 1.5 billion End of life tyres is produced annually (Dankwah *et al.*, 2012). In the United States, about 292 million used tyres are produced from automobiles and trucks; about 86 % are recycled while the remaining 14 % result in landfills (Dankwah *et al.*, 2012; Kannan *et al.*, 2014)

Liberia has abundant iron ore deposits which are currently mined and exported in the raw state (Gunn *et al.*, 2018). Notable iron ore deposits in Liberia include the Nimba Range Deposit, Bong Deposit, Wologizi Range Deposit, and Gangra Iron Ore Deposit (Gunn *et al.*, 2018).

One of the key natural resources supporting Liberia's expanding economy is iron ore. Liberia has large stockpiles of low-grade and transition hematite iron ores which can be upgraded to high grade by getting rid of the silica. This can accomplish the quest for domestic iron and steel industries to support large external trade in Africa, and the world at large. Stockpiles of lowgrade iron ore in Gangra are illustrated in Figure 1.1

Lowgrade iron ore of 50 wt% to 55 wt% Fe content and transition of less than 50 wt% Fe content are found in Gangra. Due to the lowgrade nature of Gangra iron ore, an upgrade to about 60% Fe in the concentrate is required.

However, there is no coal deposit in Liberia. Hence, it would be advantageous for the country to utilise the generation of carbonaceous material from used vehicle tyres to

generate carbon for the iron and steel-making processes in Liberia. This would help ensure effective management of ELT(s) while obtaining carbon sources for metallurgical processes. The Stockpile of End-of-life tyres in Gangra is shown in Figure 1.2.

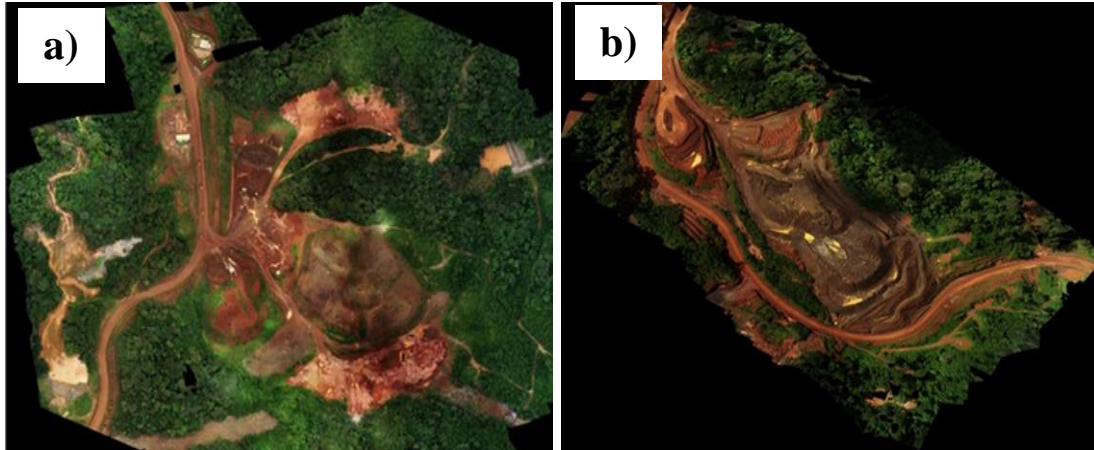


**Figure 1.1 Drone Image of Gangra Lowgrade Stockpiles: (a) Permanent Low-grade Dump (b) Valley Dump (Source: Author's Construct, 2023)**



**Figure 1.2 Stockpile of End-of-Life Tyres along the Mt. Gangra Haul Road (Source: Author's Construct' 2023)**

Previous research investigated the reduction of iron oxide using carbonaceous materials generated from end-of-life tyres (Dankwah *et al.*, 2012; Dankwah *et al.*, 2013; Abotar *et al.*, 2020).

Further information is needed on the production of metallic iron from Gangra iron ore and its amenability to reduction by using carbonaceous materials generated from End-of-life vehicle tyres, which this research seeks to ascertain.



## 1.2 Objectives of Research

The major objectives for this thesis are to:

- i. determine the mineralogical, and geological compositions of Gangra Iron Ore
- ii. ascertain Gangra Iron Ore's suitability for reduction using reductant produced from ELT(s); and
- iii. produce metallic iron from Gangra Iron Ore.

## 1.3 Method Used

The methods used for this research work are as follows:

- i. Conduct petrographic studies on the iron ore by creating thin and polished sections to determine the geological and mineralogical characteristics of Gangra iron ores;
- ii. Conduct X-ray diffraction (XRD), Scanning Electron Microscopic (SEM), Energy Dispersive Spectroscopic (EDS), and X-ray Fluorescence (XRF) of iron Metal and iron ores samples; and
- iii. Conduct experimental work: crushing, grinding, milling, pulverising, drying, microwaving, furnace reduction, microscopy study.

## 1.4 Facilities Used

- i. University of Mines and Technology (UMaT) internet and library facilities;
- ii. The University of Mines and Technology's Petrographic Laboratory;
- iii. The University of Mines and Technology's Environmental Monitoring Laboratory;
- iv. ArcelorMittal Liberia Mine Laboratory; and
- v. University of Mines and Technology (UMaT)'s Minerals Engineering Laboratory.

## 1.5 Organisation of the Report

This project is divided into five main Chapters. Chapter One focuses on the introduction, project objectives, facilities used, and possible methods used in executing the project. Chapter Two deals with a literature review related to the project. Chapter Three deals with experimental methods. Chapter Four deals with results and discussions.

Lastly, Chapter Five focuses solely on conclusions and recommendations.

## CHAPTER 2

### LITERATURE REVIEW

#### 2.1 Introduction

The development of the global economy is significantly influenced by the steel sector which is also responsible for significant environmental impacts such as greenhouse gas emissions, resource depletion, and waste generation. As the world seeks sustainability, the concept of green steelmaking has emerged to alleviate these challenges and promote a more environmentally friendly steel production process (Siddiqui, 2023). Due to its heavy use of fossil fuels, the steel industry accounts for about 7% of global anthropogenic CO<sub>2</sub> emissions. Direct reduction of iron ore with low-CO<sub>2</sub> hydrogen is said to have a high potential to reduce CO<sub>2</sub> emissions.

In the Western Area of Nimba County, ArcelorMittal Liberia has revived and expanded former iron ore mining as well as to upgrade the related infrastructure (rail, port, quarries, and community infrastructure). The Western Area includes Mounts Tokadeh and Gangra's proposed open-cast mines and Yuelliton, the latter two being developed as one unified enterprise. A defunct mine is a considerably larger abandoned mine at Nimba, which is not a part of the Western, and both are present at Tokadeh (Anon, 2010).

ArcelorMittal Liberia owns three concessions along the Nimba Mountains in northeastern Liberia. The deposits are called Tokadeh, Gangra, and Yuelliton. The Tokadeh deposit was mined from 2011-2016, producing direct transport Ore and development of the transition zone will begin soon. The Gangra deposit is currently being mined and the mining of the Yuelliton deposit is ongoing. (Barbosa *et al.*, 2016).

All deposits share roughly the same geological composition. First, itabirite, a metamorphosed striped iron layer that forms the basis of the deposit. The weathered profile then forms a ground-to-surface transition zone and finally, the laterite horizon or Canga. The deposits consist of three iron oxides, magnetite, hematite, and goethite, with quartz being the most important (and sometimes the only) dike rock. The proportions of these mineral phases vary from the bottom to the top of the deposit and from deposit to deposit (Barbosa *et al.*, 2017).

The Liberian deposit of ArcelorMittal is in the northern part of the Nimba region in northeastern Liberia. Currently, only one deposit is used to produce DSO (Direct Shipping Ore) products. Development of other deposits in the area has not yet been defined but is

expected to be developed soon. Liberian iron ore is suitable for manufacturing various types of end products such as DSO, sintered linings, and fine concentrates (Siboni *et al.*, 2015). A map of Mt. Beaton, Mt. Gangra, Mt. Tokadeh, and Mt. Yuelliton is shown in Figure 2.1 and the location of the study area is shown in Figure 2.2. Mount Gangra has an elevation of 1013 m and is currently being mined by ArcelorMittal Liberia Limited, likewise Mt. Yuelliton with an elevation of 1049m, and Mt. Beaton with an elevation of 1005 m which is to be explored soon (Anon, 2010)

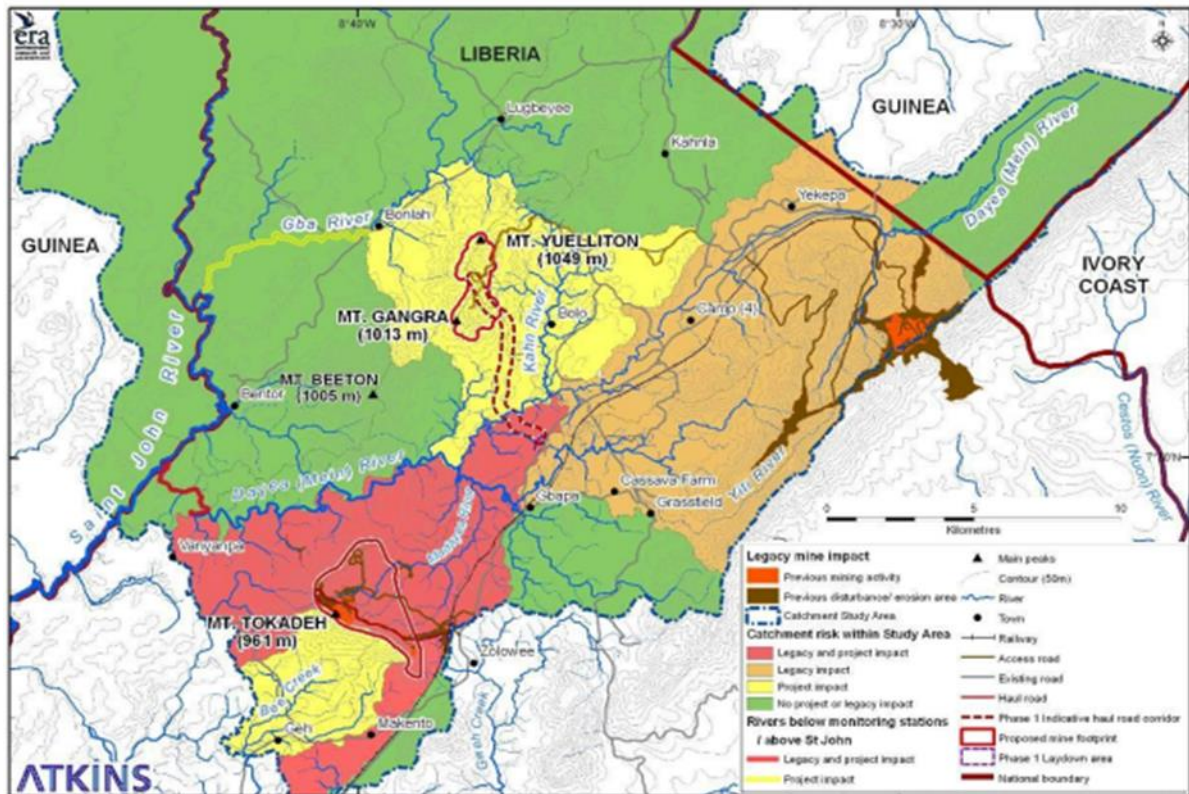


**Figure 2.1 Map of Mount Beaton, Gangra, and Yuelliton from the Old Nimba Mine (Source: Anon, 2010)**

The Tokadeh, Gangra, and Yuelliton ore production as well as the implementation of ore concentration is at full speed this 2023. Construction of a concentrator, a coal-fired power plant, tailings facilities, and possibly a reservoir will be needed for these operations, which will also necessitate improvements to the rail, port, and community infrastructure. In 2009, the Environmental Impact Assessment (EIA) for Phase 2 began (Anon, 2010).



**Figure 2.2 Map of Liberia showing ArcelorMittal Concession Area (Source: Amikiya 2014)**

Gangra Mountain consists of three pits that produce large volumes of Direct Shipping Ore (DSO). These three pits are Pit 1, Pit 2, Pit 3 Bottom North, and Pit 3 Bottom South. The Direct Shipping Ore (DSO) mined from these pits is transported to Mount Tokadeh where it is stored, crushed, screened, and finally loaded onto wagons and transported to Buchanan Port for shipment. Drone Photograph of Mt. Gangra Figure 2.3, Mt. Gangra Pit-3 Top Figure 2.4a, and Pit-2 Figure 2.4b.



**Figure 2.3 Drone Image of Gangra Mine (Source: Author's Construct, 2023)**

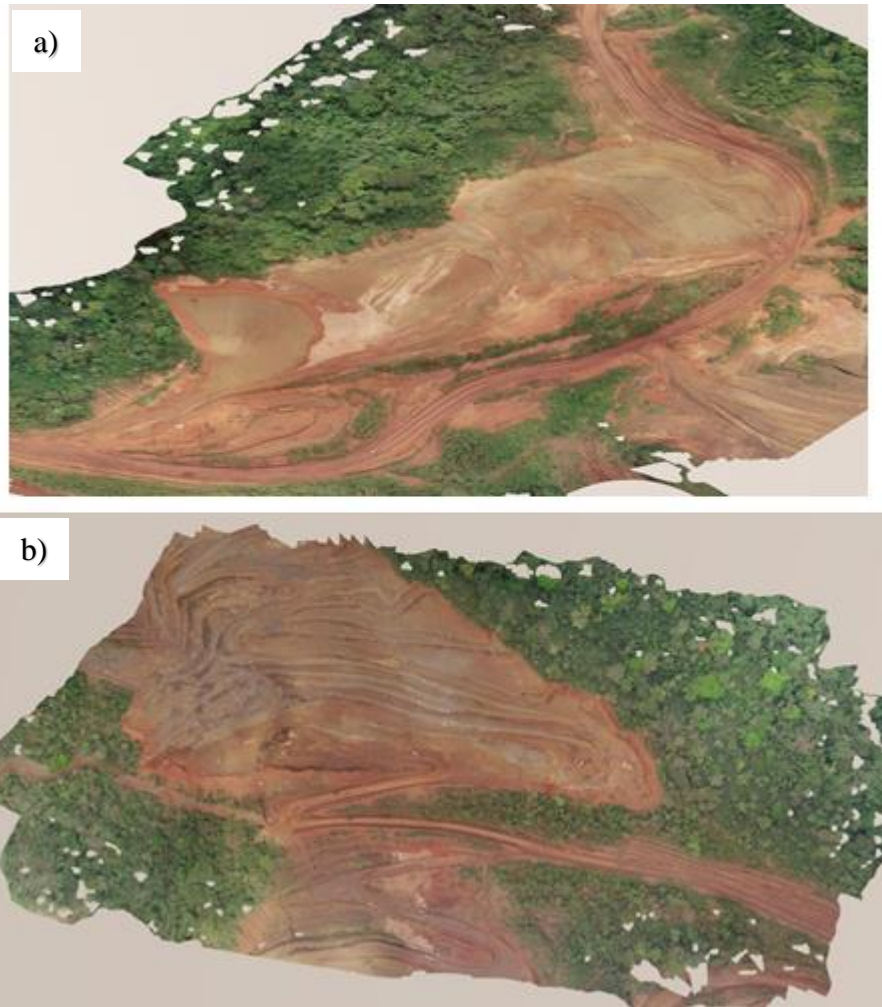


**Figure 2.4 Drone Images of (a) Gangra Pit -2 (b) Gangra Pit 3- Top**  
(Source: Author's Construct, 2023)

## 2.2 Iron Ore

Iron ore is one of the most important dry goods and a common source of abundant iron (Fe) on Earth. This mineral is the main raw material for steel production and plays an important role in human life. According to (World Steel Association, 2020), the total crude steel production in 2019 was 1,875,155,000 tons, which has been on an increasing trend since 2000 (Sani, 2021).

It is surprising that, unlike other countries in the world, Figure 2.5, China, which accounts for up to 85% of global production and boasts almost stable production, has been the major country that has achieved significant development in steel production over the past 20 years (Sani, 2021).

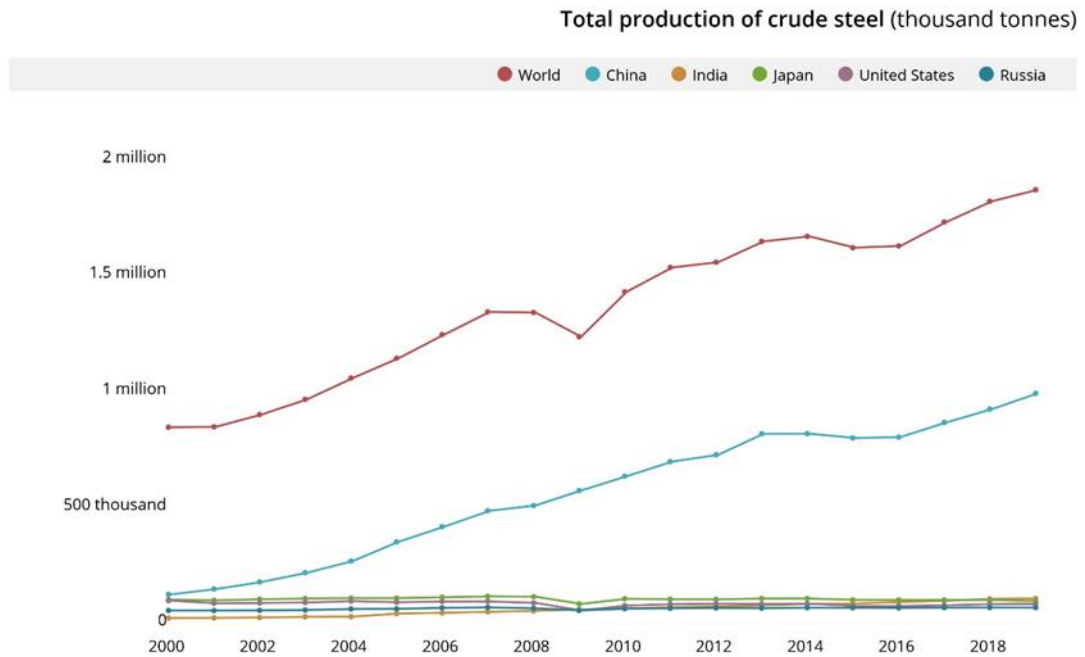


**Figure 2.5 Total Production of Crude Steel (Thousand Tonnes) World and Top five Steel Producers (Source: Sani, 2022)**

According to the Steel Production Report Figure 2.5, China is the main export destination for most iron ore exporting countries. According to this, almost 74% of this critical raw material leaked to China in 2019. Meanwhile, Australia and Brazil are the two dominant countries in iron ore exports, accounting for almost 82% of seaborne iron ore trade in 2019 (Sani, 2022).

Therefore, three countries are generally considered to be the major players in the world's iron ore trade. China is the largest importer (accounting for almost 74% share of the import market). The remaining two are Australia and Brazil, with market shares of approximately 58% and 24%, respectively Figure 2.6, and Market Share Figure 2.7 (Sani, 2022).

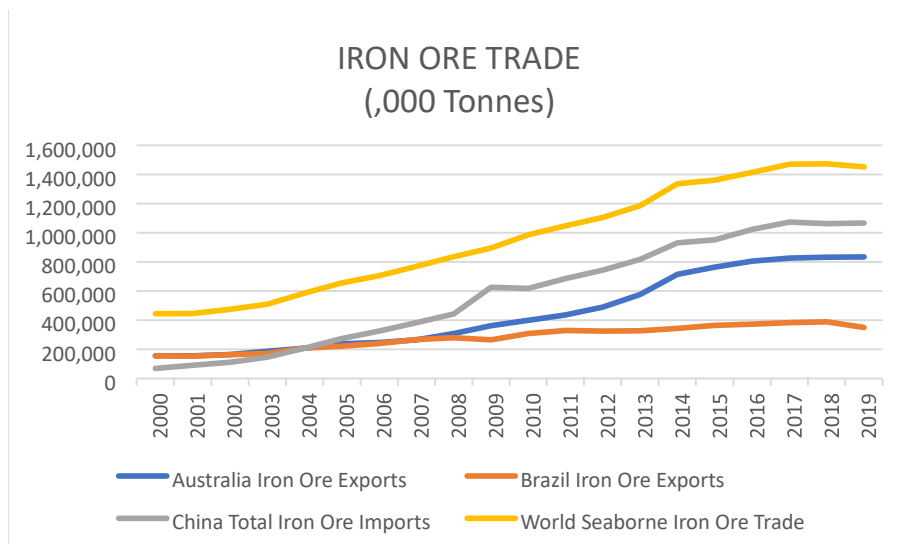


Figure 2.6 Overview of Iron Ore Trade Together with Main Players (Sani, 2022)

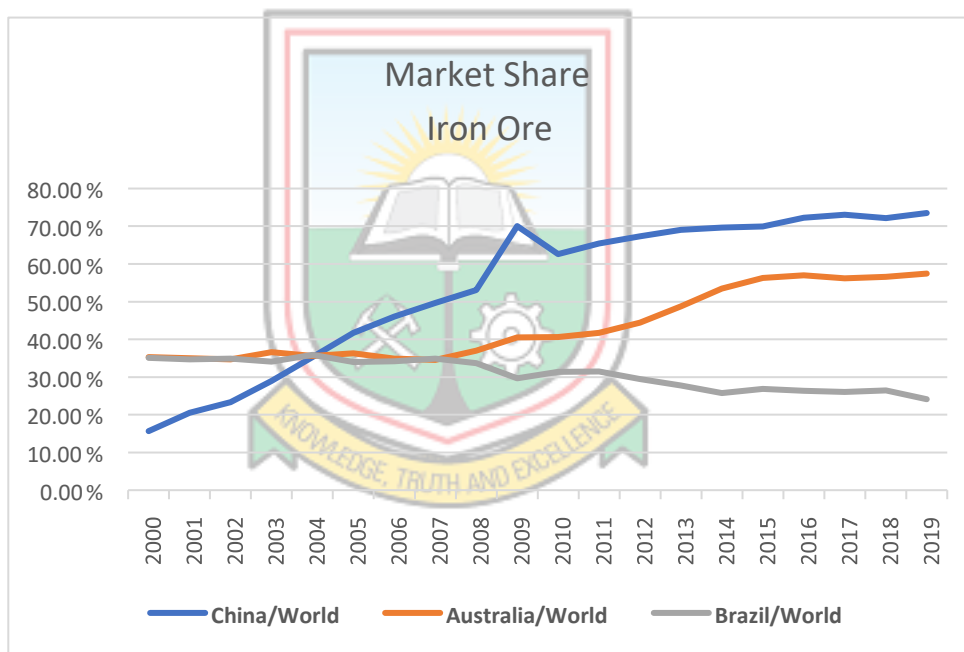


Figure 2.7 Market Share of Iron from 2000-2019 (Sani, 2022)

### 2.3 Iron Ore Deposits Formation

Mineral deposits are produced by processes that either enrich elements in their mineral forms or result in extraordinary quantities of other minerals. Because of the extreme concentrations, these deposits are known as ores, from which valuable rocks and minerals can be recovered from the ground (Howard, 1987).

Iron ore deposits are mineral bodies with adequate size, iron content, and chemical makeup with both physical and economic properties to be an immediate or potential source of iron

(Amikiya, 2014). Three geological processes form iron ore deposits: Formation of layered deposits, and magmatism. Formation of segregation or alternate deposits and accumulations by Weathering on the surface and just below it (US EPA, 1994). The varieties of iron ores contain their main iron minerals and the geological processes involved in the creation of iron ore deposits Table 2.1.

### 2.3.1 Iron Ore Formation Processes

The most prevalent processes are chemical and physical processes of metal or mineral enrichment. It involves the breakdown of rock chemical constituents, their movement in solutions, as well as precipitation of these constituents as minerals ore at specific depositional sites, usually controlled by chemical contrast, i.e., the chemical environment has undergone significant changes. When crystallised from the solution, the heavier iron-bearing minerals segregate by gravity, forming iron-rich sediments. The subsidence of surface water or the rise of groundwater through rock formations can lead to the deposition of iron-bearing minerals and the leaching of gangue minerals such as silica (Amikiya, 2014).

**Table 2.1 Geological Mechanisms of Iron Formation**

| <b>Geological Mechanism</b>                     | <b>Principal iron mineral</b>                     |
|---|---|
| <b>Sedimentation</b>                            |   |
| Banded iron formation                           | Magnetite, Hematite, Siderite, Iron silicate      |
| Iron stones                                     | Chamosite, Limonite, Hematite, Siderite           |
| <b>Igneous Activity</b>                         |   |
| Magmatic segregations                           | Titaniferous, Ilmenite, Magnetite, Iron silicates |
| Pyrometasomatic                                 | Magnetite   |
| <b>Surface or Near-Surface Weathering</b>       |   |
| Secondary enrichment of low-grade iron deposits | Magnetite, Limonite, Siderite                     |

(Source: Amikiya, 2014)

Global crude steel production, reported by 64 countries to the World Steel Association, was 140.7 million tons (Mt) in December 2022, down 10.8% from December 2021. Steel production by region Table 2.2. Africa's production in December 2022 was 1.1 million tonnes (Mt), down 8.9% from December 2021. Asia and Oceania produced 104.9 million tonnes, down 9.2% (Anon, 2023).



**Table 2.2 Crude Steel Production by Region**

|                                 | Million Tonnes              |                       | Million Tonnes  |                           |
|---------------------------------|-----------------------------|-----------------------|-----------------|---------------------------|
|                                 | Million/Tonnes<br>Dec. 2022 | % Change<br>Dec-22/21 | Jan-Dec<br>2022 | %Change Jan<br>Dec. 22/21 |
| <b>Africa</b>                   | 1.1                         | -8.9                  | 14.9            | -6.6                      |
| <b>Asia and Oceania</b>         | 104.9                       | -9.2                  | 1,351.3         | -2.3                      |
| <b>EU (27)</b>                  | 9.2                         | -16.7                 | 136.7           | -10.5                     |
| <b>Europe, Other</b>            | 3.4                         | -19.2                 | 44.7            | -12.2                     |
| <b>Middle East</b>              | 3.7                         | 0.4                   | 44.0            | 7.7                       |
| <b>North America</b>            | 8.8                         | -9.9                  | 111.4           | -5.5                      |
| <b>Russia, CIS, and Ukraine</b> | 6.2                         | -28.4                 | 85.2            | -20.2                     |
| <b>South America</b>            | 3.3                         | -3.8                  | 43.3            | -5.0                      |
| <b>Total 64 Countries</b>       | 140.7                       | -10.8                 | 1,831.5         | -4.3                      |

(Source: Anon., 2023)

The 27 EU member states produced 9.2 million tonnes, a decrease of 16.7%. European residual production was 3.4 million tonnes, a decrease of 19.2%. The Middle East produced 3.7 million tonnes, up 0.4%. North American production fell 9.9% to 8.8 million tonnes. Production in Russia, other CIS countries, and Ukraine fell by 28.4% to 6.2 million tonnes. South America produced 3.3 million tonnes, with a decrease of 3.8% (Anon, 2023).

China's production in December 2022 was 77.9 million tons, down 9.8% from December 2021. India's production was 10.6 million tons. 44.44 million tons, an increase of 0.8%. Japan's production decreased by 13.1% to 6.9 million tons. The United States produced 6.5 million tons, down 8.3%. Russian production was estimated at 5.5 million tonnes, down 11.3%. South Korea produced 5.2 million tons, down 11.6%. German production was 2.7 million tonnes, down 14.6%. Turkey's production decreased by 20.0% to 2.7 million tons. Brazil produced 2.5 million tonnes, down 5.2%. Iran produced 2.7 million tonnes, up 3.3% (Anon, 2023). Ten Steel producing countries Table 2.3.

**Table 2.3 Ten Steel Producing Countries**

| Countries     | Million Tonnes |                    | Million Tonnes |                        |
|---------------|----------------|--------------------|----------------|------------------------|
|               | Dec. 2022      | % Change Dec-22/21 | Jan-Dec 2022   | %Change Jan Dec. 22/21 |
| China         | 77.9           | -9.8               | 1,013.0        | -2.1                   |
| India         | 10.6           | -0.8               | 124.7          | -5.5                   |
| Japan         | 6.9            | -13.1              | 89.2           | -7.4                   |
| United States | 6.5            | -8.3               | 80.7           | -5.9                   |
| Russia        | 5.5            | -11.3              | 71.5           | -7.2                   |
| South Korea   | 5.2            | -11.6              | 65.9           | -6.5                   |
| Germany       | 2.7            | -14.6              | 36.8           | -8.4                   |
| Turkey        | 2.7            | -20.0              | 35.1           | -12.9                  |
| Brazil        | 2.5            | -5.2               | 34.0           | -5.8                   |
| Iran          | 2.7            | 3.3                | 30.6           | 8.0                    |

(Source: Anon., 2023)

The estimated ranking of the top 10 producing countries is based on year-to-date aggregate.

### 2.3.2 Mineral Types found in Iron Ore

Almost 300 minerals contain iron, however, just a few of these are significant sources of iron ore (Amikiya, 2014). The main minerals that makeup iron ore are listed in Table 2.4.

**Table 2.4 Properties of Major Iron Minerals**

| Mineral       | Chemical Formula  | Theoretical Iron Content, % | Specific Gravity | Mohs Hardness |
|---------------|---|-----------------------------|------------------|---------------|
| Hematite      | Fe <sub>2</sub> O <sub>3</sub>  | 70                          | 5.1              | 5-6           |
| Magnetite     | Fe <sub>3</sub> O <sub>4</sub>  | 72                          | 5.2              | 5.5-6         |
| Martite       | α-Fe <sub>2</sub> O <sub>3</sub>  | 70                          | 5.3              | 5.5-6.5       |
| Goethite      | FeO (OH)  | 63                          | 3.3-4.3          | 5-5.5         |
| Siderite      | FeCO <sub>3</sub>   | 48                          | 4                | 4             |
| Chamosite     | (Mg, Fe, Al) <sub>6</sub> (Si, Al) <sub>4</sub> O <sub>14</sub> (OH) <sub>8</sub> | 45                          | 3.1              | 3             |
| Pyrite        | FeS <sub>2</sub>  | 47                          | 4.9              | 6-6.5         |
| Limonite      | FeO (OH). n (H <sub>2</sub> O)  | 63                          | 3-4              | 5-5.5         |
| Lepidocrocite | γ-Fe <sub>2</sub> O <sub>3</sub> .H <sub>2</sub> O                                | 60                          | 4.1              | 5             |
| Greenalite    | Fe <sub>3</sub> Si <sub>2</sub> O <sub>5</sub> (OH) <sub>4</sub>                  | 45                          | 2.9              | 3             |
| Ilmenite      | FeTiO <sub>3</sub>  | 37                          | 4.7-4.79         | 5-6           |

(Source: Amikiya, 2014)

Hematite, magnetite, martite (a pseudomorph of hematite to magnetite), goethite, and limonite are the principal iron-bearing minerals in the Mt. Gangra deposit. Group minerals identified in the deposit include quartz and aluminum minerals. DSO deposits are generally rarer than magnetite-bearing BIFs and other rocks that constitute the main source, or pisolitic rocks, but their high iron content requires less processing, making mining and processing easier, and the cost is significantly lower.

However, DSOs typically have high contents of phosphorus, water (particularly in pisolite sediments), and aluminum (clays in pisolite), and may contain significantly higher concentrations of punitive elements. Export-grade DSO ores are typically in the 62-64% Fe range. The Direct Shipping Ore (DSO) of Mt. Gangra Figure 2.8.

There are many types of iron minerals, but the most used are magnetite  $\text{Fe}_3\text{O}_4$  (72% Fe), hematite –  $\text{Fe}_2\text{O}_3$  (70% Fe), goethite  $\alpha\text{FeO OH}$  (61% Fe), Lepidocrocite  $\gamma\text{FeO}$ , etc. 61% Fe), siderite -  $\text{FeO CO}_2$  (48% Fe) and chamosite  $3\text{FeO Al}_2\text{O}_3 \cdot 2\text{SiO}_2 \cdot 6\text{H}_2\text{O}$  (35% Fe). Iron ore may contain gangue minerals such as feldspar, quartz, calcite, dolomite, clay, and carbonaceous material. Iron ore may also contain phosphorus, silica, potassium, zinc, sulfur, and sodium (Adeleke, 2014).

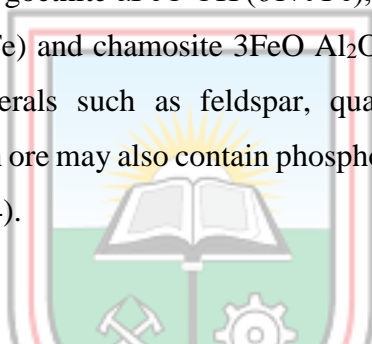


**Figure 2.8 Mt. Gangra High-Grade Direct Shipping Ore (DSO) (Source: Author's Construct, 2023)**

## 2.4 Types of Iron Minerals

The Types of iron minerals are as follows:

- i. The term "Natural Ore" refers to hematite ( $\text{Fe}_2\text{O}_3$ ) and dates back to the early days of mining when specific hematite ores with up to 66% iron content could be delivered straight to blast furnaces for the production of steel. Most hematite deposits, like banded iron formations (BIF), are of sedimentary origin. Hematite, magnetite, and fine-grained recrystallized quartz alternately make up the layers that makeup BIF. Although the process of how they were created is not entirely understood, it is known that iron from shallow Precambrian waters was chemically precipitated between 1.8 and 2.6 billion years ago (Amikiya, 2014);
- ii. Magnetite, a naturally occurring metallic mineral ( $\text{Fe}_3\text{O}_4$ ) is found in large enough amounts to be used as iron ore. It contains both ferrous oxide ( $\text{FeO}$ ) and ferric oxide ( $\text{Fe}_2\text{O}_3$ ). High-quality magnetite ores typically contain more than 60% iron and contain impurities such as silica, alumina, and phosphorus. Magnetite is produced by crushing magnetite from gangue minerals and separating it with a magnet. This separation is usually so efficient that low-grade magnetite ores can be processed more easily than comparable hematite ores (Amikiya, 2014);
- iii. Martite ( $\text{Fe}_2\text{O}_3$ ) is a secondary hematite formed by the chemical substitution of magnetite formed at depth and under pressure. Along crystal planes, substitution often occurs from the magnetite grain's periphery to its core (Amikiya, 2014);
- iv. Secondary minerals like goethite and limonite ( $\text{FeO}(\text{OH})$ ) are created when iron carbonate, hematite, and magnetite are oxidized. The hematite has been replaced by goethite in the nodules of goethite found in quartz. Hematite is manganese-free, whereas carbonates and martite are replaced by goethite, which contains significant levels of Mn (up to 27 wt% Mn) (Petruk, 2000; Amikiya, 2014). These hydrated iron oxides contain up to 60–63% iron. They can originate rather close to the surface and can occur as main minerals due to the weathering of exposed ores;
- v. Iron ore ( $\text{FeCO}_3$ ), known as Siderite, represents only a tiny portion of the total iron ore deposits in the world. It has 48.3% iron in its pure form, but heat readily breaks it down into hematite, which has 70% iron; and
- vi. Along with limonite and siderite, the mineral chamosite ( $(\text{Mg}, \text{Fe}, \text{Al})_6(\text{Si}, \text{Al})_4\text{O}_{14}(\text{OH})_8$ ) is also present, but in much smaller amounts. Along with other

minerals like quartz and calcite, this ore typically contains some sulfur and phosphorus (Amikiya, 2014). Types of iron-bearing minerals Figure 2.9.



**Figure 2.9 Types of Iron Ore Minerals (Source: Anon., 2020)**

## 2.5 Gangue Minerals

All iron ores contain embankment rock, a type of impurity. The existence of some elements in small amounts can have bad or good effects on iron ore properties and steel mill operations. To improve the efficiency of the blast furnace and the product quality, flux is frequently added to the iron ore raw material in the blast furnace. Iron ore should only contain iron and oxygen in its ideal state, but it typically also contains several other components that are unsuitable for modern steel (Amikiya, 2014).

## 2.6 Reviews of Ore Geology of Liberia

The Republic of Liberia in West Africa is primarily composed of Archean (Liberian age) and Precambrian rocks in the west, and Proterozoic (Eburnean) rocks in the east. Liberia's geology contains gold, iron ore, diamonds, base metals, bauxite, manganese, feldspar, and kyanite by comparison with similar terrain elsewhere in the world, particularly in West Africa (Gunn *et al.*, 2018).

There are abundant itabirite-type iron reserves in Liberia and was Africa's largest producer before the 1989 civil war. Iron ore production is currently limited to a single mine, Yekepa, in the Nimba Mountains. Other important deposits, some previously mined, include Bong, Western Cluster, Putu, and Goe Fantro (Gunn *et al.*, 2018).

### 2.6.1 Geology of the Study Area

Northern Liberia is a portion of the West African Craton, a collection of extremely old pre-Cambrian rocks with radiometric ages ranging from 2.2 to 3.0 billion years. The bedrock in

the Western Area deposits and the Nimba Range can be separated into two supergroups (Berge, 1974).

The Yekepa Supergroup and the Nimba Supergroup. The more experienced is Yekepa Supergroup. Between the Nimba and Tokadeh-Beeton-Gangra-Yuelliton mountains, a large valley is formed by banded gneisses and ortho-amphibolite. The Tokadeh-Yuelliton and Nimba ranges are home to the Nimba Supergroup. Pelitic schists and the Nimba Itabirites, which are metamorphosed, banded (i.e., initially sedimentary), iron-formations and the ore bodies that ArcelorMittal propose to extract, make up the unconformably overlying rocks, which are older than the Yekepa rocks.

Nimba itabirite is a 250–450 m thick unit composed of recrystallized (metamorphic) striped iron layers. It occurs along the ridges of the Tokadeh-Beeton-Gangra Yuelliton and Nimba (and Gbahrn) Mountains. This ore is formed from coarse siliceous low-carbonate iron oxide layers (Berge, 1974). Iron exists as hematite, magnetite, or martite (a special type of hematite).

The Nimba Mountains, which are shared by Liberia, Guinea, and the Ivory Coast, include the West Nimba Region iron ore deposit. The majority of the iron ore resources in the Nimba Mountains are of the Achaean Itabirite variety overlying gneiss bedrock complexes and associated with metavolcanic sediment layers closely embedded therein (Coakley, 2004). According to Heneghan (2010), the Achaean Iron Formation in the western area is part of the West African Craton.

In the northwestern Nimba Mountains of Liberia, Nimba-Itabirite changes into an epidote-amphibolite facies, and in the Tokadeh Yuelliton ridge, it changes into an upper amphibolite-lower granite facies. In the northern region of Mount Nimba, the magnetite oxide facies iron layer recrystallizes to gray itabirite (Berge, 1974). Facies are rock formations with particular characteristics, commonly formed under specific sedimentary conditions, and are unique entities that reflect specific processes or environments (Amikiya, 2014).

Historically, iron ore was mined in both Liberia and Guinea sections of the Nimba Greenstone Belt. In Liberia, the bulk of the Nimba iron ore currently mined was in one of two parallel belts of the northeasterly impacted Achaean Banded Iron Formation (BIF) (Berge *et al.*, 1977).

## 2.6.2 Liberia's Iron Ore Mining History

Since the start of the civil war in 1990, Liberia, a nation with a long history of iron ore mining, has been regarded as one of the most promising prospects. The political climate in Liberia has been stable for 17 years and is currently luring sizable foreign investment (Tomlinson, 2004).

In the 1960s and 1970s, the Liberian Mining Company (LMC) was the first of four iron mining firms to produce and ship significant amounts of iron ore. As a result, Liberia became the third-biggest exporter of iron ore in the world at the time and the largest in Africa. For the exploitation of the Mano River iron ore deposit, the National Iron Ore Company (NIOC) entered into a concession agreement in 1958.

Operating since 1960/61, the Liberian American-Swedish Mineral Company Joint Venture (LAMCO JV) has been producing iron ore. In the Nimba Mountains, LAMCO JV has created a very rich iron ore deposit (Amikiya, 2014).

Following a concession agreement with German investors, the Bong Mining firm (BMC), a fourth mining firm, was established in 1958. He inaugurated the mine in 1965. Germany's greatest investment in sub-Saharan Africa at the time was the "Bong Mine," as the company was known locally and is still known in Liberia (Van der Kraaij, 2010; Amikiya, 2014). Distribution of principal iron Deposits in Liberia Figure 2.10.

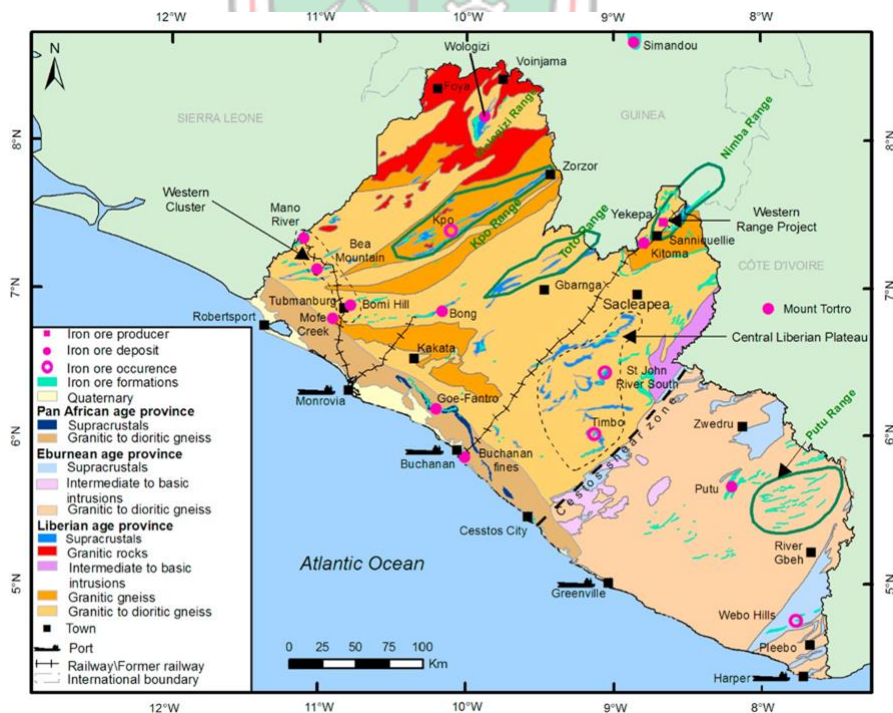


**Figure 2.10 Distribution Map of the Principal Iron Ore Deposits in Liberia (Gunn *et al.*, 2018)**

## 2.7 ArcelorMittal Liberia Proposed Iron Ore Beneficiation Plant

ArcelorMittal's Liberia planned enrichment plant is made to yield 15 million tonnes of concentrate per year, with 23 million tonnes per year (2015-2017) of oxides from Tokadeh Mine and 2018-2026) transition raw ore that can be processed. A Gangra deposit is required. Concentrate production consists of thoroughly washed fines, as ore with a marketable 65% iron concentrate grade requires relatively small particles (1 mm). (Amikiya, 2014). Table 2.5 shows the product specifications of the planned facilities.

**Table 2.5 Specifications for the Proposed Magnetic Separation Plant's Final Products**

| Component                      | Concentration, % |
|--------------------------------|------------------|
| Fe                             | > 66.5           |
| SiO <sub>2</sub>               | < 3.0            |
| Al <sub>2</sub> O <sub>3</sub> | < 1.0            |
| Mn                             | < 0.02           |
| P                              | < 0.07           |

(Source: Amikiya, 2014)

### 2.7.1 Process Description

A combination of magnetite, martite, and hematite makes up the ore mineral. Additionally, oxide ores contain significant levels of hydrated minerals such as goethite and limonite. Quartz makes up the majority of the vein minerals, along with several aluminum minerals such as hydra claystone (Al (OH)<sub>3</sub>) and boehmite (AlO (OH)), as well as other silicates like amphibole, biotite, and feldspar. The majority of the iron in magnetite is also largely bonded to hematite, which is crucial. Therefore, a processing plan that combines ore crushing with low- to medium-intensity magnetic and gravity separation is appropriate (Amikiya, 2014).

ArcelorMittal's suggested treatment process overall block diagram, simplified in Figure 2.11. The ore is transported by mining trucks to the primary crusher's dump hopper. A feed conveyor transports the ore to the coarse crusher before the jaw crusher.

A slat conveyor and a belt conveyor transport the ground ore to the primary ball mill, where the particle size is around 175 mm. Wet grinding decreases the size of the ore particles during primary grinding to roughly 6 mm. The primary ball mill's output is filtered through a 6 mm screen, and the larger material is sent back through a down comer equipped with water jets and siphons.



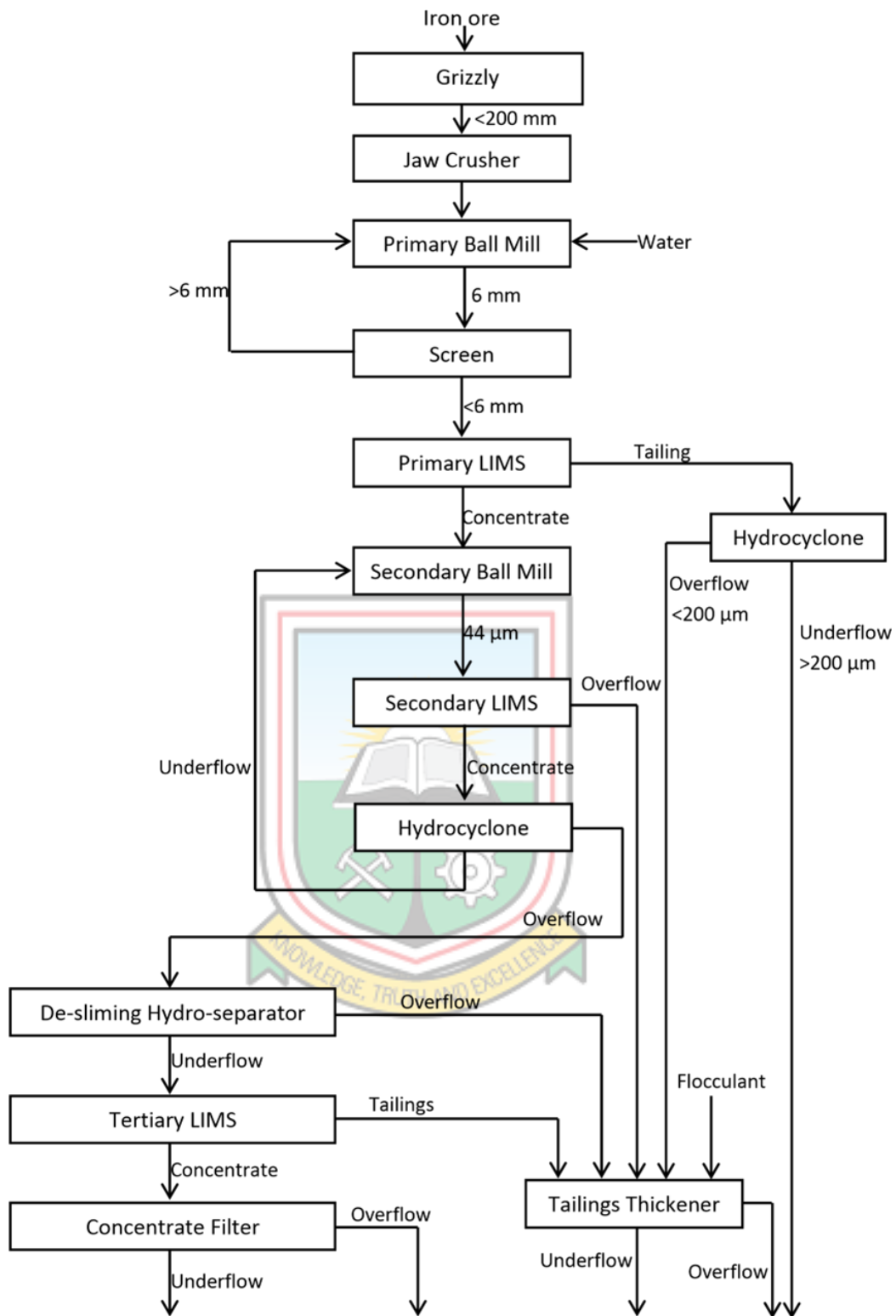


**Figure 2.11 ArcelorMittal Liberia Proposed Process Block Diagram (Amikiya, 2014)**

A primary 44 Low-Intensity Magnetic Separator (LIMS) is where the undersize is pumped. Gravity allows the main LIMS concentrate to enter the secondary ball mill. The 200 m particles are separated from the primary LIMS bottoms in a hydrocyclone before being

transferred to a residue thickener. Conversely, underflow (less than 200 meters) is pumped into the process water reservoir.

The primary LIMS concentrate is ball-milled to a final released particle size below 44 m at a rate of about 80%. With a secondary low-intensity magnetic separator and a classifying hydrocyclone, the ball mill runs in a closed circuit. The ball mill's output travels to the pump box and then to the secondary LIMS. There is a frequency converter in the pump. Water is added to the pump box to adjust the fill level. A density meter in the pump outlet line measures the density of the slurry, and the pump speed is adjusted.

The secondary LIMS tailings enter the tailing concentrator by gravity. Gravity is used to move the secondary LIMS concentration into a suitable classifier hydrocyclone feed pump box. The underflow of the hydrocyclone returns to the ball mill by gravity. The overflow from the hydrocyclone is the product of the secondary crushing circuit and flows to the associated desludging hydraulic separator (Amikiya, 2014)

Based on the difference in specific gravities, the Death Slugger is a tank that separates magnetite fine particles from siliceous sludge. Only the magnetite is delivered to the tertiary magnetic separator to remove non-magnetic small particles after the descender is set up such that only the sludge overflows and only the magnetite remains (Amikiya, 2014)

Tailings from the tertiary magnetic separator flow by gravity into the tailing's concentrator. The concentrate from the tertiary magnetic separator is the final product and flows to the concentration concentrator. The concentrate from the tertiary magnetic separator is concentrated to 70% solids in a concentrate filter using disc filters. Underflow density is controlled by recirculation. The thickener overflow flows by gravity into the process water reservoir. Filter cake with a moisture content of about 9% falls onto a conveyor belt and is transported to a storage site before being loaded onto the train.

Secondary and tertiary LIMS tailings, hydrocyclone overflow tailings, and desludging overflow tailings are all fed into the tailings thickener. Pumped to the pump box and then to the tailings pond are concentrate underflow with about 45% solids and liquid cyclone underflow. A flocculent is used in the tailings thickener to create a clear overflow that flows gravitationally into the process water tank (Amikiya, 2014).

## 2.8 Iron Production

The world's steel industry relies heavily on iron, one of the oldest metals known to man. One of the most prevalent metals on the planet, iron is traded and consumed in a variety of ways across the globe. Iron has several desired qualities, including hardness, strength, formability, ductility, durability, and ease of alloying with other metals to create different grades of steel (Adeleke, 2014). Steelmaking begins with the production of iron. According to Strazov (2006), the steel industry is the most energy and capital-intensive manufacturing sector in the world.

In the steel business, "iron" also refers to carbon-saturated intermediates (such as "pig iron") and finished goods (such as "cast iron") in addition to the chemical element in its purest form. "Steel" refers to an iron and carbon alloy, with "carbon steel" being the most basic and popular variety.

To improve or worsen certain physical qualities for certain uses, many additional elements are added to steel to create more complex steel alloys. "Stainless steel" is created by mixing chromium or nickel with steel, and is used frequently in cookware since it is known for resisting corrosion. Molybdenum, vanadium, manganese, tungsten, and titanium are more examples. To obtain or improve several desired qualities, an alloying element is used. According to the (IEA's 2020 report), there are currently over 3,500 distinct steels in use, many of which have only been created in the past 20 years.

Iron ore is transformed into molten iron during the initial stage of the steelmaking process. The blast furnace route and the direct reduction route are generally used to accomplish this. The iron ore, coke (made from coal), and limestone used in the blast furnace route are fed into the furnace, where high heat and reducing agents turn the iron ore into liquid iron (Siddiqui, 2023).

### 2.8.1 Blast Furnace

An integrated steelmaking plant's blast furnace is its most crucial component. It is regarded as essential to the ISP (Industrial Steel Production). The blast furnace's function is to turn sinter from sinter plants, coke from coke ovens, and raw materials for RMHP into pig iron, sometimes known as "hot metal." Coke acts as a heat source and reducing agent, while limestone and dolomite are used as fluxes to combine with gangue to form slag. Blast furnaces are so-called because they use blast air as the source of oxygen for the process (Vishwakarma, 2016).

For more than 200 years, the primary method of producing pig iron has been blasting furnaces (BFs). BF has developed into a very effective chemical reactor throughout time, capable of ensuring stable operation with a variety of feedstocks. However, sintering and coke production, along with related environmental concerns, are frequently a part of modern efficient blast furnace operation.

More than 90% of the iron produced now comes through the BF process, with the remaining 10% coming from other processes such as direct reduction (DR), mini blast furnaces (MBF), Corex, Finex, and Ausmelt. High-quality iron is also in dire need of supply. High-quality metallurgical coal remains a challenge on a global scale. Alternative ironmaking techniques that are more environmentally friendly and require less metallurgical coal are becoming more widely accepted as a replacement for the BF method. 2016 (Dutta and Sah, 2016). Blast Furnace Figure 2.12.

1.63 billion tons of crude steel were produced globally in 2016, with the blast furnace and basic oxygen converter process routes accounting for 73.7% of the total production. Coke is utilized as a reducing agent and energy source in blast furnaces. As a result, a lot of head gas and carbon monoxide as well as carbon dioxide are released from the furnace (Anon., 2017).

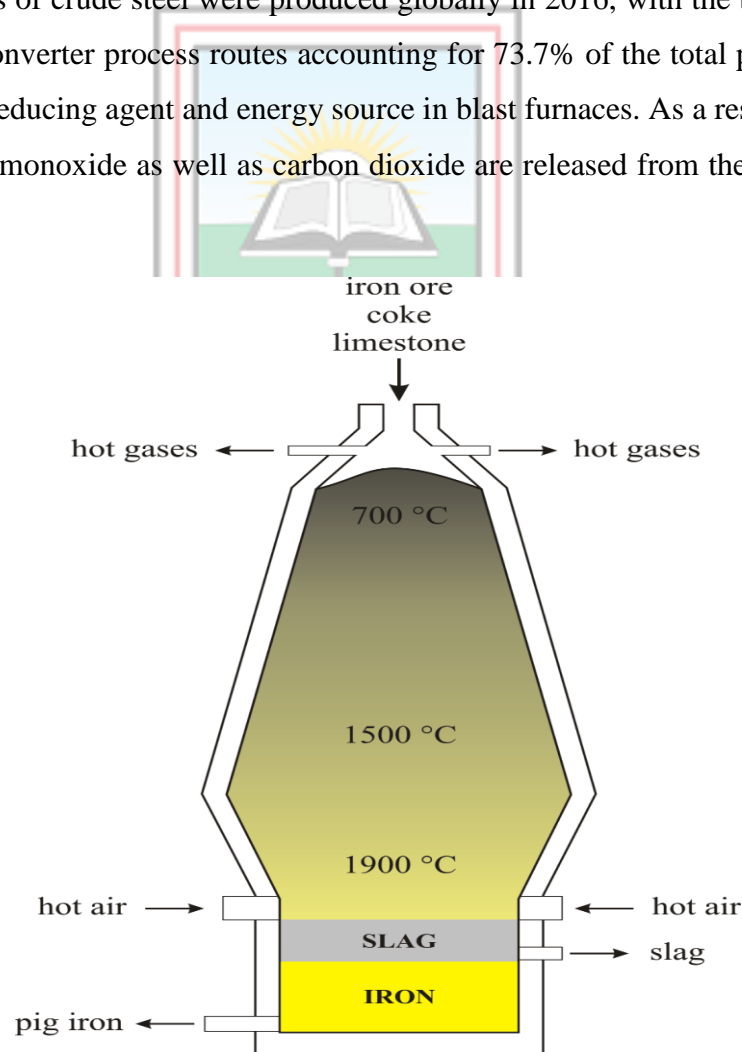


**Figure 2.12 Blast Furnace (Dankwah, 2022)**

A blast furnace is a countercurrent heat and mass exchanger where hot air is forced into the bottom of the furnace through tuyeres while solid raw materials are charged from the top of the furnace. Heat and oxygen are transmitted from the gas to the charge, respectively. Figure 2.13. Charge coke descends into the furnace as the gas rises through it. The entire process of lowering the atmosphere is particularly effective due to the reaction's countercurrent character. The ability to build massive blast furnaces made it possible to produce high-strength coke, which has led to a real advancement in blast furnace technology (Vishwakarma, 2016).

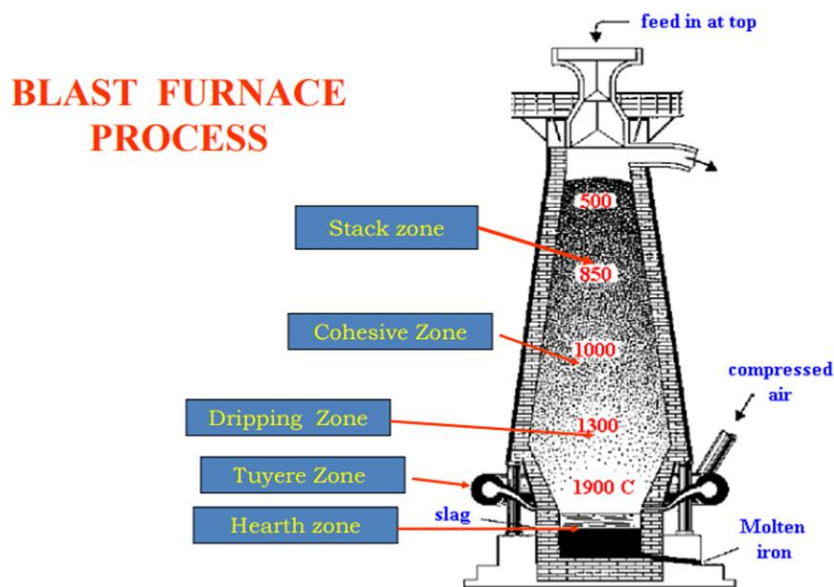


Figure 2.13 Temperature Zones of a Blast Furnace (Dankwah, 2022)

### 2.8.2 Process of Direct Reduction

Direct Reduced Iron, also known as sponge iron, is created by reducing iron ore (in the form of lumps, pellets, or granules) to a solid state using a reducing gas. To make DRI less porous and prepare it for sale or storage, it is frequently crushed. DR methods use fine ore rather than bulk low-cost off-gas to increase process flexibility and save operational costs. The CO<sub>2</sub> emissions from the DR process are only a third of those from the BF-BOF route per tonne of steel (Ramakgala and Danha, 2019).

The porous iron created by the DR process is known as DRI or Sponge Iron. The DR process employs coal or reformed natural gas as a reductant to remove detachable oxygen from iron oxide below the melting point of iron. It is a solid-state reaction process (i.e., solid-solid, or solid-gas reaction). Oxides minuscule clumps or lumps of ore that do not alter the ore's form.

Sponge iron is solid porous iron that forms clumps or pellets with lots of air-filled voids when the oxygen is removed (around a 27–30% weight loss) (Dutta and Sah, 2016).

Direct reduction ironmaking is a method of making iron without using a blast furnace. The production of direct reduced iron was first industrialised in the 1960s when the construction of various commercial and semi-commercial scale plants began.

Based on the reducing agent utilized, direct reduction ironmaking processes can be roughly categorized into two classes: coal- and natural-gas-based. In the former, there are procedures like MIDREX and HYL/ENERGIRON, whereas in the later, there are processes like SL/RN, FASTMET, and ITmk3 (Akihiro and Mitamoto, 2010). The worldwide Direct Reduced Iron production process in 2017-2019 Figure 2.14, while the alternative steel-making processes are shown in Table 2.6.

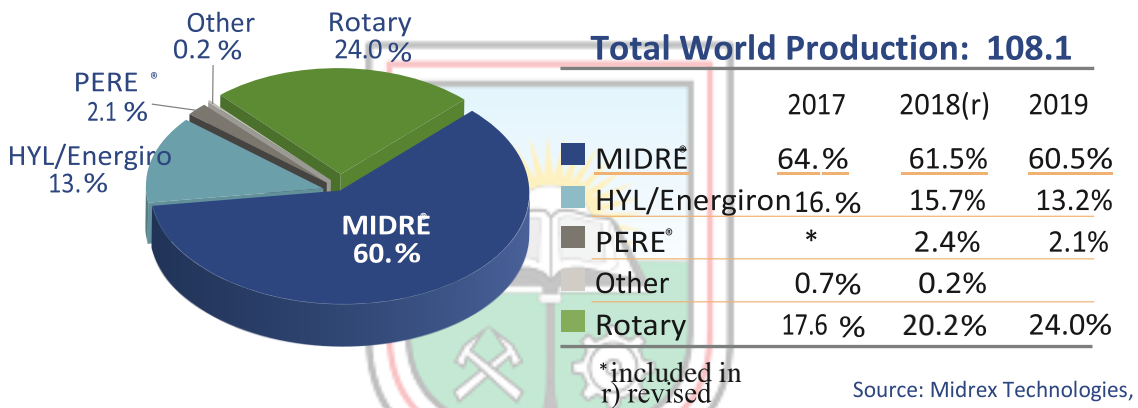


**Figure 2.14 Worldwide Direct Reduced Iron Production by Process in 2019 (Anon., 2019)**

**Table 2.6 Alternative Ironmaking Processes**

| DR PROCESS        | TYPE OF REACTORS          | CHEMICAL PROCESSES       |
|-------------------|---------------------------|--------------------------|
| Coal-based        | Rotary kiln               | ACCAR, DRC, KRUPP Rein   |
|                   | Rotary Hearth             | Fastmet, Fastmelt, ITmk3 |
| Natural Gas-Based | Shaft Furnace             | MIDREX                   |
|                   | Fluidised beds or Retorts | HYL-III                  |

(Modified after Ramakgala and Danha, 2019)

The use of non-coking coal and low-grade iron ore in direct reduction ironmaking can help with resource issues. Worldwide MIDREX/FASTMET plants Figure 2.15. Due to its minimal negative effects on the environment and minimal CO<sub>2</sub> emissions, the direct reduction method for producing iron is very promising (Akihiro and Mitamoto, 2010).

In recent decades, the direct reduction of iron ore has become an important step in iron production. Several direct reduction processes have been developed over the years, ranging from using fines to using lump ore and pellets. Some of these processes use natural gas as the fuel reductant, while others rely on coal. However, today more than 90% of the world's direct reduced iron (DRI) production is through vertical shaft furnace processes developed by Midrex in the United States and HyL in Mexico, both of which use pellets or lumps as feedstock (Basdag and Arol, 2002).

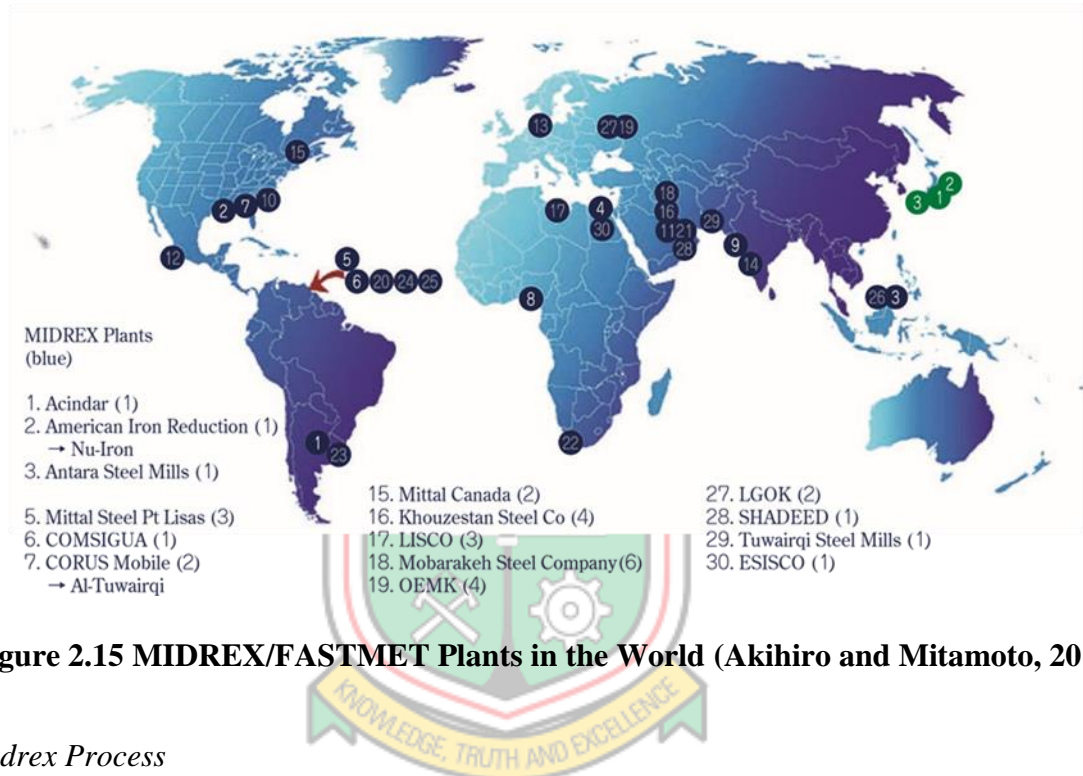


**Figure 2.15 MIDREX/FASTMET Plants in the World (Akihiro and Mitamoto, 2010)**

*Midrex Process*

Direct reduced iron (hence referred to as DRI) is produced by the MIDREX process. Using a natural gas-based reforming gas, method lowers iron ore. According to Masaaki et al. (2010), the DRI is primarily employed as a clean iron supply to replace scrap iron in electric arc furnaces (EAFs). Appearances of Direct Reduced Iron and Hot Briquetted Iron Figure 2.16. World's MIDREX Plants Figure 2.17 and MIDREX process flowsheet Figure 2.18. 58 modules operating and 19 nations are currently working on 4 modules. According to Masaaki *et al.* (2010), the MIDREX Process has a total annual capacity of 48.4 million tons.

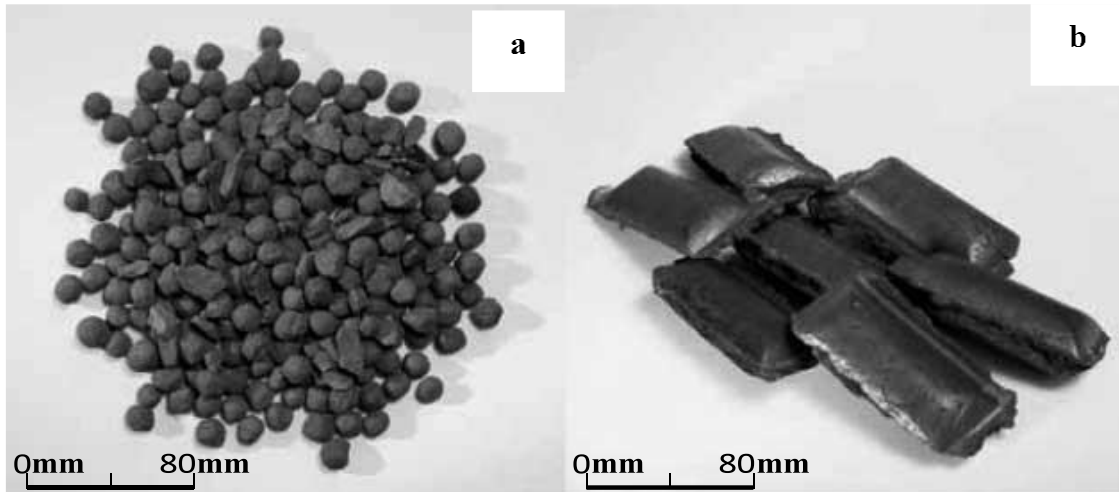
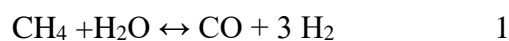


**Figure 2.16 Appearance of (a) Direct Reduced Iron and (b) Hot Briquetted Iron (Masaaki *et al.*, 2010)**



**Figure 2.17 World's MIDREX Plants (Masaaki *et al.*, 2010)**

The Midrex process differs from steam reforming in several ways. It reforms both carbon dioxide (CO<sub>2</sub>) and steam, with an oxidizer/carbon ratio of approximately 1:4, with sulfur present in the reformed gas feed, and operates at low pressure. Catalysts are required to increase the reforming reaction rate and thus achieve the required reducing gas (CO and H<sub>2</sub>) concentrations following the steam/CO<sub>2</sub> catalytic chemical reforming reaction of methane (Gines *et al.*, 2016)





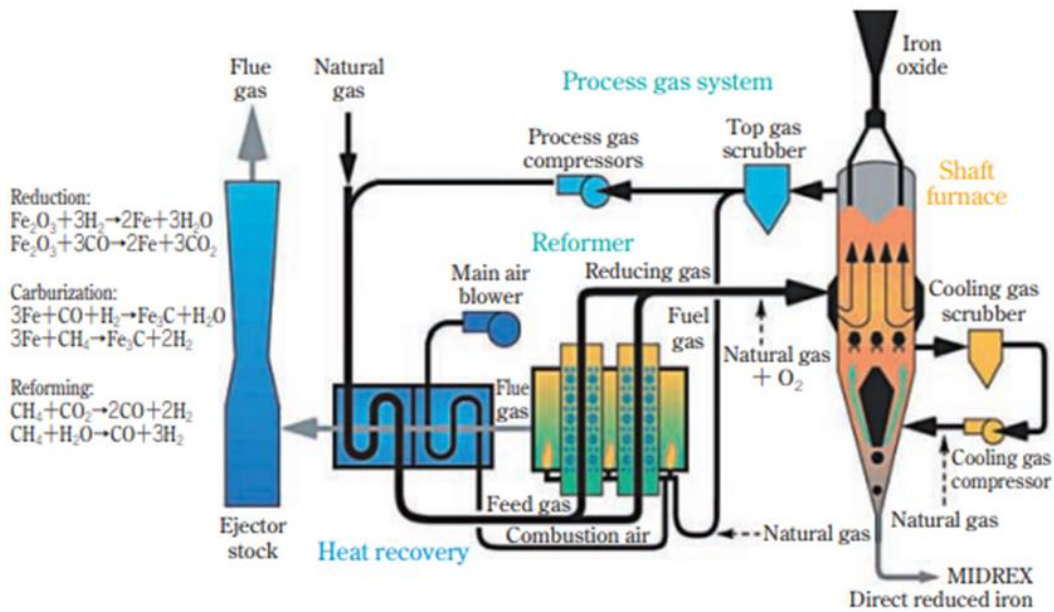


**Figure 2.18 MIDREX Process Flowsheet (Masaaki *et al.*, 2010).**

### *ITmk3 Process Technology*

The third significant development in steel production is ITmk3. Iron ore fines and pulverized coal are immediately separated from lump iron and slag by ITmk3. In comparison to the present, widely used blast furnace converter method, which is considered the first generation, and direct reduction procedures like MIDREX, which are considered the second generation (Gulhane, 2017).

Third-generation ironmaking is referred to as ITmk3. The ITmk3 process was created based on an original idea that combined iron ore and carbon technology to manufacture high-quality pig iron products (ITmk3 iron nuggets) from fine iron ore and pulverized coal. A pilot plant and a full-scale test plant were used for testing after the development phase started in 1996. The first industrial facility, which began manufacturing ITmk3 iron nuggets, was constructed in the USA. The reaction sequence of the ITmk3 takes roughly ten minutes. This method responds a great deal more quickly than the BF and DRI processes (Gulhane, 2017).

The time the feedstock spends in the furnace in a standard BF process is around 8 hours, whereas in the MIDREX process, the time it spends in the shaft furnace is only 6 hours (Kikuchi *et al.*, 2010). Blast furnace (BF) processes produce carbon-saturated pig iron at temperatures around 1,500 °C, whereas ITmk3 produces high-purity metallic iron at temperatures lower than those required for blast furnaces (Kikuchi *et al.*, 2010). Operational region of the Ironmaking process Figure 2.19.

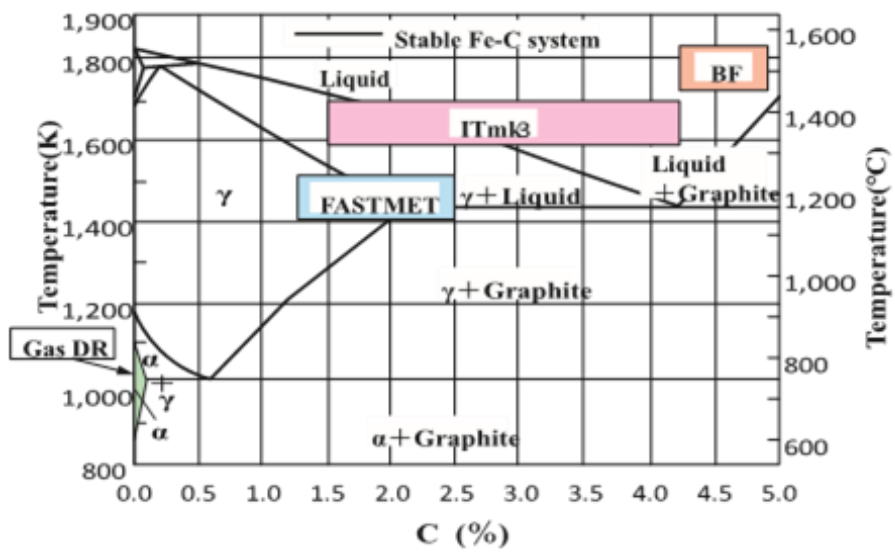


**Figure 2.19 Operational Region of Ironmaking Processes (Kikuchi *et al.*, 2010)**

*Advantages of the ITmk3 Process*

The process is simple and uses about 30% less energy than blast furnaces. Iron ore fines can be directly reduced using non-coking coal. No more sinter/pellet plants and oven batteries. A process that handles high-quality nuggets that are more soluble than pig iron during sheet manufacturing. Iron nuggets are slag-free and do not undergo re-oxidation. Low productivity and easy to transport. Foreign matter does not enter the nugget either. Specific composition values for the ITmk3 process are shown in Table 2.7. This process eliminates the need to handle molten iron. Manipulation and coordination by starting and stopping (Gulhane, 2017).

**Table 2.7 Specific Composition Values for the ITmk3 Process**

|                 |                   |
|-----------------|-------------------|
| Iron Ore fine   | 1.5 tons          |
| Non-coking coal | 0.5 tons          |
| Fuel gas        | 4.6 GJ            |
| Electric power  | 200 KWh           |
| Water           | 2 m <sup>3</sup>  |
| Air             | 85 m <sup>3</sup> |
| Nitrogen        | 12 m <sup>3</sup> |

(Source: Gulhane, 2017)

The functions of the ITmk3 process are summarised below:

- i. It is a simple process;
- ii. This enables the usage of lowgrade materials directly (e.g., fine ores and thermal coals that are not sintered or coked);
- iii. It's very energy efficient;
- iv. Low environmental impact;
- v. Changing production by starting and stopping is simpler;
- vi. Setup cost is low;
- vii. The majority of the equipment used in the procedure has been thoroughly tested and is very dependable; and
- viii. The plant is easy to operate without the need to handle molten iron, which is unprecedented in the steelmaking process. Therefore, mining company operators can operate the plant in the same way as a pelletising plant (Kikuchi *et al.*, 2010).

## 2.9 Steel Production

Steel is ubiquitous in modern society, but its production contributes to 7% of global CO<sub>2</sub> emissions. By 2050, the production of steel is expected to increase by 25–30%. The blast furnace (BF), which is the main way of generating iron, is an energy-intensive process that relies on the usage of fossil fuels (Holappa, 2020).

The conversion of iron oxide ore to molten iron is responsible for more than half of the CO<sub>2</sub> emissions from the manufacture of steel. The process of creating steel from iron ore (often hematite) and scrap is known as steelmaking. Pig iron is purified of impurities such as excess nitrogen, sulfur, silicon, phosphorus, and carbon, and alloying metals like nickel, manganese, vanadium, molybdenum, and chromium are added to the steel to give it distinct qualities. (Mondol, 2016).

One of the strongest materials on earth is steel. It influenced our civilisation and way of life while altering the path of history. However, today, scientists are modifying the molecular makeup of steel to forge new forms that may be stronger, wider, and higher than anything the world has ever seen.

It is an iron and carbon alloy. It is the most practical and affordable metal there is. Crystals make up steel, and crystal dislocations contribute to deformation. Steel is resilient and has a high compressive and tensile strength. Each patch of the patchwork-like steel is a crystal. These crystals include regular arrangements of iron atoms (Mondol, 2016).

In all industrial sectors, steel is a product that is used. The amount of crude steel produced worldwide in 2016 was roughly 1,629 billion tons. After China, the European Union is the world's second-largest producer of steel. With about 42.1 million tons, Germany comes in seventh. The blast furnace pathway (Blast Furnace Basic Oxygen Furnace - BOF) is used in integrated mills to smelt about two-thirds of the world's crude steel into oxygen steel. The remaining third is produced using electric arc furnaces (EAFs) for steelmaking (Odenthal, 2017). The Steelmaking process chain Figure 2.20.

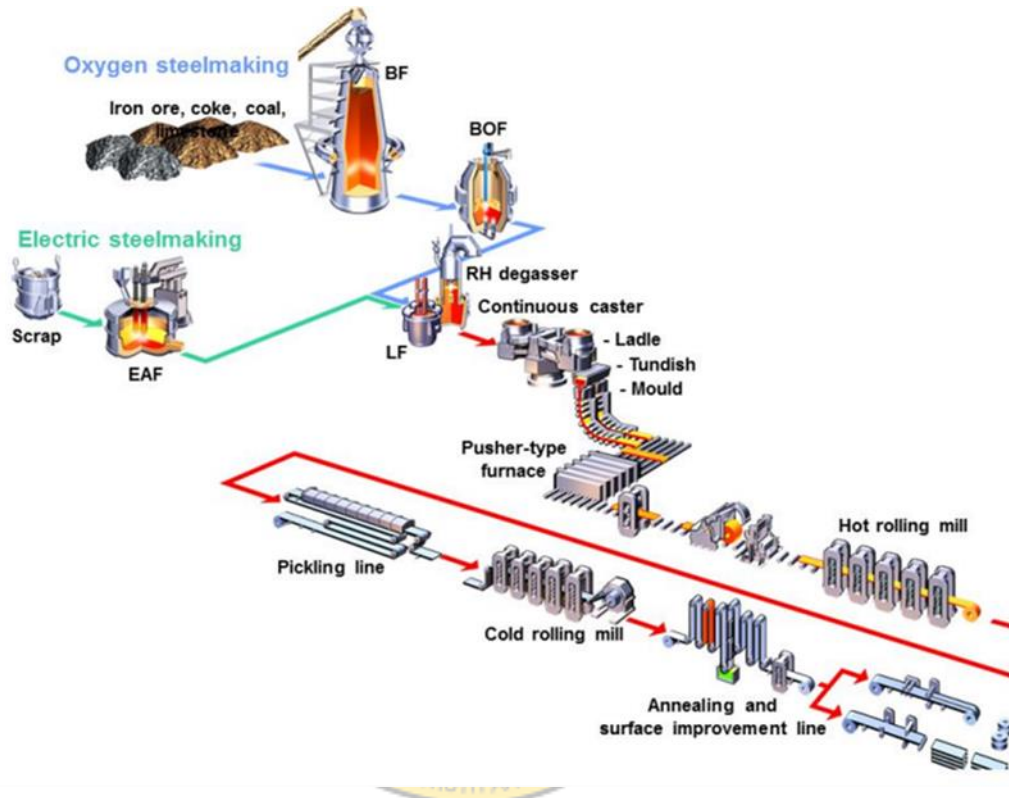


**Figure 2.20 Chain of the steelmaking process; routes for producing oxygen steel along the blast furnace (BF) and basic oxygen furnace (BOF); routes for producing electric steel along the electric arc furnace (EAF) (Odenthal, 2017)**

Both industrialized and emerging nations depend on steel as a material. Steel is a crucial raw material in the shift to renewable energy since it is used in variable degrees to make electric vehicles, solar panels, and wind turbines. To achieve the global climate protection goals, the steel industry's emissions must be decreased by at least 50% by 2050 (Dawkins *et al.*, 2023).

The sector now accounts for 7% of the energy sector's CO<sub>2</sub> emissions (including process emissions) and around 8% of the world's ultimate energy demand. Iron ore and steel scrap recycled from other products are the two main metals used in the production of steel. Iron

ore accounts for 70% of the total metal input for steel manufacturing globally; the remaining 30% is scrap (IEA. Iron and Steel Technology, 2020). The top steel producers and estimated share in 2019 are shown in Table 2.8.

The annual global production of steel is currently over 1.7 billion tons. One of the following technologies, Blast Furnace or Basic Oxide Furnace (BF-BOF), Direct Reduction of Iron in Electric Arc Furnace (DRI-EAF), or Electric Arc Furnace is used to create steel from iron ore. Direct smelting of scrap in an iron basic oxide furnace (SRI-BOF) for iron smelting and reduction (Dawkins *et al.*, 2023).

The World Steel Association identified 104 steel companies in 2019, accounting for 0.2% of global production, and producing more than 3 million tonnes annually. Just over a quarter of worldwide production is produced by the top 10 corporations, compared to 42% and 56% for the top 25 and top 50 (Anon, 2020).

There are two steps in the production of steel. Processes include the Electric Arc Furnace (EAF) and Basic Oxygen Furnace (BOF). In the converter process, impurities such as carbon, silicon, and phosphorus are removed by blowing oxygen into molten iron. To accomplish this, these elements undergo chemical reactions to oxidise and produce gaseous by-products. The steel grade and desired composition are further improved by adding steel scrap (Siddiqui, 2023).

**Table 2.8 Leading Steel Producers and Projected Market Share for 2019**

| <b>Rank</b> | <b>Company</b>           | <b>HQ</b> | <b>2019 Output (Mt)</b> | <b>Share of Global Output (%)</b> |
|-------------|--------------------------|-----------|-------------------------|-----------------------------------|
| 1           | ArcelorMittal            | Luxemburg | 97.3                    | 5.2%                              |
| 2           | China Baowu Group        | China     | 95.5                    | 5.1%                              |
| 3           | Nippon Steel Corporation | Japan     | 51.68                   | 2.8%                              |
| 4           | HBIS Group               | China     | 46.6                    | 2.5%                              |
| 5           | POSCO                    | Korea     | 43.1                    | 2.3%                              |
| 6           | Shagang Group            | China     | 41.1                    | 2.2%                              |
| 7           | Ansteel                  | China     | 39.2                    | 2.1%                              |
| 8           | Jianlong Group           | China     | 31.2                    | 1.7%                              |
| 9           | Tata Steel Group         | India     | 30.2                    | 1.6%                              |

|        |                |       |      |      |
|--------|----------------|-------|------|------|
| 10     | Shougang Group | China | 29.3 | 1.6% |
| Top 10 | –              | –     | 505  | 27%  |
| Top 25 | –              | –     | 785  | 42%  |
| Top 50 | –              | –     | 1049 | 56%  |
| Total  | –              | –     | 1869 | 100% |

(Source: Anon., 2020)

Iron alloy products and their by-products are characterised by the principle of “reduce, reuse, and recycle”, making steel a particularly recyclable raw material. Steel is an alloy of iron containing less than 1% carbon. By refining iron ore through a series of processes, integrated steel mills produce very high-quality steel with a tightly controlled chemical composition that meets all product quality standards. Flowchart of Iron and Steelmaking Processes Figure 2.21

The LD converter converts the carbon in the pig iron into carbon monoxide by blowing in pure oxygen to produce steel. The converter is fed with pig iron, scrap iron, ferroalloys, lime, and iron ore. Oxygen is blown into the converter via a lance. Using iron ore as a coolant significantly changes the proportion of pig iron scrap (Agrawal and Pandey, 2005).

Blowing high-purity oxygen into the furnace mainly oxidises and removes carbon and silicon in the hot metal. Fluxes are injected into the basic oxide furnace to remove siliceous impurities (Agrawal and Pandey, 2005).

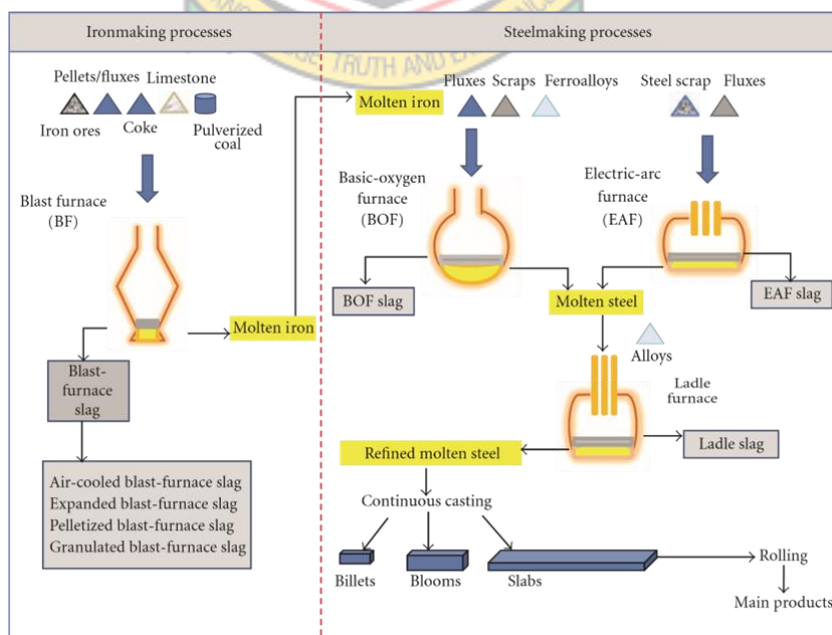


Figure 2.21 Iron and Steelmaking Processes Flowsheet (Yildirim and Prezei, 2011)

The qualities of the steel may also be improved by the addition of specific alloying components, fumes, and gases, including carbon monoxide (CO) gas and small particles of the charged materials, which are produced during the oxygen-blowing process (Agrawal and Pandey, 2005).

### 2.9.1 Basic Oxygen Furnace

The BOF process is commonly used in large-scale steel production, especially in integrated steel mills. Steel scrap is melted during the EAF process using arcs produced by graphite electrodes (Siddiqui, 2023). Steel is frequently created in basic oxygen furnaces (BOFs) using heated metal. Process automation is frequently insufficient and not at its best.

In the world, the Basic Oxygen Furnace (BOF) is responsible for producing about 70% of the steel. Scrap and hot metal are fed into the BOF, and a supersonic jet of oxygen is shot into the metal bath's surface from above through a lance. The oxidation of certain species in the metal bath causes a less dense slag layer. To prevent refractory wear and to aid in the development of slag, flux is supplied. Carbon monoxide can be created when iron oxide in the slag and carbon in the metal droplets react (Dering *et al.*, 2020).

Molten iron and iron scrap produced in the integrated steelworks' blast furnace are fed into the basic oxygen furnace, which is connected to it. An appropriate basic oxygen furnace charge typically consists of 80–90% molten iron and 10–20% scrap iron. Iron scrap in the basic oxygen furnace charge is crucial for cooling the furnace and preserving the temperature needed for the required chemical reactions to take place, which is between 1600°C and 1650°C (Yildirim and Prezei, 2011).

### 2.9.2 Electric Arc Furnace (EAF)

The electric arc furnace used to make steel was invented by Paul Héroult in 1889. The advent of large-scale electrical energy production around the turn of the 20th century coincided with the emergence of new technologies. Furnaces from the first generation ranged in capacity from 1 to 15 tons. Siemens-Martin furnaces and Bessemer/Thomas converters were at first EAF's main rivals. However, it specialises in the fabrication of specialty steels that need to be melted at high temperatures, over an extended period, and using ferroalloys. When billet casting initially gained popularity in the 1960s, EAF represented a new niche industry (Madias, 2014)

It is the perfect melting unit, according to (Madias, 2014), for so-called mini-mills feeding billet casters for the production of wire and rebar. To better support the quick tap-to-tap

times needed by billet casters, the EAF was developed as a specialized refining machine throughout the following two decades.

Steel cleaning operations were carried out in newly installed ladle furnaces. Using foam slag technology, large transformers have been built and ultra-high-power reactors have been created. As a result, the duration between taps got closer to the casting time. By 1985, new markets for the production of electrical steel included thin slab casting and direct rolling flat goods. This process route plays an important role in global steel production, reaching almost 26% share in 2014 (Madias, 2016).

The primary raw material used in the electric furnace method is recycled steel, as opposed to the converter furnace method, which primarily employs iron ore. The scrap is heated by the arc, and other alloys and fluxes can be added to change the steel's chemical makeup. The EAF process is better suited for small-scale steel production especially steel grades because it is more adaptable, effective, and ecologically benign.

When the steel has been polished, it is cast into various shapes such as slabs, blooms, and billets depending on the application. The final stages of the steelmaking process involve various finishing treatments to improve steel properties and meet specific customer requirements. These treatments include heat treatment, rolling, forging, coating, and surface finishing. Heat treatment processes such as quenching and tempering can improve the hardness, strength, and ductility of steel. Cast steel is deformed through rolling, forging, and forming processes (Siddiqui, 2023). A schematic representation of the electric arc furnace steelmaking and ladle refining process Figure 2.22.

Up to 300 tons of steel can be produced by electric arc furnaces in a single cycle, which lasts 1-3 hours. Initially, only high-quality steel was made using the electric furnace method because it was more expensive than using a converter. However, when electric furnaces grew in size over time, they became more competitive in producing different steel grades and started to rule the U.S. steel industry, making up 55% of all steel produced in 2006 (USGS Geological Survey, 1993–2006)



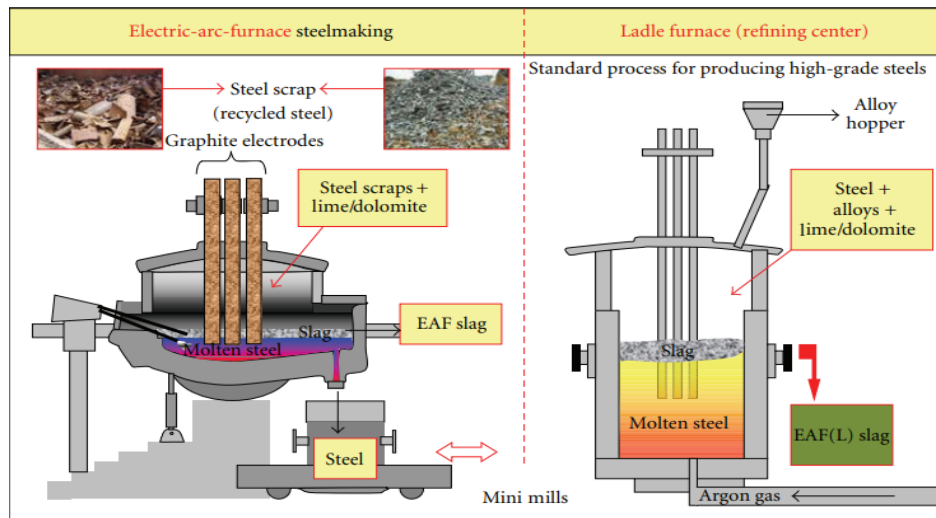


**Figure 2.22 Schematic Representation of the Electric-Arc-Furnace Steelmaking and Ladle Refining Process (Yildirim, and Prezzi, 2011)**

### 2.10 Pelletising

Pellets are balls made by rolling wet iron ore concentrate and fines with additives and binders in horizontal drums or inclined discs. The fines can have a variety of mineralogical and chemical compositions. (Moraes *et al.*, 2018).

Since one of the most important plants in the steel production chain is the iron pelletising plant, any improvement in the final production of this plant, i.e., iron pellets, is desirable and increases the productivity of the steelmaking process (Nakhaeinejad and Zarei, 2020).

The iron pellets were created by combining carbonaceous material and ore with corresponding percentages of 28% and 70%. The remaining 2% consists of wheat flour, which primarily enhances the binding properties of the formed pellets. If no admixture of carbonaceous material is required, the 28% mentioned becomes 100% equivalent, all other percentages were calculated from the equivalent mass of 28% representing the percentage of the pellet said to be reductant (Aakyiir, and Dankwah, 2017).

The three basic stages of the pelletising process are illustrated in Figure 2.23, and the process of producing Iron Ore pellets in Factories Figure 2.24. Currently, worldwide installed pelletising capacity is estimated at 480.7 million tonnes per year (Tuck and Virta, 2011).

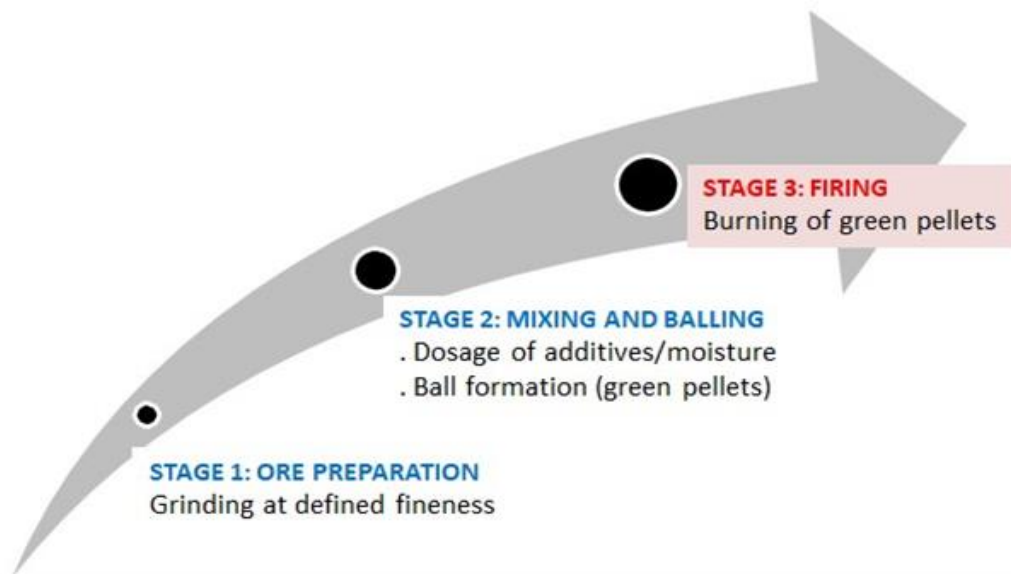


**Figure 2.23 Three (3) Basic Stages of the Pelletising Process (Mourao, 2022)**

There are three key processes in the process of pelletising iron ore:

- i. Preparation and mixing of pelleted feed: Raw materials (iron ore concentrate, additives - anthracite, dolomite - and binders) are prepared in terms of particle size and chemical specifications and fed to the pelletising process;
- ii. Balling process: green pellets are pellets that are rolled without heat treatment. Obtained under strict moisture control, it is spherical with a diameter of 8-16 mm; and
- iii. Process of Hardening: To meet physical and metallurgical requirements for handling, transportation, and ultimate use, green pellets are hardened in a high-temperature process with regulated heating rates.

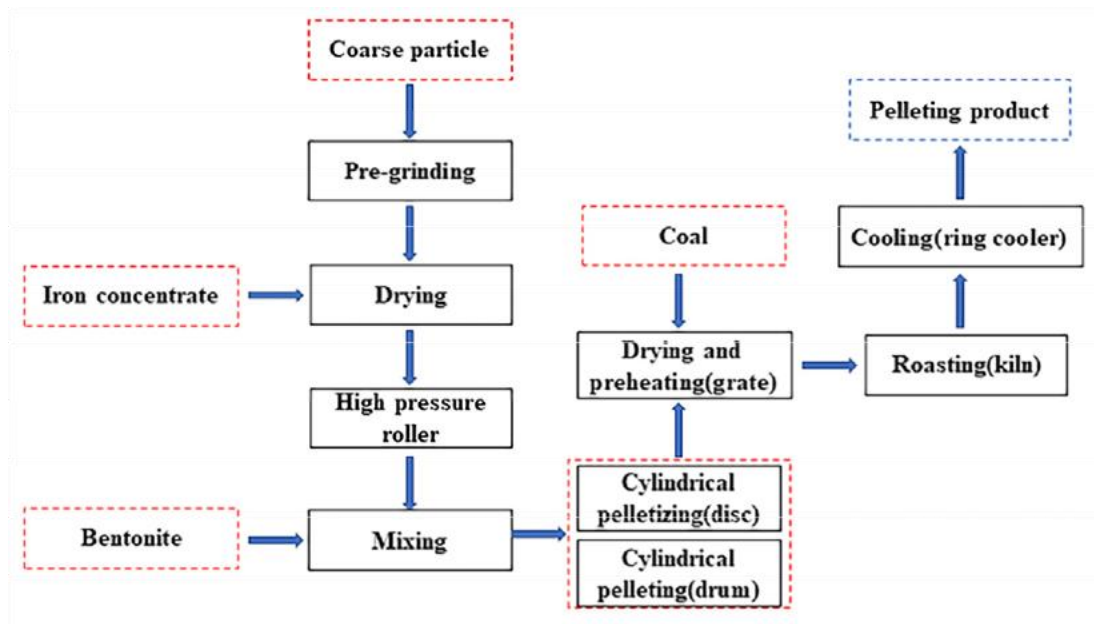


**Figure 2.24 Process Flowsheet of Producing Iron Ore Pellets in Factories (Zheo *et al.*, 2022a)**

### 2.10.1 Pelletising Binder

The iron ore pelletising binder is a very important factor as it controls both the green and hardened pellet properties. Bentonite has been the preferred choice for iron ore pellets since the beginning because of its excellent bonding properties, heat resistance, abundant availability, ease of handling, non-toxicity, and low toxicity in both fresh and dry pellets over the entire operating temperature range. It has been used as a binder. However, since bentonite is rich in silica and alumina, the gangue content ( $\text{SiO}_2$  and  $\text{Al}_2\text{O}_3$ ) in iron ore pellets increases proportionally with bentonite addition (Pal *et al.*, 2022).

The creation of iron ore pellets also requires the use of a pelletizing binder, which is crucial to the process of smelting metals. This considerably quickens the pelletization process, enhances the raw and dried pellet quality, and gets rid of pellet contamination. (Zhao *et al.*, 2022), (Forsmo, *et al.*, 2006). After long-term development, pelletising binders were gradually formed into inorganic binders, organic binders, and composite binders (Zhao *et al.*, 2022).

### 2.11 Microwave Technology

The most recent method of producing thermal energy is microwave technology, which works by rotating and moving polar molecules quickly against one another. The matter experiences thermal, electric field, and various non-thermal effects as a result of the microwave irradiation. Heat is created when electromagnetic energy is converted to thermal

energy by the thermal effect. Dipole molecules are rotated and polarized by non-thermal forces, which raises the frequency of intermolecular collisions and causes heat to be transferred from the material's core to its exterior through friction (Hu *et al.*, 2021).

Several researchers have demonstrated the effectiveness of microwave technology as a technological approach to iron ore reduction and other applications (Aguilar and Gomez, 1997; Dankwah *et al.*, 2015; Dankwah *et al.*, 2016).

Microwave reduction technology is a new phenomenon intended to address some of the environmental concerns associated with traditional blast furnace metal production. A major factor behind the use of microwaves in the steel industry is their potential to significantly reduce carbon footprint. It relies on the ability of metal oxides or carbonaceous reductants, or both, to absorb microwave energy and heat rapidly to temperatures sufficient for metal oxide reduction (Aakyiir and Dankwah, 2017). Microwave in operation Figure 2.25.



**Figure 2.25 Microwave in Operation (Aakyiir and Dankwah, 2017)**

### **2.12 End-of-Life Tyres (ELTs)**

Currently, less than 20% of end-of-life rubber tyres (ELTs) are recycled globally and it has been estimated that 4 billion ELTs are currently held in various stockpiles across the globe (Dankwah, 2018)

In recent decades, the global growth of the automotive industry and the increased use of automobiles as a primary means of transportation have led to a significant increase in tire production. As a result, our inventory of used tires has grown exponentially. Scrap tires

consist of components that cannot be decomposed under ambient conditions (Ganjian *et al.*, 2009).

From 324 million new tires sold in Europe in 2020, 89.5% (70% by weight) for passenger cars and light commercial vehicles and 4.9% (20% by weight) for heavy vehicles (trucks and buses), 3.6% (1% by weight) for motorcycles and scooters, and 1.9% (9% by weight) for agricultural and off-road vehicles (European Tire and Rubber Manufacturers Association, Statistical Report, 2021). Various sections of a scrap tire are shown in Figure 2.26.

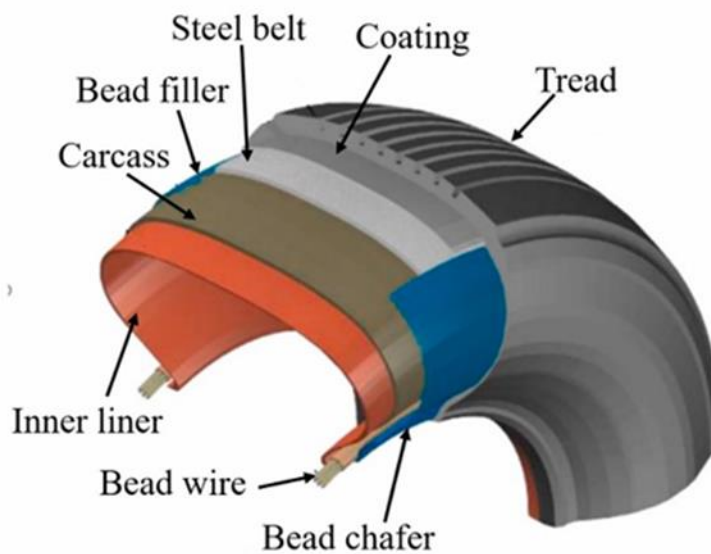


**Figure 2.26 Typical Tyre Structure (Source: Xiao *et al.*, 2022)**

There are currently 4 billion ELTs in stock worldwide, with more than 1 billion being added each year (Dankwah and Koshy, 2013).

ELT outbreaks are dangerous to both the environment and people's health as they become breeding grounds for disease-carrying mosquitoes and rodents, and fires can be caused by lightning strikes and arson (Dankwah and Koshy, 2013). Previous investigators' work showed that ELT contains large amounts of carbon and hydrogen, which can be recovered to reduce iron oxides and induce slag foaming in electric steelmaking (Dankwah *et al.*, 2012); (Dankwah and Koshy, 2013); and (Dankwah, 2018).

### 2.13 Pyrolysis of End-of-life Tyres (ELTs)

One of the eco-friendly methods for waste valorization is the pyrolysis of polymeric wastes, such as used plastic bottles, rubber tires, and pure water sachets. To lower the time, money, and energy costs associated with the pyrolysis process, however, ongoing efforts must be made (Akinbomi *et al.*, 2022).

Pyrolysis is the thermal degradation of organic materials at high temperatures, typically between 400 °C and 800 °C, in an inert environment (lack of oxygen). Nitrogen is often injected into the system to maintain the inert environment, but steam or hydrogen can also be employed. The feedstock dehydrates, cracks, isomerizes, dehydrogenates, aromatizes, and condenses as a result of the volatilization and breakdown reactions brought on by heating. As a result, solid materials are transformed into volatile gases and a carbonaceous solid residue (char), which is mostly made up of inorganics (metals, salts, etc.) and fixed carbon (Costa *et al.*, 2022). Schematic representation of pyrolysis Figure 2.27.

Pyrolysis is an effective conversion method, and it also provides several economic and social advantages as a waste tire processing technology (Jahirul *et al.*, 2021). Due to its nature and condensed processing steps, the pyrolysis process is thought to be the most environmentally friendly among comparable thermochemical processes.

The solid is broken down during the process at a significant temperature of between 300 and 900 °C in an atmosphere devoid of oxygen, resulting in the production of char, oil, and gas. H<sub>2</sub>, CO, CO<sub>2</sub>, and CH<sub>4</sub> are frequently important pyrolysis gas byproducts, although H<sub>2</sub>O and CH<sub>3</sub>OH make up most of the liquid. The remaining solid products are made up primarily of carbon and ash (Jahirul *et al.*, 2021). Pyrolysis process flowsheet Figure 2.28.

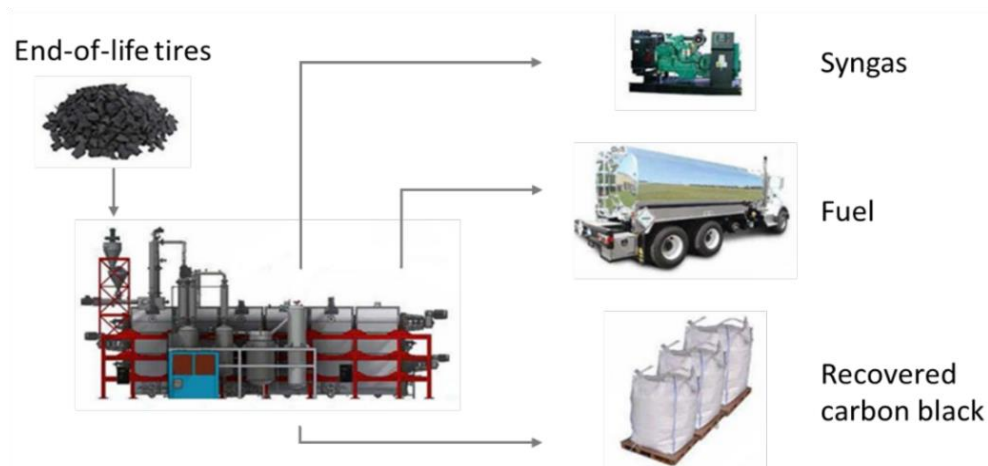


**Figure 2.27 Schematic representation of the ELTs pyrolysis and ensuing products (Costa *et al.*, 2022)**

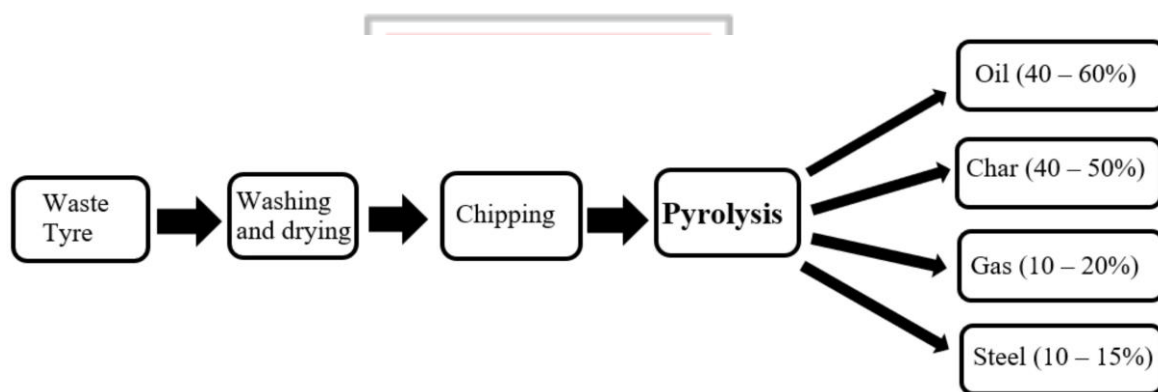


**Figure 2.28 Pyrolysis process flowsheet (Jahirul *et al.*, 2021)**

### Tyres Pyrolysis Reactor

The reactor is the key component of the pyrolysis procedure, which entails the oxygen-free degradation of used tire waste. Numerous studies on the pyrolysis reactor have focused on the key variables of heating methods and rates, waste tyre feeding, pyrolysis residence time, vapor condensation, and product collection. Fixed-bed, vacuum, fluidized bed, moving screw bed, rotary kiln, and other reactor types are being investigated for waste tyre pyrolysis (Jahirul *et al.*, 2021).

The fixed bed pyrolysis reactor, as depicted in Figure 2.29, is easily built and effective in generating clean fuel. The majority of the time, these reactors are run in batch mode. The used tire is fed into a fixed bed within a steel pyrolyser that is cylindrical. A mounted electrical heater or furnace provides heat to the waste tire through the pyrolyser wall. All of

the oxygen inside the pyrolyser is removed by purging pressurized nitrogen (N<sub>2</sub>) from the exterior cylinder (Jahirul *et al.*, 2021).

Solid char from decomposing waste tires builds up at the pyrolyser's bottom, while vapor (both condensable and non-condensable) escapes to the top. The oil is then kept and collected in a liquid storage container after the vapour is cooled by a condenser, which condenses the condensable vapour into the oil. The gaseous, non-condensable vapour is recovered as syngas. Fixed bed reactors have a longer solid residence duration, lower gas velocity, lower gas carryover rate, and a higher carbon conservation rate (Jahirul *et al.*, 2012).

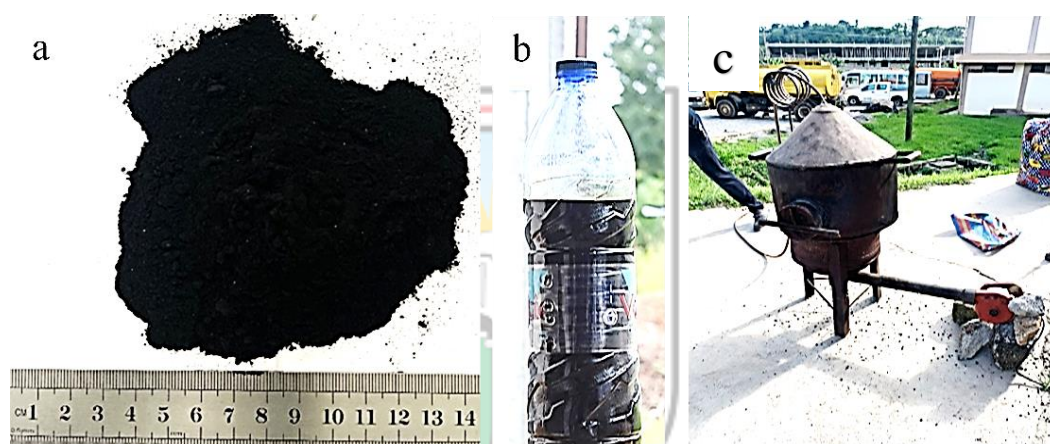


**Figure 2.29 (a) Pulverised Carbonaceous Material (b) Liquid Fuel Obtained From (ELTs) (c) Pyrolysis Reactors (Source: Author's Construct, 2023)**

The proximate analysis Table 2.9 for the End-of-Life Tyres (ELTs) was determined by some researchers.

**Table 2.9 Proximate Analysis of End-of-Life Tyres**

| Author                           | Component (wt %) |              |          |       |       |
|----------------------------------|------------------|--------------|----------|-------|-------|
|                                  | Volatile         | Fixed Carbon | Moisture | Ash   | Steel |
| Abotar and Dankwah (2020)        | 61.67            | 29.88        | 0.85     | 7.6   | -     |
| Juma <i>et al.</i> , (2006)      | 61.61            | 22.66        | 1.72     | 14.01 | -     |
| Rodrigues <i>et al.</i> , (2001) | 58.8             | 27.7         | -        | 3.9   | 9.6   |

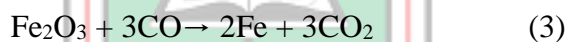


|                                   |         |       |      |       |     |
|-----------------------------------|---------|-------|------|-------|-----|
| Lee <i>et al.</i> , (1995)        | 67.3    | 28.5  | 0.5  | 3.7   | -   |
| Chang <i>et al.</i> , (1996)      | 62.32   | 26.26 | 1.31 | 10.29 | -   |
| Gonzales <i>et al.</i> , (2001)   | 61.9    | 29.2  | 0.7  | 8.0   | -   |
| Chen <i>et al.</i> , (2001)       | 93.73** | -     | 0.54 | 5.3   | -   |
| Loresgoiti <i>et al.</i> , (2004) | 59.3    | 27.6  | -    | 3.5   | 9.6 |
| Orr <i>et al.</i> , (1996)        | 68.7    | 23.3  | 0.4  | 7.6   | -   |
| Williams and Bottrill, (1995)     | 66.5    | 30.3  | 0.8  | 2.4   | -   |
| Atal and Levendis, (1995)         | 58.7    | 33.6  | -    | 7.7   | -   |

(Abotar *et al.*, 2020)

### 2.14 Reduction of Iron Oxide

One of the biggest problems we have today is attempting to reduce the effects of global warming. One of the most significant pillars of our society and technology is the manufacture and usage of iron and steel, but due to the redox reaction, it also produces the most greenhouse gas emissions. In addition,



contributes to the present reduction technology. 1.85 to 2.1 tonnes of carbon dioxide are produced during the manufacturing of 1 tonne of steel (Pineau *et al.*, 2006), (Patisson and Margaux, 2020).

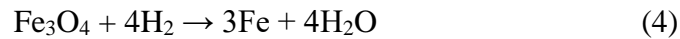
Iron ore mined from mining areas with an iron content of 56% or more is used for industrial purposes, while iron ore with low iron content is sorted in its ore state. In recent years, some researchers have attempted to study low-grade ores instead of high-grade ores (Chandio *et al.*, 2023).

Iron ore mined from mining areas with an iron content of 56% or more is used for industrial purposes, while iron ore with low iron content is sorted in its ore state. In recent years, some researchers have attempted to study low-grade ores instead of high-grade ores (Chandio *et al.*, 2023).

Currently, iron is primarily produced by reducing iron oxide. An H<sub>2</sub>/CO gas mixture is used in the so-called direct reduction process to transform iron ore into metallic iron. The

reduction behavior of iron oxides is a commonly researched subject in ferrous metallurgy as a result of the significant economic significance of iron (Gamisch *et al.*, 2022).

In general, the steam ironing process can be viewed as a heterogeneous non-catalytic gas-solid reaction and the charging and discharging stages should be considered separately. The endothermic charging stage, where the reduction of magnetite (Fe<sub>3</sub>O<sub>4</sub>) to Fe occurs, can be explained as follows:



Fe<sub>3</sub>O<sub>4</sub> is reduced by hydrogen first to wustite (also known as FeO), and subsequently to Fe. H<sub>2</sub> is oxidized during the process, resulting in water vapor. The comparable oxidation process is given by and also adheres to the two-step reaction principle:



The theoretical maximum storage of H<sub>2</sub> in Fe can be calculated as 4.8 weight percent using the mass ratio of H<sub>2</sub> and Fe in Eqs. (2) and (3). This is equivalent to 1.6 kWh (Kg of iron) of gravimetric energy storage density (ESD) (Gamisch *et al.*, 2022).

#### 2.14.1 Reduction of Iron Oxide by Carbon

Steelmaking is an energy-intensive process, consuming 70% of a steel company's total energy (Zhang, 2005). Most of the heat needed to make molten iron is typically provided by burning coke, but the price of coke continues to rise as the supply of coking coal dwindles. Additionally, iron production is one of the world's largest carbon-emitting industries. Carbon emissions from the steel industry are expected to continue increasing as pig iron production increases unless new energy sources are developed, and current steelmaking processes are significantly improved.

Renewable and carbon-neutral resources include biomass. The use of biomass energy in industry can reduce CO<sub>2</sub> emissions and fossil energy consumption. Abundant biomass resources can replace coke and charcoal in the steelmaking process. It has been reported that biomass is used in the sintering of iron ore, blast furnaces, and some innovative steelmaking processes (Zandi *et al.*, 2010; Ueda *et al.*, 2009).

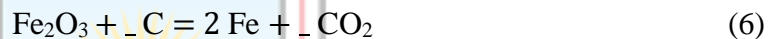
It has been demonstrated that iron ore can be reduced to iron by biomass in fluidized or fixed beds. These are all short steelmaking processes that consume less energy and are less

polluting than the blast furnace process. Iron production from biomass is expected to develop rapidly in the future (Wei *et al.*, 2016)

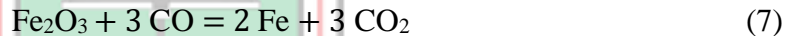
#### 2.14.2 Reduction of Iron Oxide by Hydrogen Gas

Climate change is the main reason why employing hydrogen as a reductant is a good idea. The steel sector is responsible for 4% to 7% of the world's anthropogenic CO<sub>2</sub> emissions. This is due to the nearly complete reliance on carbon (coal or coke) for the energy and chemical reduction required along the steelmaking process, with the blast furnace being the major contributor (Patisson and Mirgaux, 2020). In the blast furnace, solid iron ore in the form of sinter or pellets is converted into liquid pig iron.

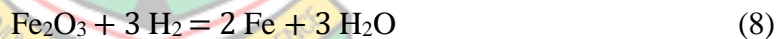
The majority of iron ores are oxides, often hematite Fe<sub>2</sub>O<sub>3</sub>, and CO<sub>2</sub> is produced when iron oxide is chemically reduced to iron oxide by C (or by CO generated from C or CH<sub>4</sub> to (FeO) (Patisson and Mirgaux, 2020). The fundamental idea of hydrogen ironmaking is to replace the C (or CO) reductant with H<sub>2</sub>, replacing:



or



with



Thus, in the chemical reduction process, harmless H<sub>2</sub>O is released in place of the greenhouse gas CO<sub>2</sub>. It is possible to produce steel with zero carbon content utilizing a hydrogen-based reduction process that uses hydrogen as the reductant rather than carbon (Siddiqui, 2023).

The clean ironmaking method known as hydrogen-based direct reduction (HyDR) uses hydrogen gas in place of coal to produce water instead of carbon dioxide. Although the HyDR process looks simple, its endothermic chemistry requires the reaction to be carried out at high temperatures (above 1000 °C), slowing commercialization (Bhaskar *et al.*, 2020).

However, above 800 °C, hydrogen is preferred to carbon monoxide due to thermodynamics, and at 850 °C, the rate of reduction by H<sub>2</sub> is significantly higher than that of CO (Spreitzer and Schenk, 2019).

Hydrogen reduction is a promising replacement for traditional fossil fuels and is best accomplished with the use of renewable energy. A significant amount of hydrogen may be

used in direct reduction procedures, which convert iron ore to metallic iron without the aid of a liquid phase. Consequently, it is feasible to lower the resulting carbon dioxide emissions. The direct carbon emissions from the usage of fossil fuels worldwide are 7% to 9% attributable to the steel production industry. For a single industrial sector, this is excessive (Spreitzer and Schenk, 2019).



## CHAPTER 3

### EXPERIMENTAL WORK

#### 3.1 Material Used

From previous experimental work conducted by (Abotar *et al.*, 2020), samples of End-of-Life vehicle tyres used for forming the carbonaceous material that was used in this research work were collected from a vulcanising shop opposite the University of Mines and Technology, (UMaT) main gate. The Carbonaceous material that was generated from these End-of-life vehicle tyres serves as the main reducing agent for this research work. The fixed carbon content of the carbonaceous material was 29.88 Wt%. This is illustrated in Table 2.9 in the literature review.

The iron ore utilised in this research was obtained from Mt. Gangra, Liberia. The iron ore consists of the low-grade and transition zone. Both were used for the reduction study.

Four boulder samples comprising Oxide, Fresh, Transition High-grade, and Transition Low-grade were used for petrographic studies in this research work.

#### 3.2 Apparatus Used

The whole experiment was done at the Minerals Engineering Laboratory, and the Geological Engineering Petrographic Laboratory of the University of Mines and Technology, Tarkwa, Ghana. The equipment used in executing the research was:

- i. Hammer;
- ii. Cone Crusher and Marcy GY-Roll Crusher;
- iii. Ball Mill of diameter 30 cm and length 23 cm;
- iv. Tumbling Mill;
- v. Riffle Sampler;
- vi. ASTM-E11 Screens;
- vii. Electronic Measuring Scale;
- viii. Firing reactor;
- ix. MWM200 AKAI Microwave Oven;
- x. Wash bottle ;
- xi. Cutter;
- xii. Polisher;
- xiii. Petrographic Microscopes (LEICA DM 2700P); and
- xiv. HSMAG Neodymium Magnet



### 3.3 Methods Used

The following outlined methods were used in carrying out this research:

- i. Iron Ore Sampling and packaging;
- ii. Samples Preparation;
- iii. Reduction Studies;
  - a. Estimating the masses and blend for the various raw materials;
  - b. Firing; and
  - c. Determination of the percent weight lost.
- iv. X-Ray Fluorescence (XRF) Analysis;
- v. Scanning Electron Microscopy- Energy-dispersive X-ray Spectroscopy (SEM-EDS) Analysis;
- vi. X-Ray Diffraction (XRD) Analysis; and
- vii. Petrographic Studies

#### 3.3.1 Iron Ore Sampling and Preparation

Representative Low-grade and transition ore samples were collected from Gangra Pit-3 top at GPS coordinates (540465 Eastern, 834083 Northern Elevation 830 RL) and (540243 Eastern, 834106 Northern, Elevation 835RL) respectively. These samples were dispatched to the ArcelorMittal Liberia Mine laboratory for X-ray fluorescence (XRF) analysis. The representative samples were crushed by a roll crusher and sent for further processing. The sample results were released after six (6) hours. Lastly, the samples were packaged and placed in a non-metallic container to avoid contamination.

#### 3.3.2 Iron Ore Preparation

The Ore samples were sent to the Minerals Engineering Laboratory of the University of Mines and Technology (UMaT), Ghana, for metallurgical processing. The iron ore samples were crushed into a smaller lump using a hammer. The smaller lumps were subjected to further crushing stage with the aid of a cone crusher. Products obtained from the cone crusher were subjected to roll crushing. The material produced from the roll crushing process was pulverised in a ball mill until 80% of the milled materials (pulverised sample)

were able to pass through the 150 microns screen. This particle size distribution is often considered optimal for subsequent processing steps, such as flotation or leaching, as it enhances the separation of the valuable minerals. Representative samples of the unpulverised and pulverised iron Ores that were processed are shown in Figure 3.1

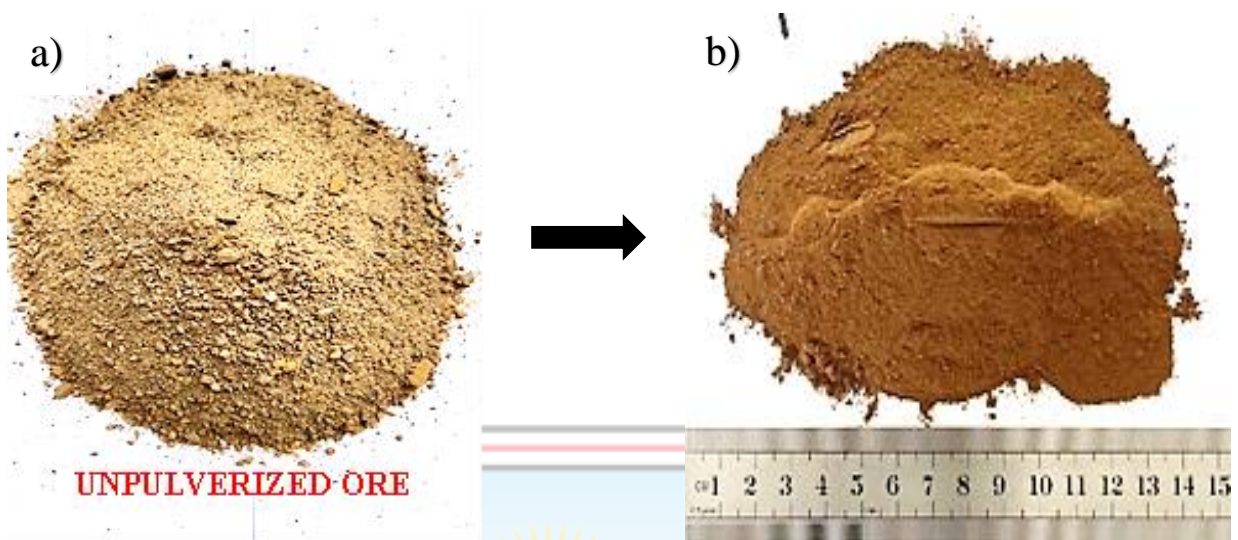


**Figure 3.1 (a) Unpulverised Iron Ore (b) Pulverised Iron Ore (Source: Author's Construct, 2023)**

### 3.3.3 Pellets Formation

Iron ore, reducing agent, and flour were combined at a ratio of 70%, 28%, and 2% respectively to form a composite pellet of mass 30 grams. Expressing the percentage ratio into weight means that every 30 grams of pellet formed will comprise 21 grams of iron ore, 8.4 grams of a reducing agent, and 0.6 grams of flour acting as a binder. The materials used in this experiment's chemical makeup Figure 3.2, and newly formed pellets are illustrated in Figure 3.3

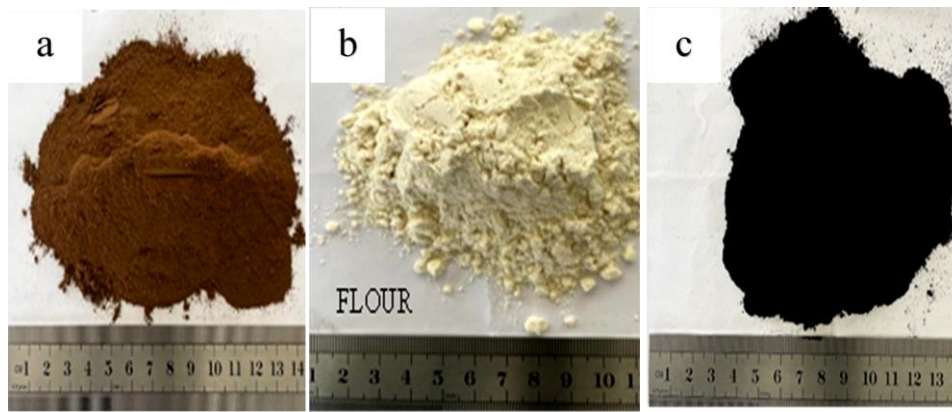


**Figure 3.2 Pellet Composition Comprising of (a) Iron Ore (b) Baking Flour (c) Carbonaceous Char (Source: Author's Construct, 2023)**

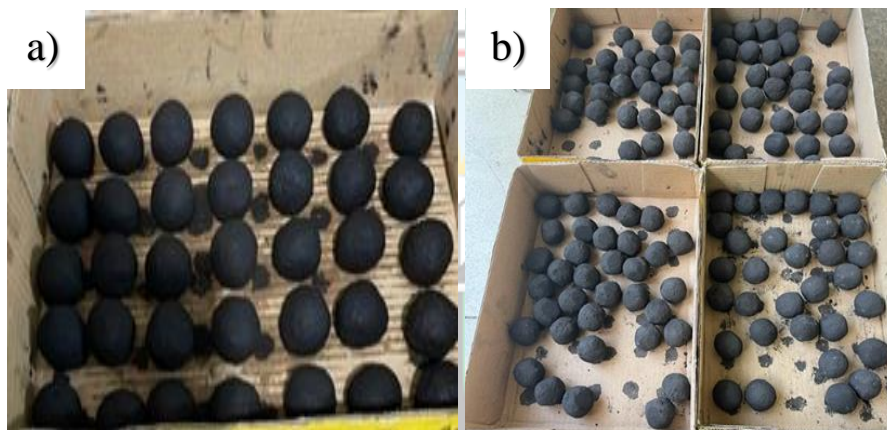


**Figure 3.3 (a) Newly Formed Pellets (b) Dried Pellets (Source: Author's Construct, 2023)**

### *Drying of Pellets*

Each material was deposited into a plastic bowl after it had been individually weighed. The mixture was stirred to ensure a homogenous mixing. To create a spherical pellet as shown in Fig 3.2 droplets of water were added to the mixture in the bowl and were mounded in a spherical form. A total of 35 Pellets were formed for both the low-grade and Transition ore at the ratio of 70 w% ore and 75 wt% ore, respectively.

Pellets were sun-dried for about 3 days. During the process, water absorbs into the pellet evaporates and the binder binds the fine materials together. This produces the ideal material for reduction.



### *Weighing of Pellet after Curing*

Following curing, every single produced pellet was weighed on an electronic balance, and the individual masses were recorded. This is done to determine whether the pellet's drying was completed entirely. Any weight exceeding thirty grams indicates that the pellet's curing was incomplete, necessitating additional days for it to finish drying.

#### 3.3.4 Microwave Reduction

The dried pellets were subjected to reduction using a domestic AKAI® microwave oven with product specifications of 2400 MW and 2.45 GHz with an output power of 1000 W. The initial weight of the dry composite pellets was noted with the aid of an electronic balance and recorded as A1, A2, A3, A4, A5, A6, A7, and A8. To prevent the pellet from getting stuck in the fireclay crucible, direct contact between the fireclay crucible and the pellet was avoided. This was achievable by using a bed of the corresponding reducing agent as a seat for the composite pellet in the crucible. The individual pellets namely A1, A2, A3, A4, A5, A6, A7, and A8 were placed in a fireclay crucible and subjected to intense microwave heating for 5 mins, 10 mins, 15 mins, 20 mins, 25 mins, 30 mins, and 40 mins respectively. The weights of the reduced pellets were recorded. The reduction results are shown in Appendixes C and D of this thesis.

#### 3.3.5 Magnetic Separation

Magnetic separations were done on the reduced material obtained after reduction. The reduced materials were crushed into fine size using a hammer. The crushed material was spread on a white A4 sheet then an HSMAG neodymium magnet with a magnetic susceptibility of 1.0 was brought 4 cm to the material.

### **3.4 Samples Analysis**

The two pulverised Iron ore samples were sent to the laboratories for XRF, XRD, and SEM-EDS analyses. Selected samples obtained after the reduction process were also sent for XRD and SEM-EDS Analyses. In addition, proximate analyses were done on the carbonaceous materials obtained from the ELT(s). A sample of the iron oxide utilised for the investigation was sent for further analysis and characterisation. Four boulder Iron ore samples comprising Oxide, Fresh, Transition High, and Transition Low were sent for petrographic study at the University of Mines and Technology (UMaT), Geological Engineering Laboratory. After the observation of these samples in thin and polished

sections, the transition high, and transition low were selected and sent for SEM-EDS Analysis.

### 3.4.1 X-Ray Fluorescence Analysis

The Chemical Compositions of the samples were determined by X-ray fluorescence (XRF) analysis. X-ray fluorescence (XRF) is a nondestructive analytical technique used to determine the elemental composition of materials. The results for the two samples were given as a multi-element analysis. Iron (Fe), which is the main metal of interest was given in percentage. Table 3.1 shows the specification standard for categorising the DSO that has been mined and shipped by ArcelorMittal Liberia Limited.

**Table 3.1 Iron Ore Grade Specification**

| Material Types | Specifications  |
|----------------|---|
| DSO1           | wt% Fe >60, wt% SiO <sub>2</sub> <5%, wt% Al <sub>2</sub> O <sub>3</sub> <3%, wt% P≤0.09  |
| DSO2           | 56<wt%Fe<60, wt% SiO <sub>2</sub> >5%, wt% Al <sub>2</sub> O <sub>3</sub> >3%, wt% P≤0.09 |
| Lowgrade       | <55-50%Fe, SiO <sub>2</sub> >10%, Al <sub>2</sub> O <sub>3</sub> <2%, wt% P≤0.09          |
| Transition     | wt% Fe <50, wt% SiO <sub>2</sub> >20%, wt% Al <sub>2</sub> O <sub>3</sub> <1%, wt% P<0.09 |

(Author's Construct, 2023)

### 3.4.2 Scanning Electron Microscopy-Energy Dispersive Spectroscopy (SEM-EDS) Analysis

The University of Mines and Technology (UMaT) Environmental Monitoring Laboratory employed a Scanning Electron Microscope with Energy Dispersive X-ray Spectroscopy (SEM-EDS) analyser of specification of 45 kv for material characterisation, geology, mineralogy, metallurgy, etc. A concentrated electron beam is employed in this microscope to scan a sample's surface. As the sample and this electron beam interact, different signals are produced.

When the electron beam makes contact with the sample, secondary electron imaging can result. SEM creates high-resolution images of the sample's surface, revealing its topography and morphology. This is done by detecting and analysing these secondary electrons.

An energy-dispersive X-ray detector is used in energy-dispersive X-ray spectroscopy (EDS). This happens when the sample and electron beam interact, emitting distinctive X-rays as a result. These X-rays are captured and their energy is determined by this EDS detector.

For the elemental analysis, the energy of the emitted X-ray is characteristic of the elements and their relative abundance in the sample. This determines the chemical composition of the sample, map element distribution, and locate specific phases or contaminants. SEM-EDS provides valuable information about the elemental composition, structure, and morphology of a wide range of materials at high spatial resolution.

### 3.4.3 X-ray Diffraction (XRD)

This technique was conducted on both the original and the reduced ore samples. Two original ore samples with ten reduced ore samples were submitted to the University of Ghana (Department of Physics) laboratory for XRD analysis. The specification of this equipment is 40 mA, 45 kv.

This technique was used to analyse the iron ore samples to determine the mineral composition and crystal structure present in the ore. Representative samples of iron ore were collected and prepared for this analysis. The original samples were typically ground into a fine powder to ensure homogeneity and to increase the surface area available for X-ray interaction.

A focused X-ray beam is directed onto the powdered iron ore sample. The X-rays used are typically high-energy rays, such as Cu-K $\alpha$  radiation, with wavelengths of around 1.54 Å. When the X-rays intersect with the crystal lattice of the iron ore sample, they undergo diffraction. The diffracted X-rays scatter in different directions, forming a diffraction pattern.

A detector positioned opposite the sample captures the diffracted X-rays. The detector records the intensity of the diffracted X-rays as a function of the scattering angle.

When the recorded diffraction pattern is examined to learn more about the iron ore's mineral makeup and crystal structure, data analysis can be done. To do this analysis, a database of well-known mineral structures is compared to the locations and intensities of the diffraction peaks in the pattern.

Mineral identification was based on the positions and intensities of the diffraction peaks, specific minerals present in the iron ore can be identified. Different minerals exhibit characteristic diffraction patterns, allowing for identification.

**Quantitative Analysis:** XRD can also be used for quantitative analysis, where the intensities of diffraction peaks are used to determine the relative abundances of minerals in the iron ore sample. This information is valuable for understanding the ore's composition and potential economic value. XRD was employed to gain insights into the mineralogy of iron

ore, identify valuable minerals, assess the quality of the ore, and optimise processing strategies for efficient extraction and beneficiation.

### 3.5 Petrographic Studies

Four rock samples comprised of oxide, fresh, transition low-grade, and transition high-grade were submitted to the University of Mines and Technology's (UMaT) Geological Laboratory for petrographic studies. Petrographic studies of these iron ore rocks involve the examination and analysis of thin and polished sections using optical microscopy. It is a valuable tool for understanding the mineralogy, texture, and geological history of rocks, including iron ore. In the context of Mt. Gangra iron ore, these petrographic studies provide detailed information about the various mineral phases present in the ore, their distribution, and their textural relationships. Samples of rocks from Mount Gangra Figure 3.4.

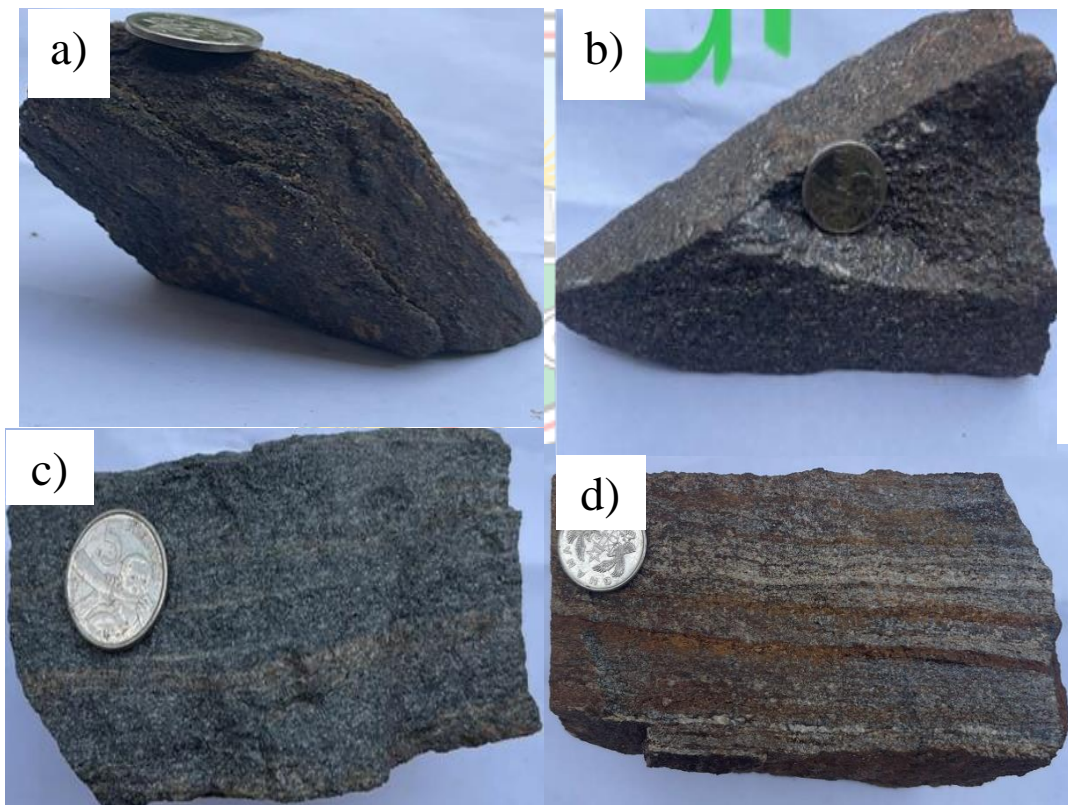


**Figure 3.4 (a) Gangra Oxide (b) Gangra Fresh Rock (c) Gangra Transition High-grade (d) Gangra Transition Lowgrade**

## CHAPTER 4

### RESULTS AND DISCUSSION

#### 4.1 Nature of Mount Gangra Iron Ores

Iron ore resources on Mount Gangra are renowned for being abundant. The ore is of excellent quality and contains considerable amounts of iron minerals. Although the precise makeup of this iron ore might vary, it often contains impurities including silica, alumina, phosphorus, and minerals like hematite ( $\text{Fe}_2\text{O}_3$ ) and magnetite ( $\text{Fe}_3\text{O}_4$ ). The chemical composition (wt%) of the lowgrade and transition iron ores was determined by XRF analyses at the ArcelorMittal Liberia Mine Laboratory, Yekepa, Liberia. This is shown in Table 4.1.

It can be seen from Table 4.1 that the low-grade ore contains a lot more iron than the transition ore. These are multi-element self-fluxing ores, including silicon dioxide ( $\text{SiO}_2$ ), aluminum oxide ( $\text{Al}_2\text{O}_3$ ), phosphorus (P), titanium dioxide ( $\text{TiO}_2$ ), magnesium oxide ( $\text{MgO}$ ), calcium oxide ( $\text{CaO}$ ), and others. The Loss on Ignition (LOI) Values for the Lowgrade (GLG-001), and transition (GLT-001) are 3.534 and 2.547 respectively.

For the lowgrade ore (GLG-001), the LOI value, 3.534, indicates that a greater proportion of the sample's weight is lost when heated. This suggests that the sample contains more volatile materials and high water (moisture) content which is 11.10%.

Conversely, the transition ore (GLT-001) has a lower LOI value of 2.547, indicating that less weight is lost during ignition, suggesting that the sample has fewer volatile compounds and a lower water content of 9.00 wt%. The interpretation of LOI values can vary depending on the specific material being analysed and the testing condition.

The silica contents of the two unpulverised ores were given as 23.446 wt. % and 29.303 wt% suggesting that the ores are high in silica. Gangra iron ores are classified based on their iron (Fe) content. For ArcelorMittal Liberia, iron ore is said to be low grade when the iron (Fe) ranges from 55-50%, and the transition is from 50% below.

**Table 4.1 Chemical Composition by XRF of the Mt. Gangra Iron Ores.**

| Sample ID and Chemical Analysis |         |                                |         |
|---------------------------------|---------|--------------------------------|---------|
| GLG-001                         |         | GLT-001                        |         |
| Multi-Elements                  | (%)     | Multi-Elements                 | (%)     |
| Fe                              | 50.147  | Fe                             | 44.814  |
| SiO <sub>2</sub>                | 23.446  | SiO <sub>2</sub>               | 29.303  |
| Al <sub>2</sub> O <sub>3</sub>  | 0.734   | Al <sub>2</sub> O <sub>3</sub> | 0.594   |
| P                               | 0.056   | P                              | 0.074   |
| Mn                              | 0.137   | Mn                             | 0.068   |
| TiO <sub>2</sub>                | 0.019   | TiO <sub>2</sub>               | 0.024   |
| CaO                             | 0.004   | CaO                            | 0.007   |
| MgO                             | 0.028   | MgO                            | 0.042   |
| Na <sub>2</sub> O               | 0.018   | Na <sub>2</sub> O              | 0.023   |
| K <sub>2</sub> O                | 0.003   | K <sub>2</sub> O               | 0.019   |
| Cr <sub>2</sub> O <sub>3</sub>  | <0.0095 | Cr <sub>2</sub> O <sub>3</sub> | <0.0105 |
| S                               | 0.008   | S                              | 0.004   |
| LOI                             | 3.534   | LOI                            | 2.547   |
| Moisture                        | 11.10   | Moisture                       | 9.00    |

(Anon, 2022)

#### 4.2 SEM-EDS Results of Mt. Gangra Lowgrade (Pulverised) Ore for Region 1

The SEM-EDS result of Gangra Lowgrade iron ore (Pulverised) before reduction at Region 1 (GLG-2567) is illustrated in Figure 4.1, and Table 4.2 respectively. This result shows the point-by-point surface analyses of the magnetic ore and gives the chemical composition of the samples. In Region 1 (GLG-2567), the ore exists as Iron (III) oxide (Fe<sub>2</sub>O<sub>3</sub>) Compound. This is hematite based on the O/Fe atom ratio of 59.92/40.08 (~1.5).

According to mineralogical research, the iron (Fe) concentration of hematite is 69.9% or 70%. The precise makeup of hematite can, however, change slightly depending on the particular geological source and the presence of impurities. From the SEM-EDS micrograph shown in Figure 4.1, the ore is moderately sorted with coarse subangular grains.

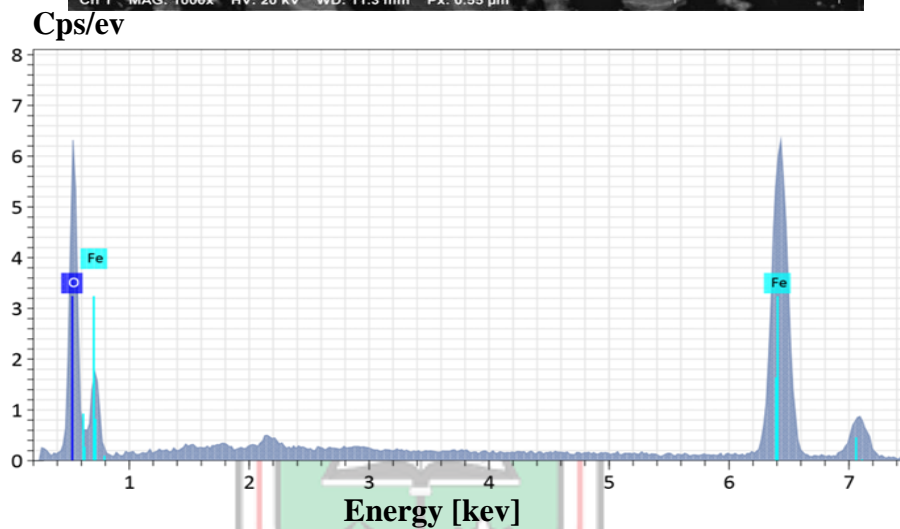
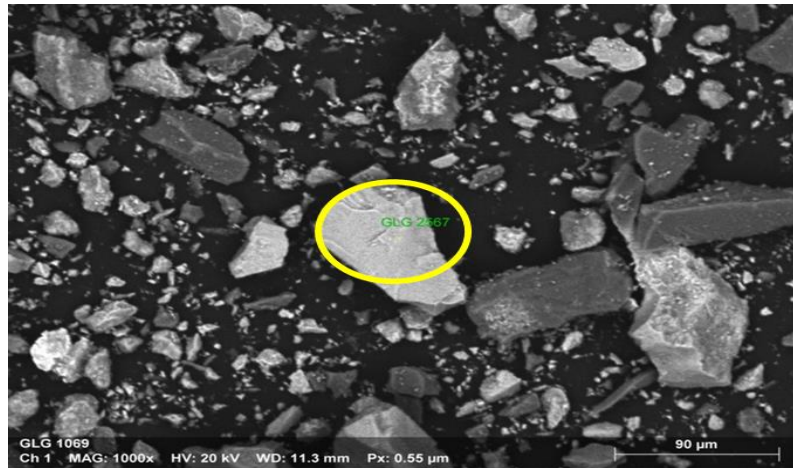


Figure 4.1 SEM Micrograph of Gangra Lowgrade Ore (Pulverised) at Region 1 (GLG-2567)

Table 4.2 EDS Chemical Analysis of Gangra Lowgrade Ore (Pulverised) at Region 1 (GLG-2567)

| Element      | Atomic No. | Mass [%]     | Mass Norm. [%] | Atom [%]      |
|--------------|------------|--------------|----------------|---------------|
| Oxygen       | 8          | 3.36         | 29.99          | 59.92         |
| Iron         | 26         | 9.02         | 70.01          | 40.08         |
| <b>Total</b> |            | <b>12.88</b> | <b>100.00</b>  | <b>100.00</b> |

Region 2 (GLG-2568), Figure 4.2, and Table 4.3 shows the results, which typically reflect the sample's elemental makeup. The presence of Iron (Fe) is a sign that a metallic iron compound is present in the sample. Silicon (Si) is a non-metallic element and is often found in minerals quartz, silicates, and various geological materials.

The presence of silicon suggests the presence of silicon-based compounds in the sample, which is common in rocks, minerals, and many natural substances.

The presence of oxygen (O) in this sample supports the existence of compounds containing oxygen. Oxygen and silicon combine to generate silicon dioxide ( $\text{SiO}_2$ ). The atomic compositions of Iron (Fe), oxygen (O), and silicon (Si) make it apparent that in addition to silica ( $\text{SiO}_2$ ), iron forms a silicide with silicon and it is predicted to be of the form  $\text{Fe}_2\text{Si}_3$ . This alloy principally consists of silicon (Si) and iron (Fe). Because it may improve the qualities of iron and steel, it is utilised in many industrial processes, such as steelmaking and foundry work. The subangular ore grains are moderately sorted.

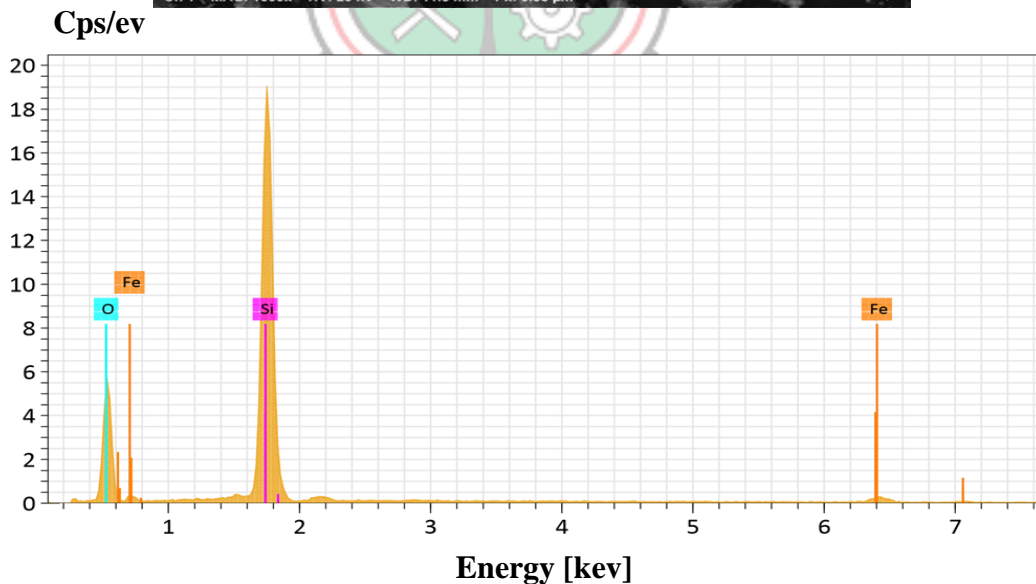


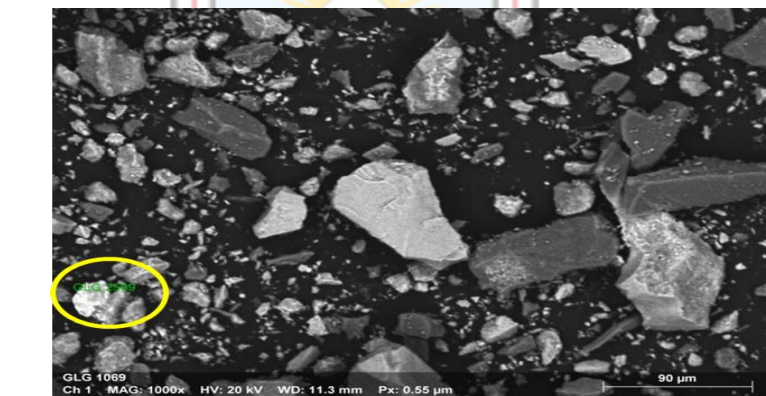
**Figure 4.2 SEM Micrograph of Gangra Lowgrade Pulverised Ore in Region 2 (2568)**



**Table 4.3 EDS Chemical analysis of Gangra Lowgrade Pulverised Ore for Region 2 (GLG-2568)**

| Element      | Atomic No. | Mass [%]     | Mass Norm. [%] | Atom [%]      |
|--------------|------------|--------------|----------------|---------------|
| Oxygen       | 8          | 38.03        | 49.14          | 63.48         |
| Silicon      | 14         | 37.43        | 48.35          | 35.59         |
| Iron         | 26         | 1.94         | 2.51           | 0.93          |
| <b>Total</b> |            | <b>77.41</b> | <b>100.00</b>  | <b>100.00</b> |

In Region 3 (2569), Figure 4.3, the presence of aluminum (Al) indicates the existence of aluminum-containing compounds in this sample likewise as silicon and iron. With some amount of oxygen trapped in the system, Iron (Fe) combines with Oxygen (O) to form a Fe (II/ III) oxide compound which is Magnetite. The mass percent of iron (Fe) is said to be 80.52, Table 4.4. Magnetite is an iron oxide mineral known for its strong magnetic properties and high iron content making it valuable ore for steel production. From the SEM-EDS micrograph Figure 4.3, the ore grains are subangular and moderately sorted.



Cps/ev

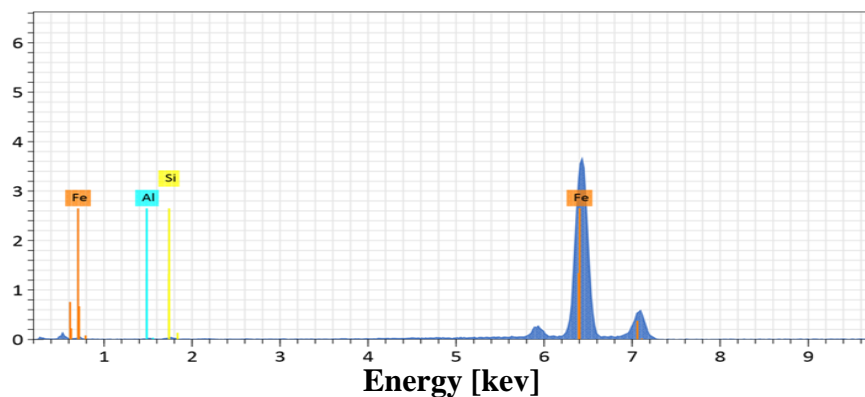


**Figure 4.3 SEM Micrograph of Gangra Lowgrade Ore (Pulverised) for Region 3 (GLG-2569)**

**Table 4.4 EDS Chemical Analysis of Gangra Lowgrade Pulverised Ore for Region 3 (GLG-2569)**

| Element   | At. No | Mass [%]     | Mass Norm. [%] | Atom [%]   |
|-----------|--------|--------------|----------------|------------|
| Aluminium | 13     | 0.97         | 7.92           | 13.67      |
| Silicon   | 14     | 1.42         | 11.56          | 19.17      |
| Iron      | 26     | 9.88         | 80.52          | 67.16      |
|           |        | <b>12.27</b> | <b>100</b>     | <b>100</b> |

### 4.3 SEM-EDS Results of Mt. Gangra Transition (Pulverised Ore)

The SEM-EDS results of Gangra Transition iron ore (Pulverised) before reduction are illustrated in Figures 4.4, and 4.5, Table 4.5, and Table 4.6 respectively. These are the point-by-point surface analyses of the magnetic ore.

In Region 1 (GLT-2572), Figure 4.4, and Table 4.5, predictable mineralogical phases based on atom% are aluminum oxide ( $\text{Al}_2\text{O}_3$ ), silicon carbide (SiC), and iron silicide with the formula (FeSi). This substance is frequently employed as an alloying and deoxidizing agent in the steelmaking sector. Smelting a combination of silicon and iron sources, such as ore and quartz, results in ferrosilicon ( $\text{Fe}_2\text{Si}_3$ ). To meet the needs of varied applications, it is available in grades with varying silicon contents. From the SEM-EDS micrograph Figure 4.4, the ore has a subangular grain and it is moderately sorted.

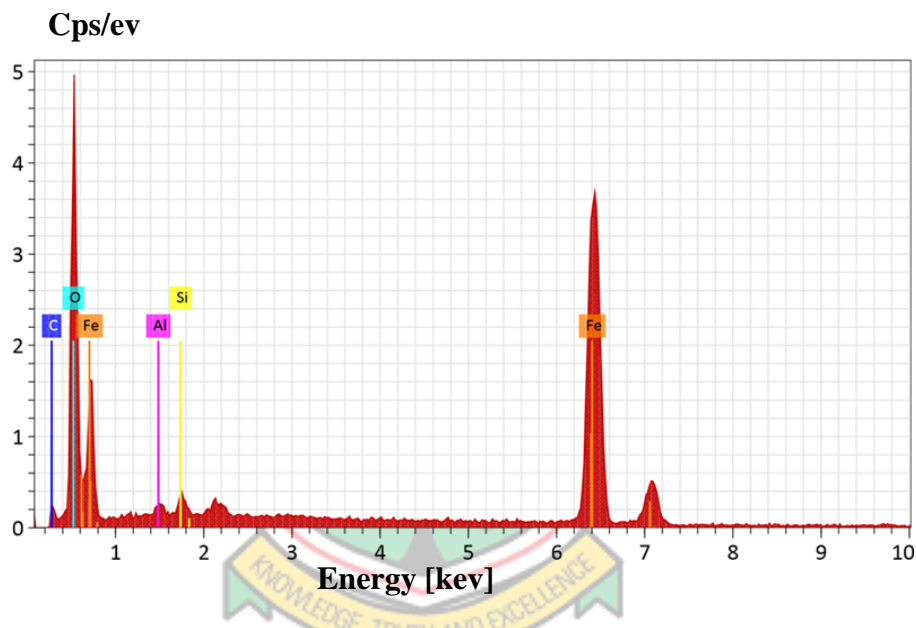
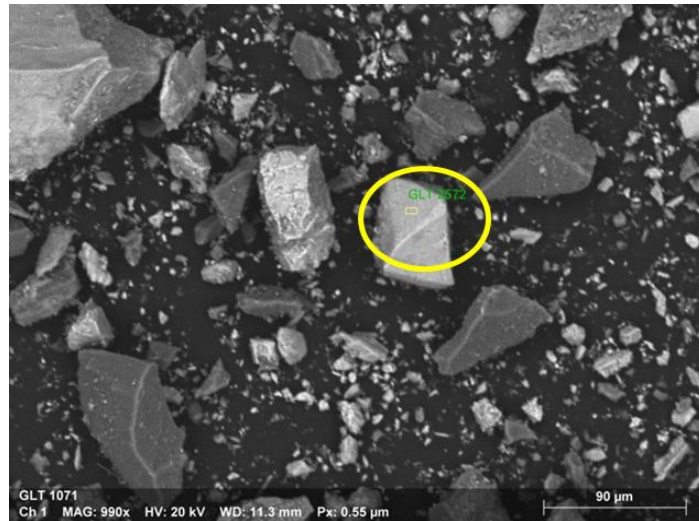


Figure 4.4 SEM Micrograph of Gangra Pulverised Transition Ore for Region 1(2572)

Table 4.5 EDS Chemical Analysis of Gangra Transition Pulverised Ore for Region 1 (GLT-2572)

| Element   | At. No.    | Mass [%]     | Mass Norm. [%] | Atom [%]      |
|-----------|------------|--------------|----------------|---------------|
| Carbon    | 6          | 2.82         | 6.07           | 10.82         |
| Oxygen    | 8          | 17.41        | 37.54          | 50.21         |
| Aluminium | 13         | 12.78        | 27.54          | 21.85         |
| Silicon   | 14         | 7.44         | 16.04          | 12.22         |
| Iron      | 26         | 5.94         | 12.81          | 4.91          |
|           | <b>Sum</b> | <b>46.39</b> | <b>100.00</b>  | <b>100.00</b> |

Predictable phases in Region 2 (GLG-2574), Figure 4.5, and Table 4.6, are silicon carbide (SiC), and iron silicide

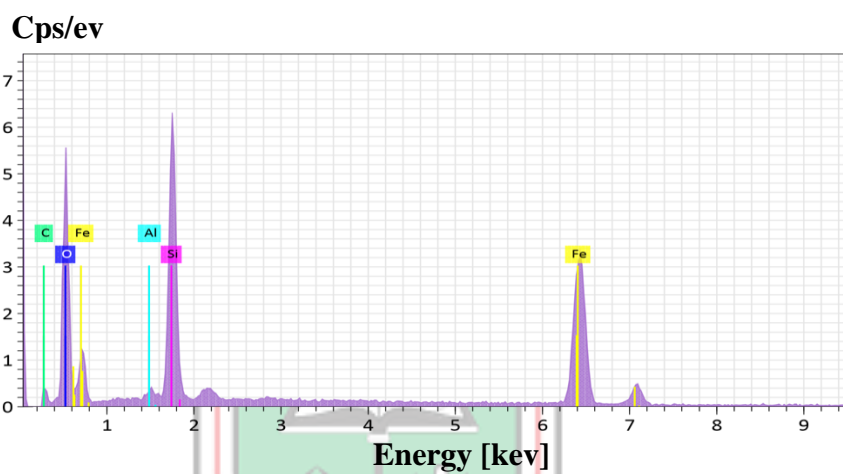
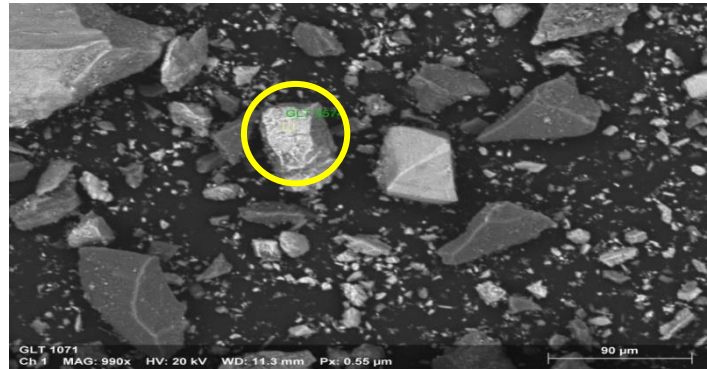


Figure 4.5 SEM Micrograph of Gangra Pulverised Transition Ore at Region 3.

Table 4.6 EDS Chemical Composition of Gangra Transition Ore (Pulverised) for Region 3 (GLG-2574)

| Element   | Atomic No. | Mass [%]     | Mass Norm [%] | Atom [%]      |
|-----------|------------|--------------|---------------|---------------|
| Carbon    | 6          | 6.35         | 9.95          | 16.78         |
| Oxygen    | 8          | 24.84        | 38.92         | 49.29         |
| Aluminium | 13         | 2.17         | 3.40          | 2.55          |
| Silicon   | 14         | 25.02        | 39.21         | 28.29         |
| Iron      | 26         | 5.44         | 8.53          | 3.09          |
|           | <b>SUM</b> | <b>63.82</b> | <b>100.00</b> | <b>100.00</b> |

#### 4.4 SEM-EDS Results of Gangra Lowgrade Iron Ore (Reduced)

The SEM-EDS micrograph of Gangra Lowgrade iron ore (Reduced) after reduction is illustrated in Figures 4.6, 4.7, and 4.8, and analysis Tables 4.7, 4.8, and 4.9, respectively.

It is apparent from Region 1 (M1-2751), Figure 4.6, and Table 4.7 that the compounds formed after reduction are silicon carbide (SiC) which comes about from the reaction of silicon(Si) with carbon (C), ferrosilicon ( $\text{Fe}_2\text{Si}_3$ ), which comes from the reaction of iron (Fe) with Silicon (Si), and silica ( $\text{SiO}_2$ ) which was present in the unreduced ore. From the SEM micrograph (Figure 4.6), the ore is spherical and shows a good reduction rate.

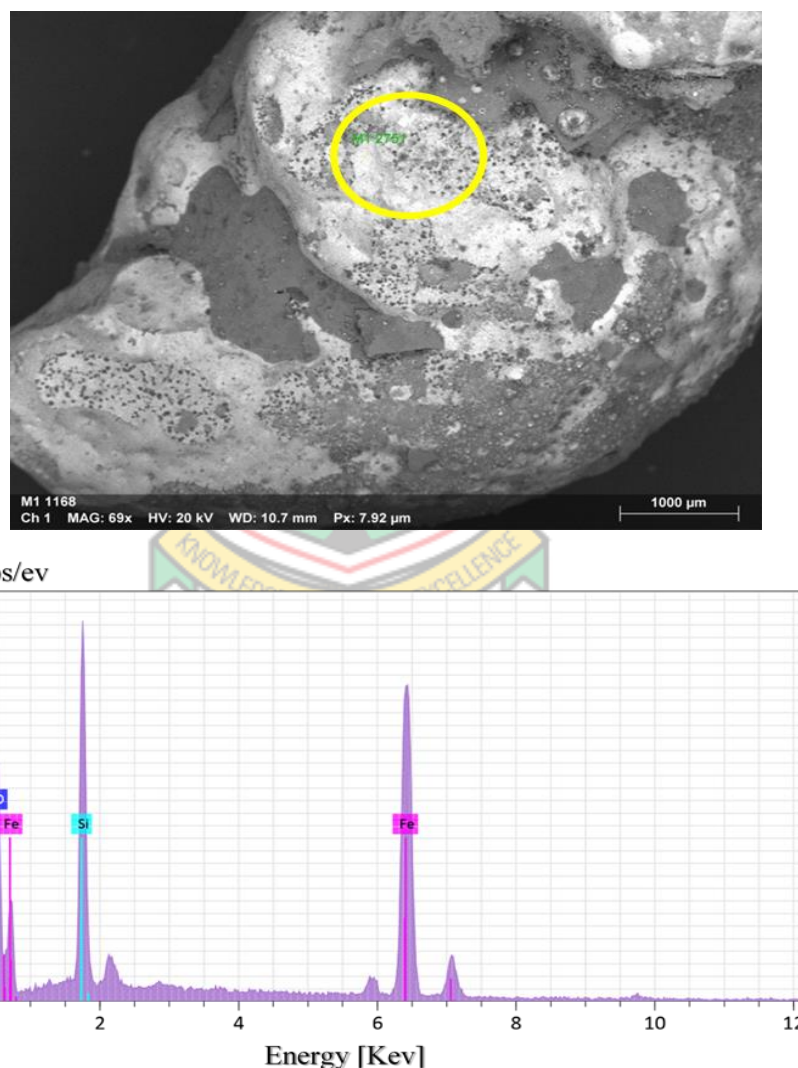


**Figure 4.6 SEM Micrograph of Gangra (Reduced) Lowgrade Ore at Region 1 (M1-2751)**

**Table 4.7 EDS Chemical Analysis of Gangra Lowgrade Reduced Ore at Region 1 (M1-2751)**

| Element | Atomic No. | Mass [%]     | Mass Norm. [%] | Atom %        |
|---------|------------|--------------|----------------|---------------|
| Carbon  | 6          | 3.34         | 11.29          | 21.29         |
| Oxygen  | 8          | 7.54         | 25.53          | 36.13         |
| Silicon | 14         | 12.51        | 42.34          | 34.13         |
| Iron    | 26         | 6.15         | 20.83          | 8.45          |
|         | <b>Sum</b> | <b>29.54</b> | <b>100.00</b>  | <b>100.00</b> |

In Region 2 (2752), Figure 4.7, and Table 4.8, the predicted phases are Ferrosilicon ( $\text{Fe}_2\text{Si}_3$ ), Silicon Carbide ( $\text{SiC}$ ), and Silica ( $\text{SiO}_2$ ). Ferrosilicon plays a vital role in the production of high-quality steel and allows for the customisation of steel properties to meet various industrial requirements. Different compositions of ferrosilicon ( $\text{Fe}_2\text{Si}_3$ ) are used depending on the specific needs of the steel being produced.

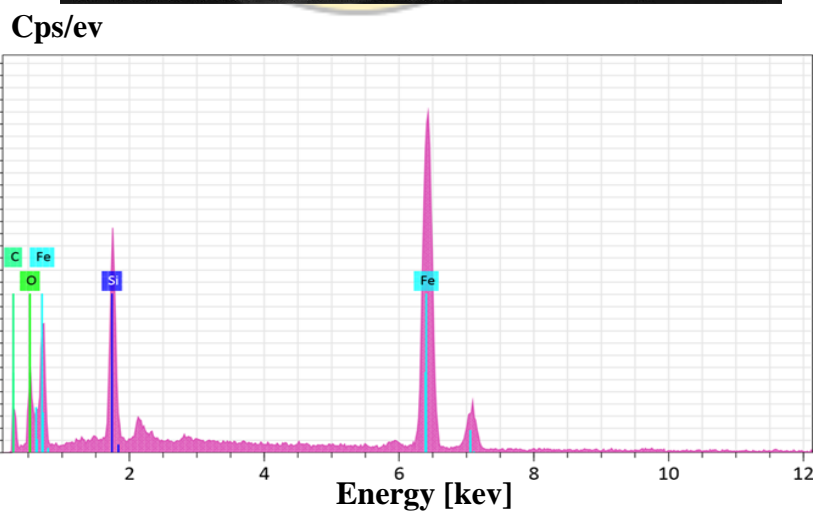


**Figure 4.7 SEM Micrograph of Gangra Lowgrade Reduce Ore for Region 2 (M1-2752)**

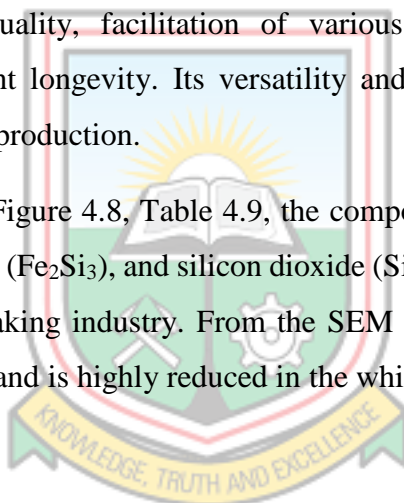
**Table 4.8 EDS Chemical Analysis of Gangra Lowgrade (Reduced) Ore for Region 2 (M1-2752)**

| Element | Atomic No. | Mass [%]     | Mass Norm. [%] | Atom [%]      |
|---------|------------|--------------|----------------|---------------|
| Carbon  | 6          | 6.30         | 18.66          | 35.37         |
| Oxygen  | 8          | 3.68         | 10.90          | 15.51         |
| Silicon | 14         | 17.10        | 50.63          | 41.04         |
| Iron    | 26         | 6.69         | 19.81          | 8.07          |
|         | <b>SUM</b> | <b>33.33</b> | <b>100.00</b>  | <b>100.00</b> |

Silicon Carbide (SiC) has many applications in the steel industry, ranging from abrasive and refractory materials to deoxidation and improving the wear resistance of steel components. Its properties make it a valuable material in steel manufacturing processes and related applications.

The steel industry depends heavily on silica (SiO<sub>2</sub>) for several reasons, including the enhancement of steel quality, facilitation of various manufacturing processes, and maintenance of equipment longevity. Its versatility and refractory properties make it a valuable material in steel production.

In Region 3 (M1-2753), Figure 4.8, Table 4.9, the compounds that are formed are silicon carbide (SiC), ferrosilicon (Fe<sub>2</sub>Si<sub>3</sub>), and silicon dioxide (SiO<sub>2</sub>). All these compounds played a vital role in the steelmaking industry. From the SEM micrograph (Figure 4.8), the ore shows spherical particles and is highly reduced in the white or lighter region.



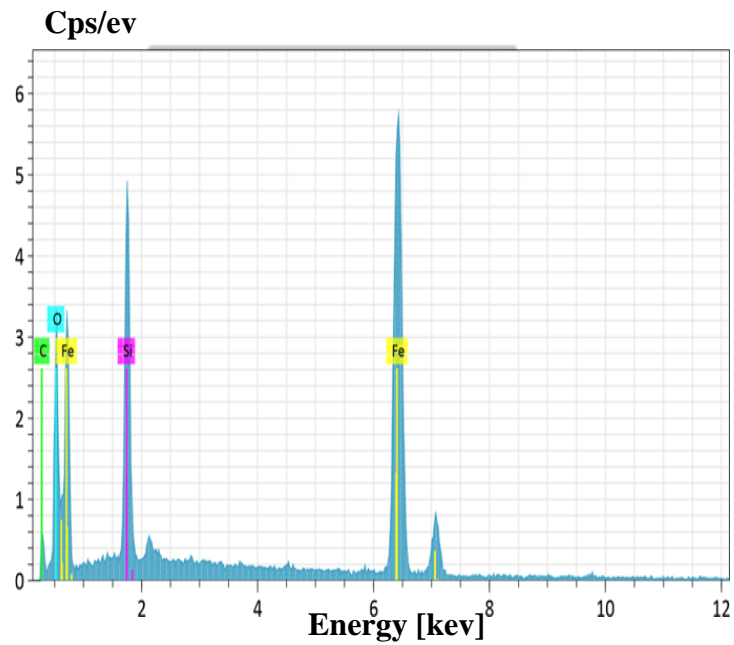


**Figure 4.8 SEM Micrograph of Gangra Lowgrade Ore (Reduced) for Region 3 (M1-2753)**

**Table 4.9 EDS Chemical Analysis of Gangra Lowgrade Reduced Ore at Region 3 (M1-2753)**

| Element | Atomic No. | Mass [%]     | Mass Norm. [%] | Atom [%]      |
|---------|------------|--------------|----------------|---------------|
| Carbon  | 6          | 6.35         | 12.31          | 22.86         |
| Oxygen  | 8          | 10.69        | 20.71          | 28.87         |
| Silicon | 14         | 28.13        | 54.50          | 43.28         |
| Iron    | 26         | 6.44         | 12.48          | 4.99          |
|         | <b>SUM</b> | <b>51.61</b> | <b>100.00</b>  | <b>100.00</b> |



#### 4.5 SEM-EDS Results of Gangra Transition Ore (Reduced)

In Region 1 (C1-2745), Figure 4.9 of Gangra Reduced Transition Ore, the compounds that are formed are ferrosilicon ( $\text{Fe}_2\text{Si}_3$ ), silicon carbide ( $\text{SiC}$ ), and silicon dioxide ( $\text{SiO}_2$ ) Table 4.10. All these compounds are essential in steel production. The lighter region shows that the ore was highly reducible with a high percentage of silicon (Si).

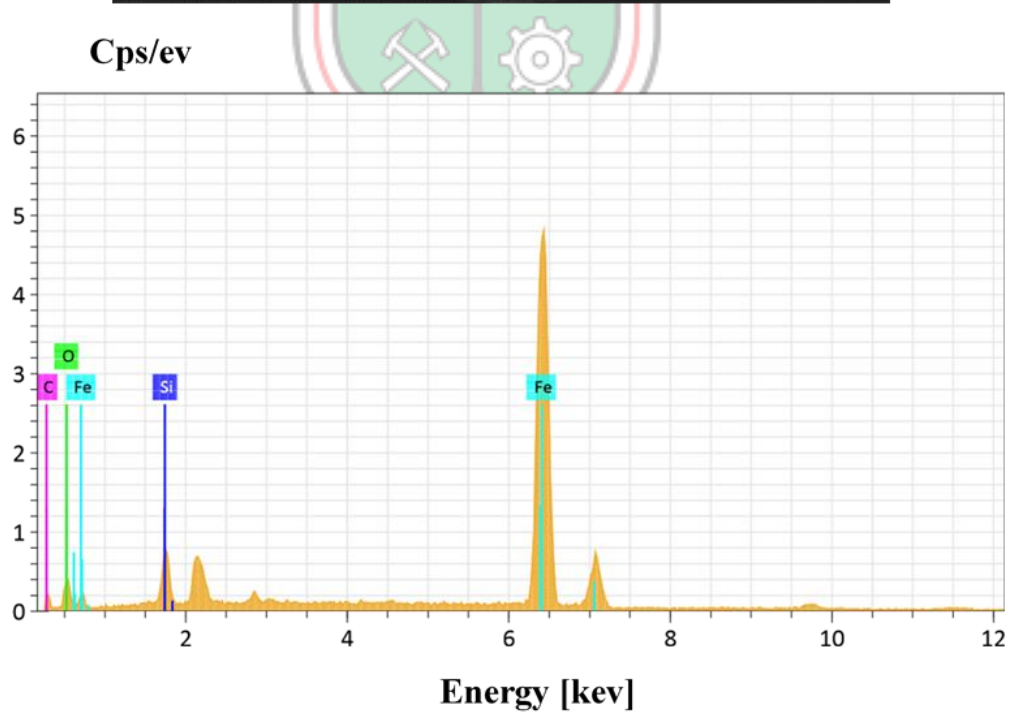
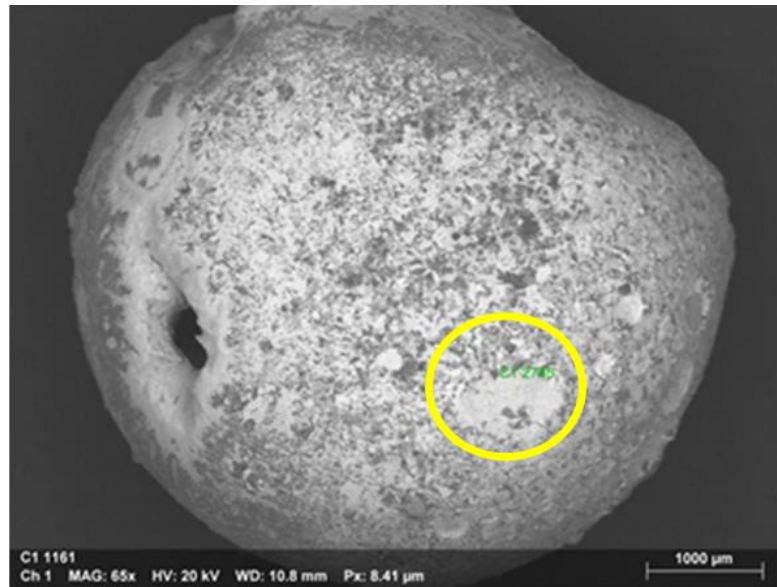
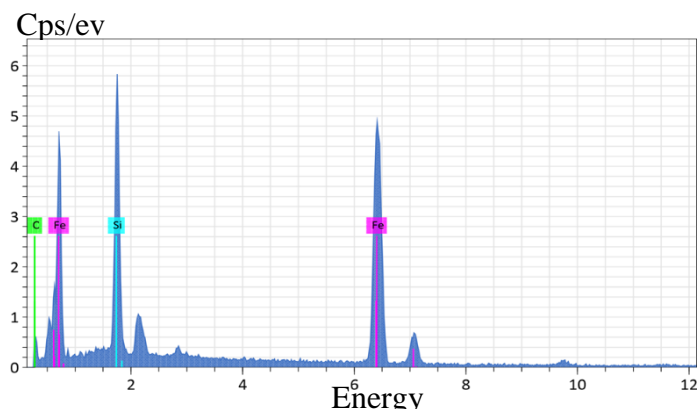
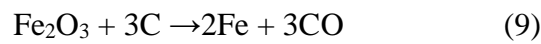


Figure 4.9 SEM Micrograph of Gangra Transition Ore (Reduced) at Region 1 (C1-2745)

**Table 4.10 EDS Chemical Analysis of Gangra Transition Ore (Reduced) at Region 1(C1-2745)**

| Element | Atomic No. | Mass [%]     | Mass Norm. [%] | Atom [%]      |
|---------|------------|--------------|----------------|---------------|
| Carbon  | 6          | 1.40         | 8.85           | 23.60         |
| Oxygen  | 8          | 0.76         | 4.82           | 9.66          |
| Silicon | 14         | 4.82         | 30.37          | 34.64         |
| Iron    | 26         | 8.88         | 55.97          | 32.11         |
|         | <b>Sum</b> | <b>15.86</b> | <b>100.00</b>  | <b>100.00</b> |

In Region 2 (C1-2746), Figure 4.10, and Table 4.11, the predicted phases are Ferrosilicon ( $\text{Fe}_2\text{Si}_3$ ), silicon carbide ( $\text{SiC}$ ), and elemental silicon ( $\text{Si}$ ). These predicted phases suggest a simultaneous reduction of all the silica and all the hematite in the Gangra Transition ore by the carbon from the ELT, following the reactions below:



**Figure 4.10 SEM Micrograph of Gangra Transition Ore (Reduced) for Region 2 (C1-2746)**

**Table 4.11 EDS Chemical Analysis of Gangra Transition Ore (Reduced) at Region 2 (C1-2746)**

| Element | Atomic No. | Mass [%]     | Mass Norm. [%] | Atom [%]      |
|---------|------------|--------------|----------------|---------------|
| Carbon  | 6          | 9.55         | 20.55          | 39.88         |
| Silicon | 14         | 30.35        | 65.33          | 54.22         |
| Iron    | 26         | 6.56         | 14.12          | 5.90          |
|         | <b>Sum</b> | <b>46.46</b> | <b>100.00</b>  | <b>100.00</b> |

In Region 3 (C1-2747), Figure 4.11, Table 4.12, the compounds that are present are titania ( $\text{TiO}_2$ ), silicon carbide ( $\text{SiC}$ ), silica ( $\text{SiO}_2$ ), and metallic iron ( $\text{Fe}$ ).

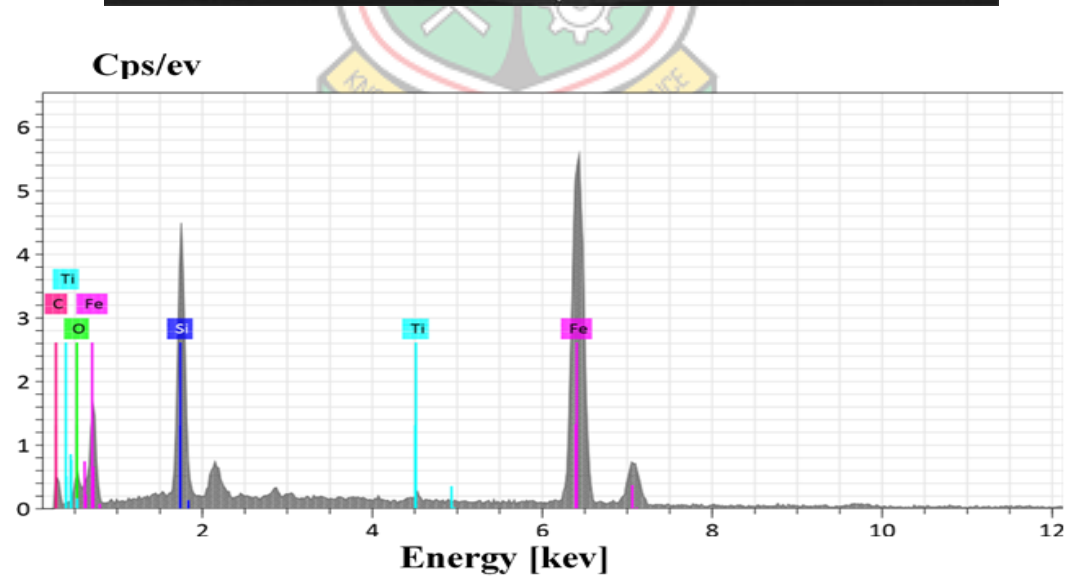


**Figure 4.11 SEM Micrograph of Gangra Transition Ore (Reduced) at Region 3 (C1-2747)**

**Table 4.12 EDS Chemical Analysis of Gangra Transition Ore (Reduced) at Region 3 (C1-2747)**

| Element  | Atomic No. | Mass [%]     | Mass Norm. [%] | Atom [%]      |
|----------|------------|--------------|----------------|---------------|
| Carbon   | 6          | 4.93         | 16.19          | 33.48         |
| Oxygen   | 8          | 1.49         | 4.88           | 7.57          |
| Silicon  | 14         | 16.45        | 53.99          | 47.76         |
| Titanium | 22         | 0.33         | 1.09           | 0.56          |
| Iron     | 26         | 7.27         | 23.86          | 10.62         |
|          | <b>Sum</b> | <b>30.46</b> | <b>100.00</b>  | <b>100.00</b> |

In Region 4, (E1-2748), Figure 4.12, and Table 4.13, the compounds that are present are ferrosilicon ( $\text{Fe}_2\text{Si}_3$ ), unreduced silica ( $\text{SiO}_2$ ), and elemental silicon (Si). Ferrosilicon also helps remove oxygen and other impurities from molten steel and can enhance the properties of steel, such as strength, and corrosion resistance.

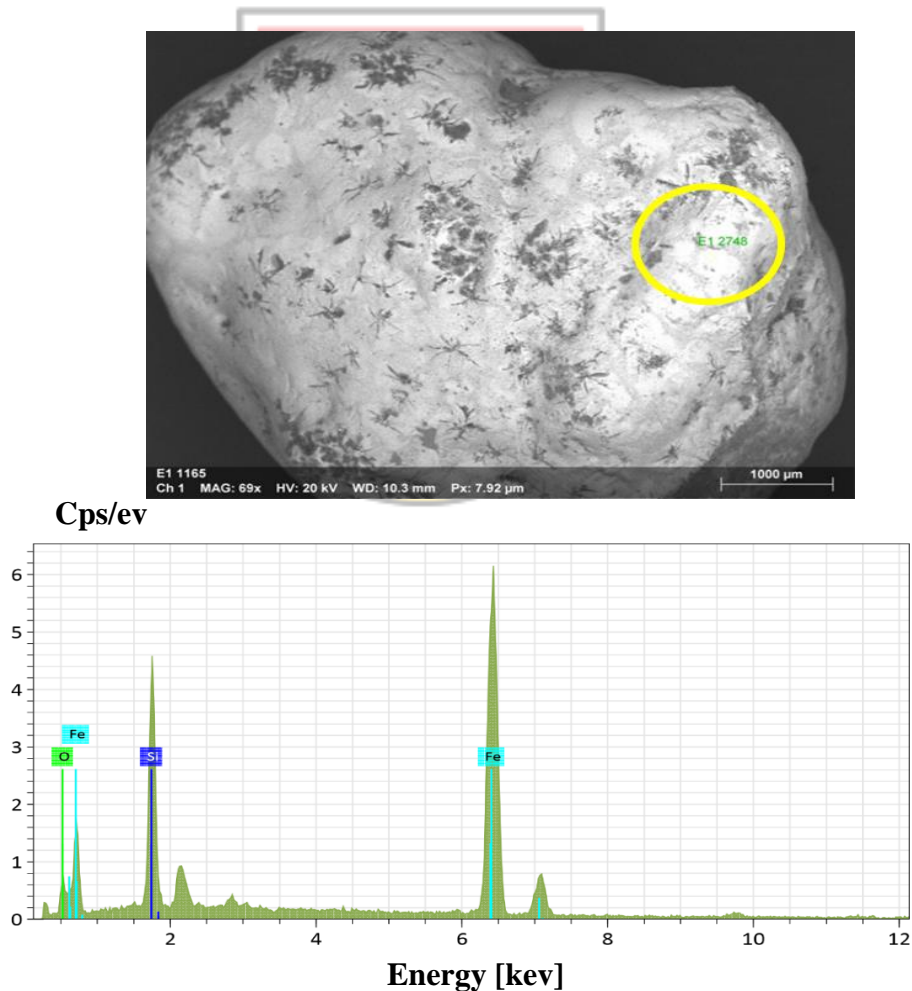


**Figure 4.12 SEM Micrograph of Gangra Transition (Reduced) at Region 4 (E1-2748)**

**Table 4.13 EDS Chemical Analysis of Gangra Transition (Reduced) Ore at Region 4 (E1-2748)**

| Element | Atomic No. | Mass [%]     | Mass Norm. [%] | Atom [%]       |
|---------|------------|--------------|----------------|----------------|
| Oxygen  | 8          | 1.20         | 4.42           | 8.74           |
| Silicon | 14         | 17.96        | 66.42          | 74.76          |
| Iron    | 26         | 7.88         | 29.15          | 16.50          |
|         | <b>SUM</b> | <b>27.03</b> | <b>100.00</b>  | <b>1.00.00</b> |

In Region 5, (E1-2749), Figure 4.13, and Table 4.14, the compound that is formed after the reduction process is ferrosilicon ( $\text{Fe}_3\text{Si}_4$ ). The absence of oxygen suggests a complete reduction of both hematite and silica contents of the Gangra Transition ore.

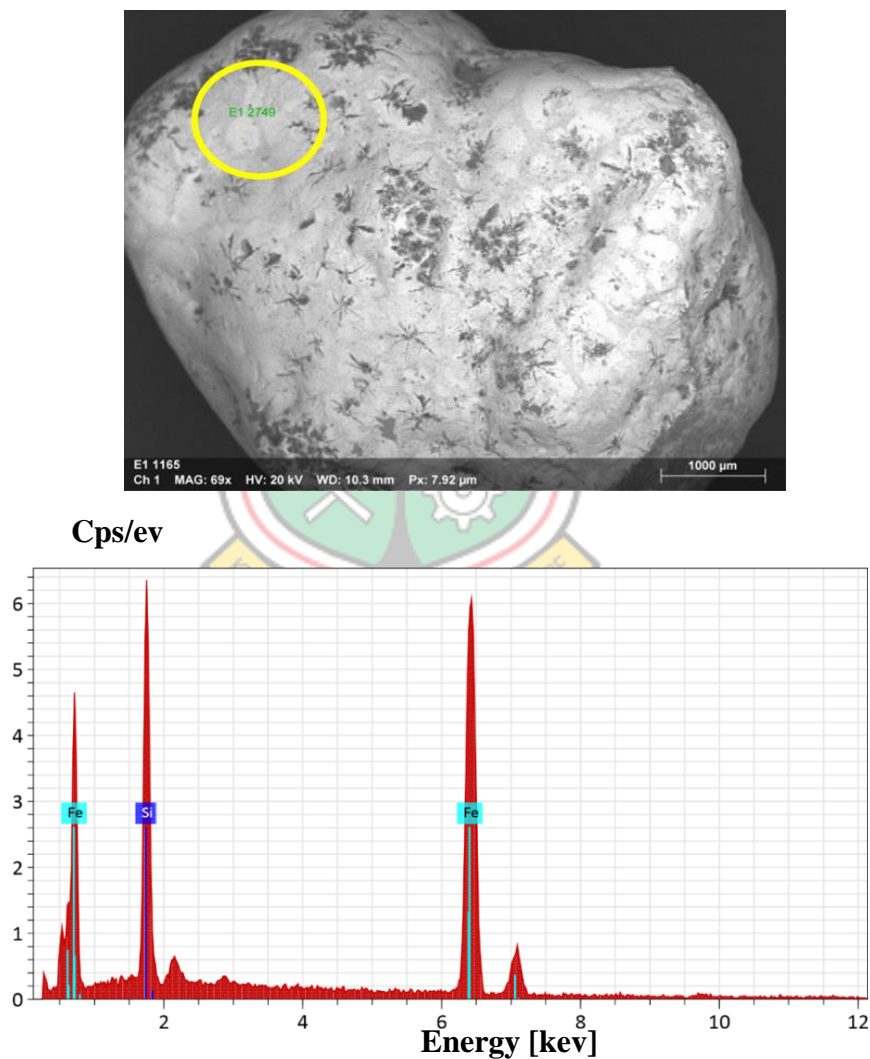


**Figure 4.13 SEM Micrograph of Gangra Transition Ore (Pulverised) for Region 5 (E1-2749)**

**Table 4.14 EDS Chemical Analysis of Gangra Transition Ore (Reduced) for Region 5 (E1-2749)**

| Element | Atomic No  | Mass [%]     | Mass Norm. [%] | Atom [%]      |
|---------|------------|--------------|----------------|---------------|
| Silicon | 14         | 6.25         | 39.78          | 56.78         |
| Iron    | 26         | 9.49         | 60.22          | 43.22         |
|         | <b>SUM</b> | <b>15.71</b> | <b>100.00</b>  | <b>100.00</b> |

In region 6, (E1-2750), (Figure 4.14), and (Table 4.15), the compounds that are formed are ferrosilicon ( $\text{Fe}_2\text{Si}_3$ ), silicon carbide ( $\text{SiC}$ ), and silicon dioxide or silica ( $\text{SiO}_2$ ).

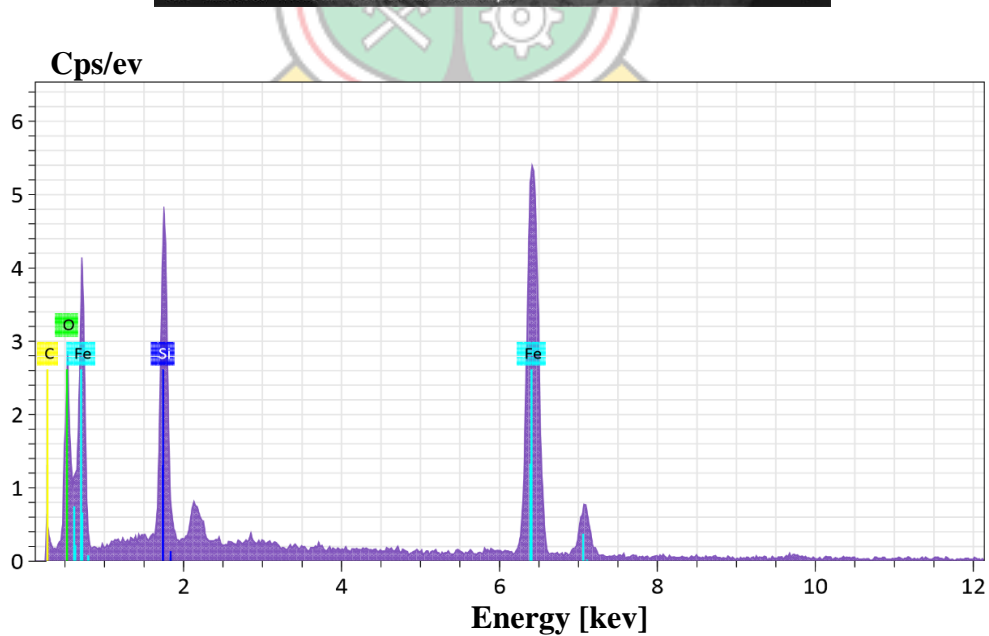
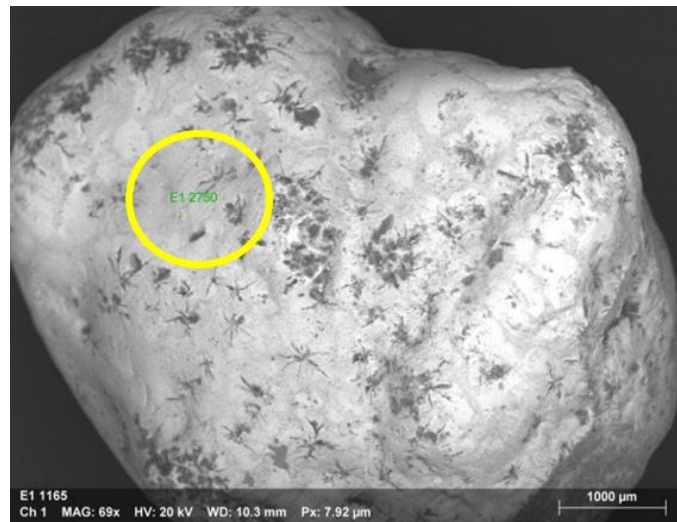


**Figure 4.14 SEM Micrograph of Gangra Transition Ore (Reduced) at Region 6 (E1-2750)**

**Table 4.15 EDS Chemical Analysis of Gangra Transition Ore (Reduced) at Region 6 (E1-2750)**

| Element | Atomic No. | Mass [%] | Mass Norm. [%] | Atom [%] |
|---------|------------|----------|----------------|----------|
| Carbon  | 6          | 4.86     | 11.41          | 21.87    |
| Oxygen  | 8          | 8.00     | 18.76          | 27.00    |
| Silicon | 14         | 23.36    | 54.81          | 44.93    |
| Iron    | 26         | 6.40     | 15.02          | 6.19     |

#### 4.6 X-ray Diffraction Results for Low-grade and Transition Ore (Pulverised)

The X-ray Diffraction results for both Gangra lowgrade and transition ores (Pulverised) (Figure 4.15) show that the ores are dominantly composed of hematite ( $\text{Fe}_2\text{O}_3$ ) as the main phase, with Silica having to be the major impurity. The diffraction patterns provide information about the crystalline structure of the hematite and silica phases in the samples.

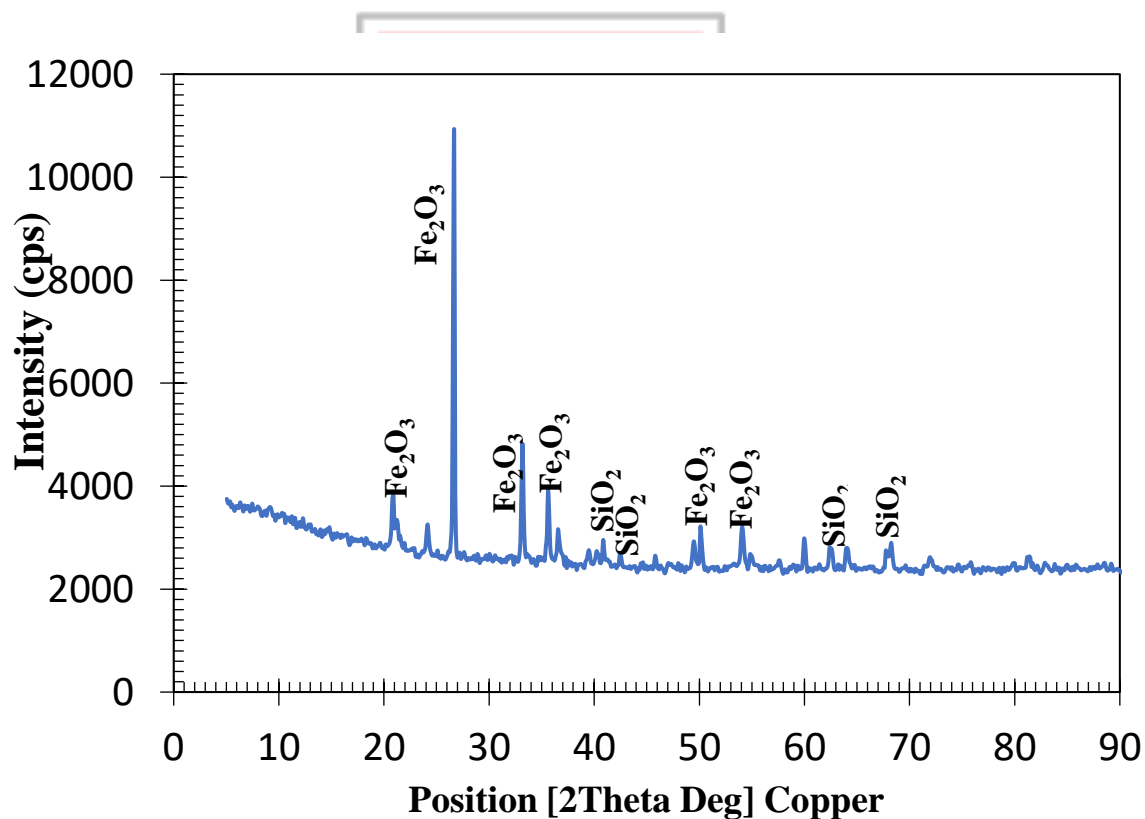


**Figure 4.15 XRD Spectrum of Gangra Lowgrade Ore (Pulverised)**

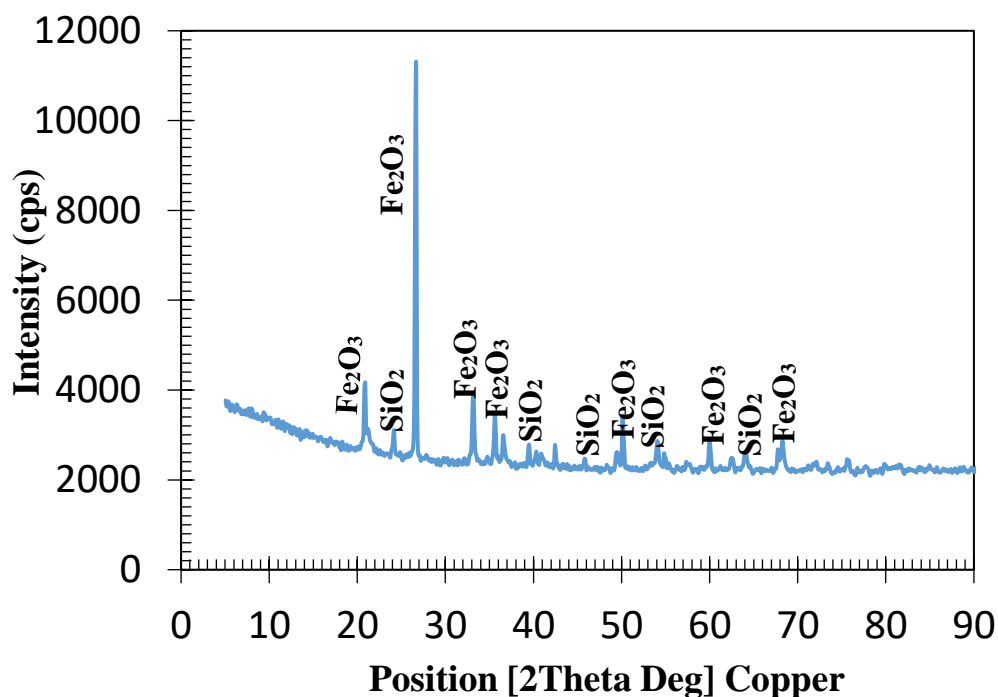
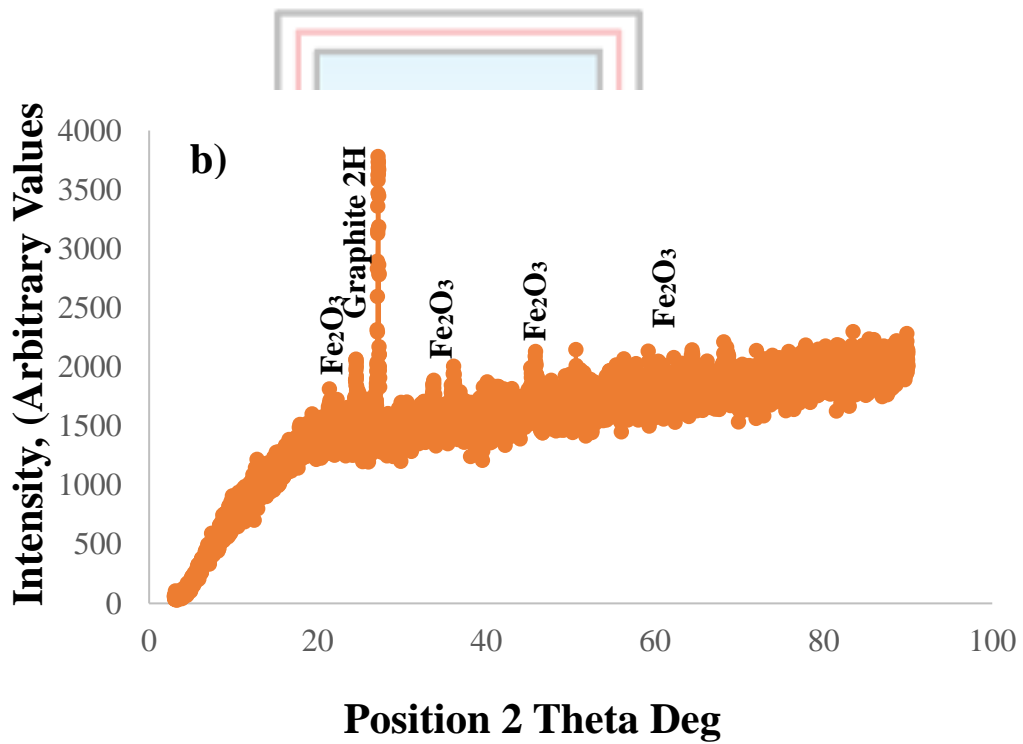
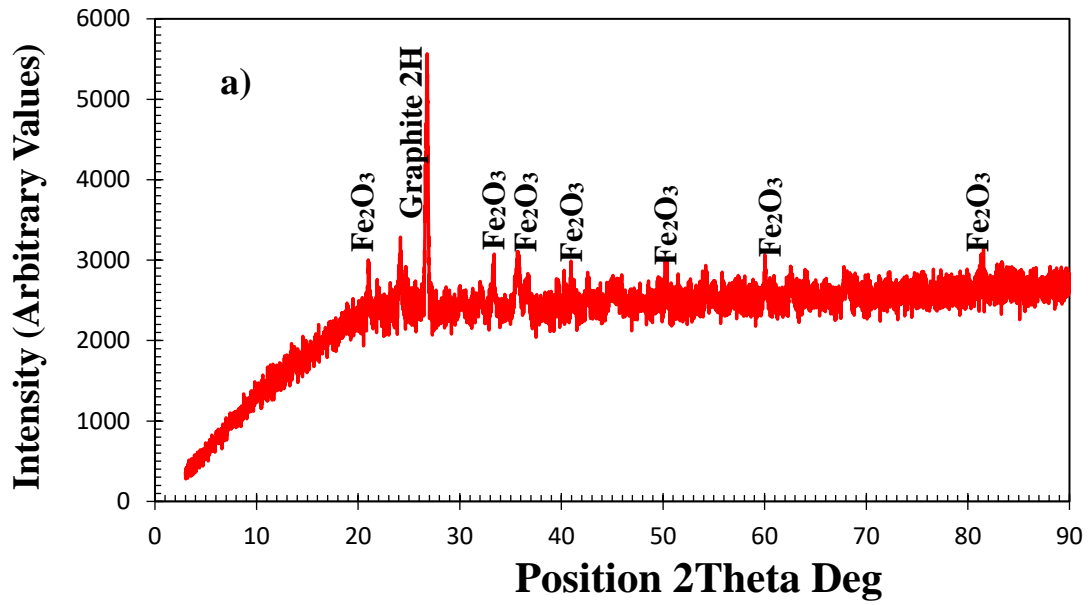


Figure 4.16 XRD Spectrum of Gangra Transition Ore (Pulverised)

#### 4.7 X-ray Diffraction (XRD) Results of Gangra Transition and Lowgrade Ores (Reduced)

The X-ray Diffraction (XRD) results of Gangra Transition Ore (Reduced) samples B2, and C2, Figure 4.17, and reduced lowgrade ore (Sample Z3, and Z4), Figure 4.18, reveal that the iron ores are predominantly composed of hematite and Graphite 2H which is a graphitic carbon with a hexagonal structure. Graphite 2H on the other hand, is a form of carbon allotrope meaning that the samples contain a combination of iron oxide (Fe) and carbon (C).





**Figure 4.17 XRD Spectrum of Gangra Transition Ore (Reduced) (a) Sample B2 and (b) Sample C2**

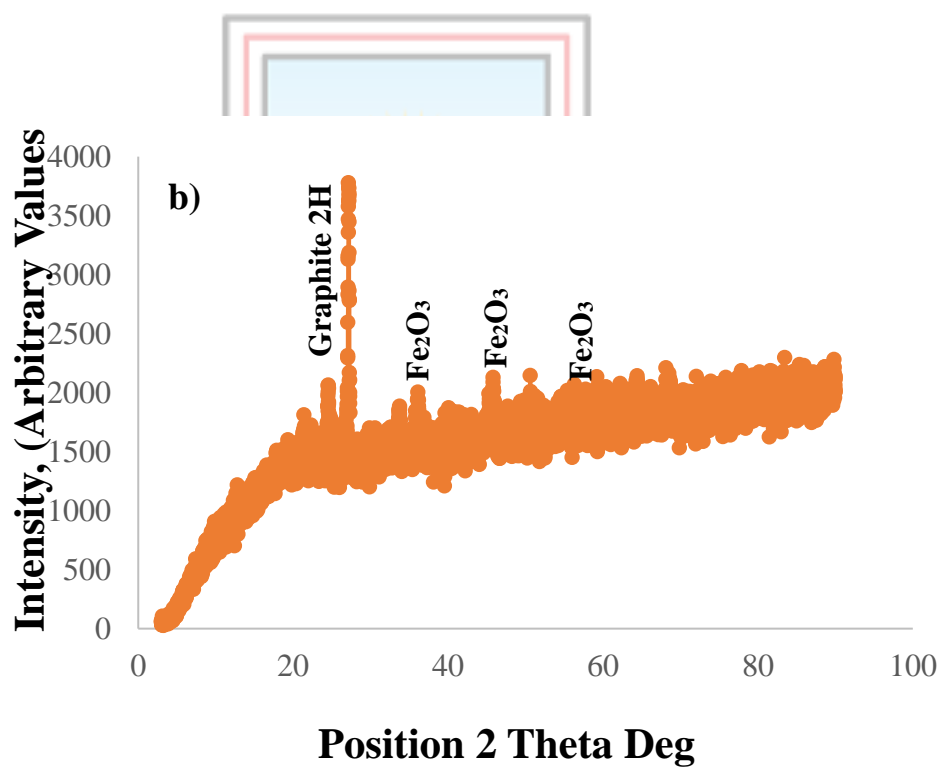
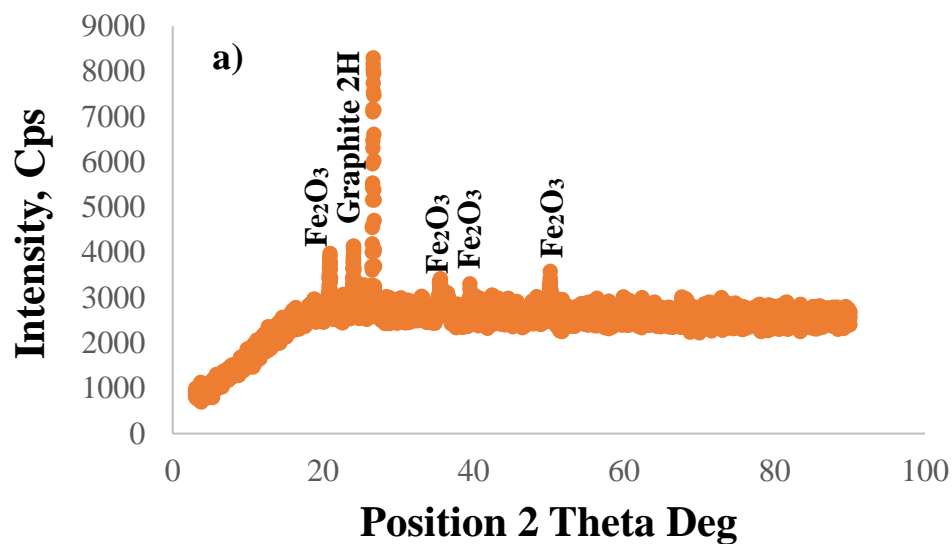
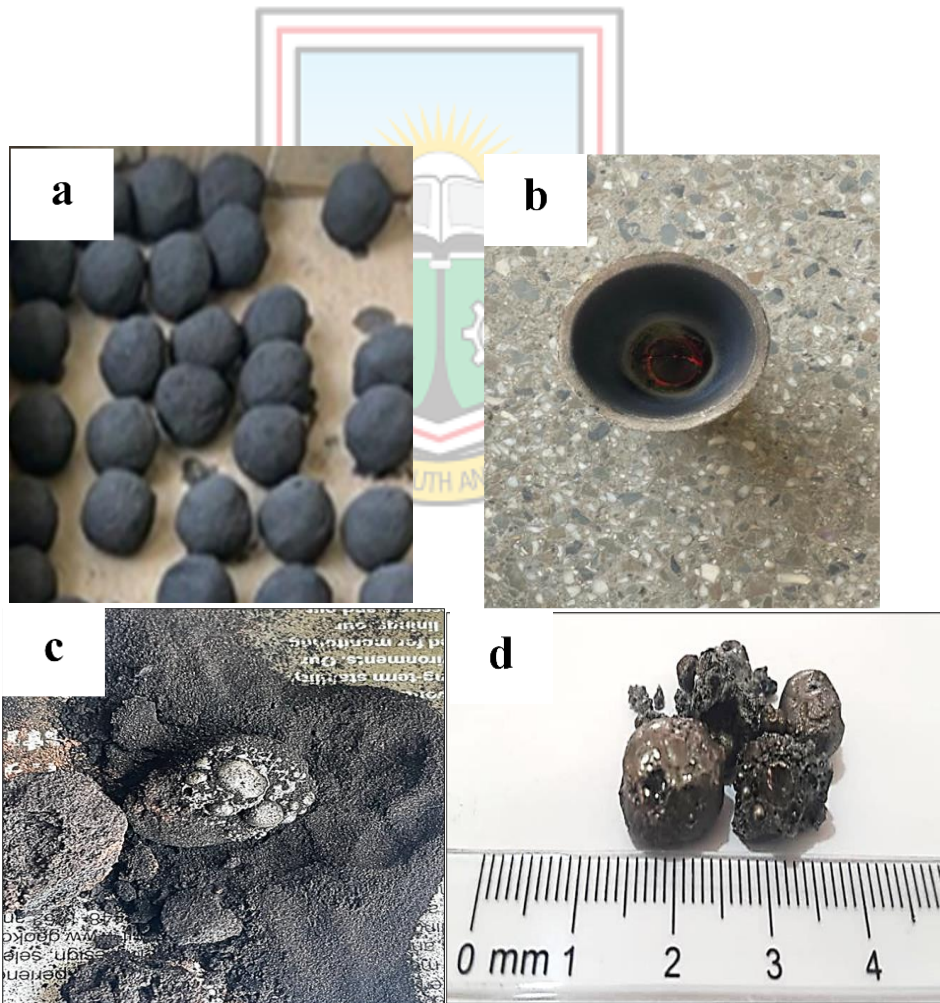


Figure 4.18 XRD Micrograph of Gangra Lowgrade Ore (Reduced) (a) Sample Z1, and (b) Sample Z2

#### 4.8 Formation of Iron Metal (Reduction Studies)

In this experiment, it was observed that the transition ore was more reducible than the lowgrade ore because the transition ore formed well-developed iron metal when subjected to microwave reduction Figure 4.19.

The silica in Gangra iron ore was also very reducible with the presence of excise carbon. It was also observed that the metal that was formed has an irregular sponge-like structure or shape Figure 4.19. This is a solid-state reaction and the pellets that were reduced were 100% magnetic. Both ore showed magnetic characteristics when subjected to a low-intensity magnet. The non-magnetic material was removed after magnetic separation. SEM-EDS results revealed that the iron metals along with the iron filings have high percentages of carbon (C), and silica ( $\text{SiO}_2$ ) using ELT as a reducing agent. The reduction tables for both ores are shown in Appendix B.



**Figure 4.19 Iron Metal Produced after Microwave Reduction (a) Carbon Pellets (b) Fire Clay Crucible (c) Mixture of Iron Ore with Carbon (d) Reduced Iron Ore**

Out of 29.40 wt. %, 24.97 wt. % (90%) of the material was attracted by the magnet (HSMAG Neodymium) of susceptibility of 1.0, leaving behind (10%) of the non-magnetic portion. For the pure iron (Fe) metal, it was strongly attracted to the magnet.

The material is a ferrosilicon [ $\text{Fe}_2\text{Si}_3$ ] compound, it contains iron and silicon and was attracted to the magnet due to the iron content. The samples contained hematite [ $\text{Fe}_2\text{O}_3$ ], and magnetite [ $\text{Fe}_3\text{O}_4$ ], marking up 70% lead to the magnetic characteristic of the ores Table 4.17. The other components of the rocks which make up 30%. These are either iron-bearing minerals or contain the inclusion of hematite, magnetite, or iron-bearing minerals. These minerals are pyrrhotite [ $\text{Fe}_{1-x}\text{S}$ ], ilmenite [ $\text{FeTiO}_3$ ], arsenopyrite [ $\text{FeAsS}$ ], pyrite  $\text{FeS}_2$ , garnet [ $\text{X}_3\text{Y}_2(\text{SiO}_4)_3$  where X and Y represent different elements that can vary, such as Al, Fe, Mg, and Ca]; amphibole [ $[\text{Ca}, \text{Na}]_{2-3}(\text{Mg}, \text{Fe}, \text{Al})_5(\text{Si}, \text{Al})_8\text{O}_{22}(\text{OH})_2$  (these are iron-bearing minerals and could be magnetic); erskebornite [ $\text{CuFeS}_2$ ]. Quartz [ $\text{SiO}_2$ ], and plagioclase [ $\text{NaAl}_2\text{Si}_2\text{O}_8$ ] are non-magnetic but contain the inclusion of iron-bearing minerals. Carbon [C], silica [ $\text{SiO}_2$ ], alumina [ $\text{Al}_2\text{O}_3$ ], and silicon carbide [ $\text{SiC}$ ] were left behind because they are non-magnetic. The efficiency of the separation varies depending on the specific composition and particle sizes of the materials involved.

#### 4.9 Petrographic Studies of Thin Sections

##### Gangra Fresh Rock

The rock shows early foliation of medium-grained quartz which is elongated and marked by amphibole, sheared partially altered. The quartz is recrystallised into fine to medium grains with triple junctions. The original quartz is marked by elongated fine to medium-grained opaque minerals.

Second-generation quartz marks a foliation that is strong in the rock. It is also drawn out and shows recrystallisation into finer grains. The quartz is marked by a strong band of medium-grained opaque minerals. This leaves the rock in an alternation of quartz-rich against opaque-rich bands. The earlier foliation is also marked by garnet which shows the inclusion of quartz and opaque minerals. This garnet has internal foliation that is marked by amphibole, chlorite, quartz, and fine opaque minerals. Yet the garnet is sheared parallel to the second foliation.

Garnet 2 is coarse-grained and marks the main foliation it contains the inclusion of opaque minerals and quartz yet does not show internal foliation.

Opaque mineral 3 is coarse-grained and overprints mark the main foliation. It rarely has inclusions of quartz. This opaque mineral is, however, overprinted by garnet 3.

Thin Section of Gangra Fresh Rock Figure 4.20. The model percentages of the minerals found in the rock are shown in Table 4.16

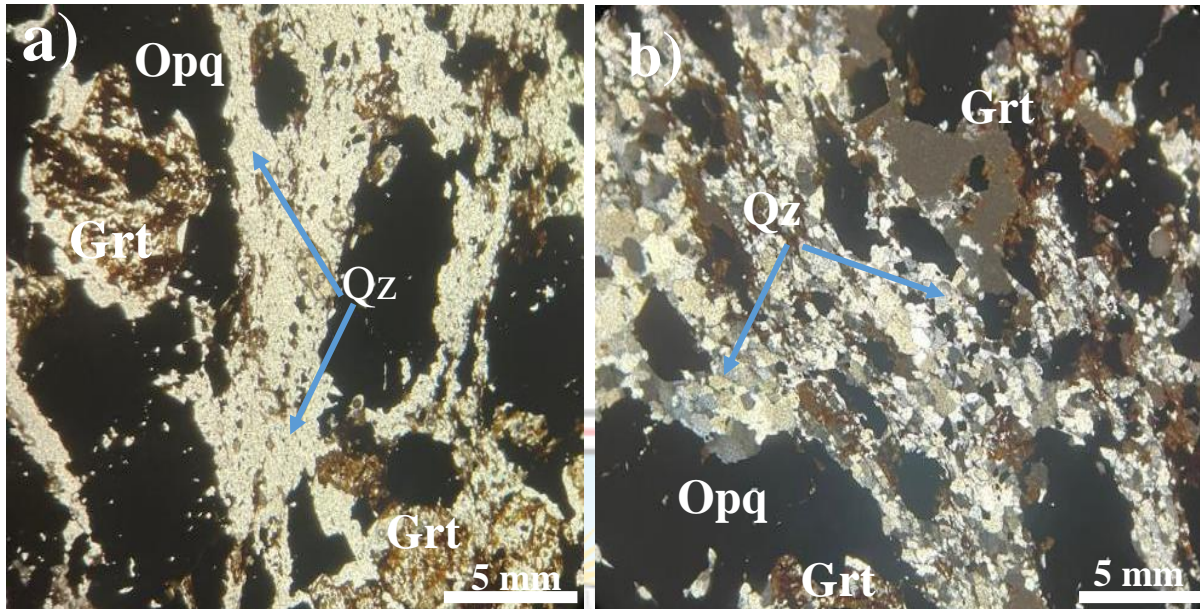


**Figure 4.20 Photomicrograph of Thin Sections under PPL (a) and XPL (b) of Fresh Rock (opq = Opaque Minerals; Qtz = quartz; and Grt = Garnet)**

Gangra Transition High-grade

The first foliation is made up of medium-grained subhedral plagioclase that is crowded with opaque minerals. This shows rare albite twinning with an extinction angle of 28.5 to 29 degrees. This is along the foliation that contains medium-grained quartz that is crowded and weakly recrystallised into medium to fine grains. The foliation is cut by secondary foliation marked by medium-grained amphiboles. These amphiboles have an extinction of 11. This is in line with plagioclase which is dusty with an albite twinning of 10 (Oligoclase). The amphibole is overprinted by pyroxene and shows weak pleochroism and extinction of 21 degrees (labradorite).

Quartz 2 is parallel to a foliation marked by amphibole which is sheared, medium-grained, and shows pleochroism that is yellowish to brownish green with an extinction angle of 9.5 degrees. Quartz is granular and shows a triple junction of recrystallisation of earlier quartz. This quartz has fine to medium grained opaque minerals at the margins.

Quartz 3 is at a higher angle and medium-grained. It is dusty and shows partial recrystallisation into medium to fine grains. It is overprinted by fine to medium-grained opaque minerals. These opaque minerals are coarse-grained and aggregate into sheared opaque minerals that mark the rock bands. These are overprinted by fine granules of garnet in the coarse-grained section.

Thin section of Gangra Transition high-grade Ore Figure 4.21. The modal percentages of the various minerals that are found in the rock are shown in Table 4.16.

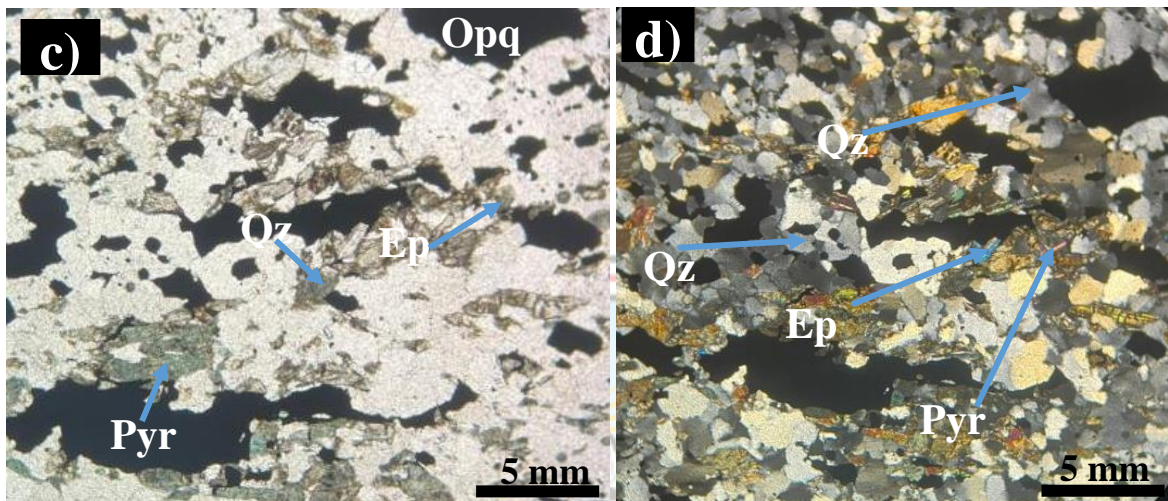


**Figure 4.21 Photomicrograph of Thin Sections under PPL (c) and XPL (d) of Gangra Transition High-grade (opq = Opaque Minerals; qtz = quartz; pyr = Pyroxene; and Ep = Epidote)**

#### Transition Low-grade

The transition low-grade is composed of quartz, garnet, amphibole, and opaque minerals. Most minerals within the transition lowgrade (L1) exhibit a hypidiomorphic to granular texture. The rock is largely dominated by quartz which has a percentage of 65%, amphibole 2%, garnet 3%, and 30% opaque minerals. The modal percentages of these minerals are shown in Table 4.16 The thin section of Gangra transition lowgrade Figure 4.22.

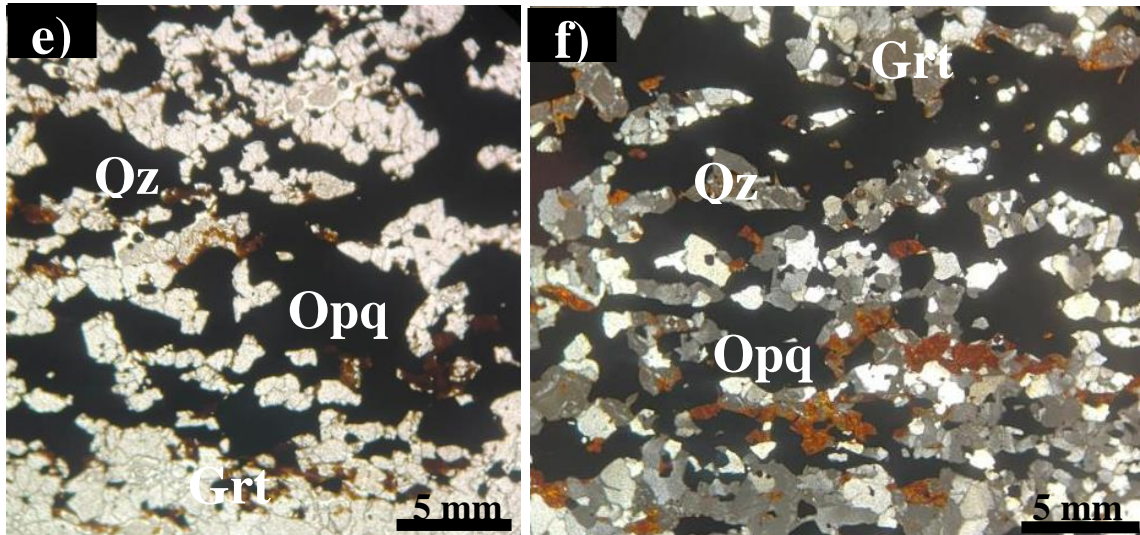


**Figure 4.22** Photomicrograph of Thin Sections under PPL (e) and XPL (f) of Gangra Transition Low-grade (opq = Opaque Minerals; qtz = quartz; and Garnet)

#### Gangra Oxide

Gangra oxide is composed of quartz, garnet, amphibole, and opaque minerals. Most minerals within the oxide (G1) exhibit a fine-grained texture. The rock is largely dominated by quartz which has a percentage of 50%, 5% amphibole, 10% garnet, and 35% opaque minerals. The modal percentages of these minerals are shown in Table 4.16 The thin section of Gangra oxide Figure 4.23.

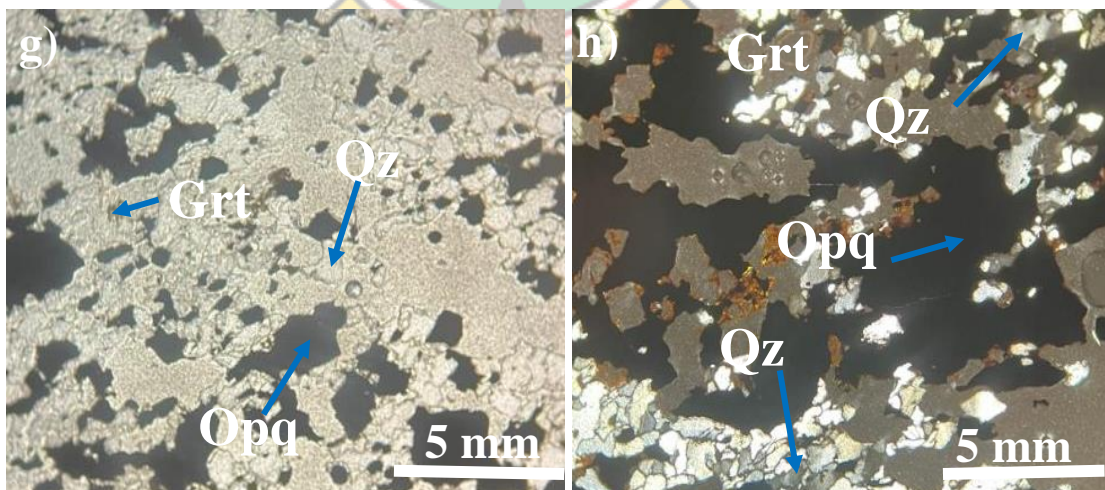


**Figure 4.23** Photomicrograph of Thin Sections under PPL (g) and XPL (h) of Gangra Oxide (opq = Opaque Minerals; qtz = quartz; and Garnet)

**Table 4.16 Modal Composition of the Rocks in Thin Section**

| <b>MINERALS</b> | <b>FRESH (F1*)</b> | <b>TRANSITION LOW (L1*)</b> | <b>OXIDE (G1*)</b> | <b>TRANSITION HIGH (T1)</b> |
|-----------------|--------------------|-----------------------------|--------------------|-----------------------------|
| Quartz          | 44                 | 65                          | 50                 | 30                          |
| Amphibole       | 5                  | 2                           | 5                  | 10                          |
| Garnet          | 10                 | 3                           | 10                 | 2                           |
| Chlorite        | 1                  |                             |                    |                             |
| Opaque mineral  | 40                 | 30                          | 35                 | 45                          |
| Plagioclase     |                    |                             |                    | 3                           |
| Pyroxene        |                    |                             |                    | 10                          |
| <b>TOTAL</b>    | <b>100%</b>        | <b>100%</b>                 | <b>100%</b>        | <b>100%</b>                 |

#### 4.10 Petrographic Studies (Polished Section)

##### Gangra Fresh Rock

Gangra fresh rock is composed of 14% pyritic magnetite, 10% hematite, 40% magnetite, 10% ilmenite, and 1% erskebornite. The rock is also composed of 25% gangue minerals. This rock has a granular texture. The modal percentages of the minerals are illustrated in (Table 4.17). Photomicrographs of Gangra Fresh rock in Plane Polarised Light (PPL), and Cross Polarised Light (XPL) are shown in Appendix A.

##### Gangra Oxide

Gangra oxide is composed of 2% pyritic magnetite, 5% hematite, 30% magnetite, 12% ilmenite, and 1% pyrrhotite. The rock is also composed of 50% gangue minerals and exhibits a granular texture. The modal percentages of the minerals found in this rock are illustrated in Table 4.17. Photomicrographs of Gangra oxide in Plane Polarised Light (PPL), and Cross Polarised Light (XPL) are shown in Appendix A.

##### Gangra Transition Lowgrade

Gangra transition low-grade is composed of 15% pyritic magnetite, 20% hematite, 20% magnetite, 10% ilmenite, and 10% erskebornite. The rock is also composed of 35% gangue minerals and exhibits a granular texture. The modal percentages of these minerals are illustrated in Table 4.18. Photomicrographs of Transition low-grade in Plane Polarised Light (PPL), and Cross Polarised Light (XPL) are shown in Appendix A.



Gangra Transition high-grade

Gangra transition high-grade is composed of 25% pyritic magnetite, 2% hematite, 27% magnetite, 5% ilmenite, and 1% arsenopyrite. The rock is also composed of 40% gangue minerals and exhibits a granular texture. The modal percentages of the minerals found in this rock are illustrated in Table 4.17. Photomicrographs of Gangra transition high-grade in polished section are illustrated in Appendix A.

**Table 4.17 Modal Composition of Rocks in Polished Section**

| Mineral           | Mineral Formula                | G1* | G1 | F1* | F1         | L1* | L1 | T1* | T1         |
|-------------------|--------------------------------|-----|----|-----|------------|-----|----|-----|------------|
| Gangue            |                                | -   | 50 | -   | 25         | -   | 35 | -   | 40         |
| Pyritic Magnetite | FeS <sub>2</sub>               | 35  | 2  | 40  | 14         | 30  | 15 | 45  | 25         |
| Hematite          | Fe <sub>2</sub> O <sub>3</sub> |     | 5  |     | 10         |     | 20 |     | 2          |
| Magnetite         | Fe <sub>3</sub> O <sub>4</sub> |     | 30 |     | 40         |     | 20 |     | 27         |
| Ilmenite          | FeTiO <sub>3</sub>             |     | 12 |     | 10         |     | 10 |     | 5          |
| Pyrrhotite        | Fe <sub>1-x</sub> S            |     | 1  |     | -          |     | -  |     | -          |
| Erskebornite      | CuFeSe <sub>2</sub>            |     | -  |     | 1          |     | 10 |     | -          |
| Arsenopyrite      | FeAsS                          |     | -  |     | -          |     | -  |     | 1          |
| <b>TOTAL</b>      |                                |     |    |     | <b>100</b> |     |    |     | <b>100</b> |

#### 4.11 Petrographic Studies VS Scanning Electron Microscopy

The petrographic studies of these iron ore rocks which involve examining polished sections under an optical microscope, provide valuable information about the mineral composition and texture of those rocks. These studies provide help to identify minerals like hematite, magnetite, ilmenite, erskebornite, arsenopyrite, and pyritic magnetite as well as associated rock formation minerals identified in thin sections like quartz, garnet, pyroxene, epidote, amphibole, and plagioclase. The thin section analysis allows for the characterisation of mineral phases, their distribution, and their association with one another.

Linking the SEM-EDS (Scanning Electron Microscope-Energy Dispersive X-ray Spectroscopy) analysis to the petrographic studies, the SEM-EDS provides elemental composition data. It determines the elemental composition of minerals, helping to confirm the presence of specific elements (silicon, iron, aluminum, oxygen, and carbon) in the identified minerals. For mineral identification, this petrographic study helps identify the minerals present in those rock samples but does not provide detailed information about their chemical composition.

For phase characterisation, SEM-EDS help differentiates between various iron oxides, such as ferrosilicon, iron silicide, silicon carbide, and iron II/III oxide, by analysing their

elemental composition. In summary, the petrographic studies provide a mineralogical context while the SEM-EDS analysis offers detailed elemental and chemical information. Combining both approaches leads to a comprehensive understanding of these iron ore samples.

#### **4.12 Geological Compositions of the Rock Samples**

##### **Gangra Fresh Rock**

Geologically, Gangra fresh rock is of metamorphic origin with foliated medium-grained quartz that has been recrystallised into fine to medium grains with triple junctions. This rock also exhibits earlier foliation that is marked by high-temperature andesine garnet which shows the inclusion of quartz and opaque such as pyritic magnetite, hematite, magnetite, ilmenite, and trace of erskebornite. This garnet is marked by amphibole, chlorite, quartz, and fine opaque minerals.

##### **Gangra Transition High-grade**

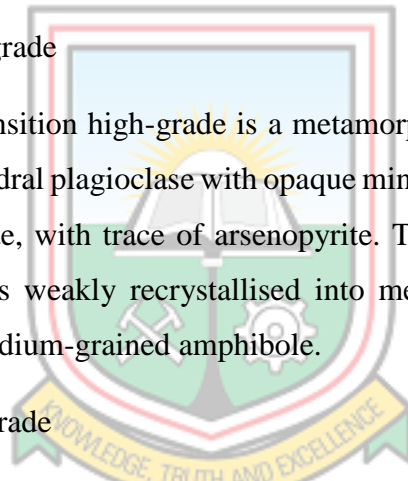
Geologically, Gangra transition high-grade is a metamorphic rock with foliation made up of medium-grained subhedral plagioclase with opaque minerals such as magnetite, hematite, pyritic magnetite, ilmenite, with trace of arsenopyrite. The foliation that is composed of medium-grained quartz is weakly recrystallised into medium to fine grains. Secondary foliation is marked by medium-grained amphibole.

##### **Gangra Transition Low-grade**

Geologically, this Gangra transition low grade is a metamorphic rock because it exhibits hypidiomorphic to granular texture and is composed of quartz, high-temperature andesine garnet, amphibole, and opaque minerals such as pyritic magnetite, hematite, ilmenite, and erskebornite.

##### **Gangra Oxide**

Gangra oxide is a metamorphic rock that exhibits fine-grained texture. It is largely dominated by 50% quartz, followed by 5% amphibole, 10% garnet, and 35% opaque minerals such as hematite, magnetite, ilmenite, and traces of pyritic, and pyrrhotite.



## CHAPTER 5

### CONCLUSIONS AND RECOMMENDATIONS

#### 5.1 Conclusions

Studies have been done on the properties of the low-grade and transition iron ore found in Mt. Gangra, Liberia. The selected ores were categorised as transition low-grade, and transition high-grade based on grade. The transition low-grade ore has an Iron (Fe) content of 44.814 Wt. %, while the low-grade ore has an iron (Fe) content of 50.147 Wt.%. Other ores include oxide, and fresh.

Intense of (Iron, Fe) content of these four rock samples from Mount Gangra, the oxide ranges from (50<% Fe<58% Fe), the fresh rock ranges from (20<%Fe< 35%), the transition high-grade ranges from (42<%Fe<50%Fe), and the transition low-grade ranges from 35<%Fe<42%Fe).

Mineralogically, a total of 50% gangue minerals (quartz, amphibole, plagioclase, garnet, chlorite, and pyroxene) are found in the oxide ore, 25% in the fresh rock, 35% in the transition low-grade ore, and 45% in the transition high-grade ore. The ores also contain ore minerals such as (hematite, magnetite, ilmenite, pyrrhotite, erskebornite, arsenopyrite, and pseudomorphic pyrite) with a total of 40% in the oxide ore, 30% in the fresh rock, 35% in the transition low-grade ore, and 45% making up the transition high-grade ore.

The ores also contain ore minerals such as (hematite, magnetite, ilmenite, pyrrhotite, erskebornite, arsenopyrite, and pseudomorphic pyrite) with a total of 40% in the oxide ore, 30% in the fresh rock, 35% in the transition low-grade ore, and 45% making up the transition high-grade ore. The material is a ferrosilicon [ $\text{Fe}_2\text{Si}_3$ ] compound, 90% attracted to the magnet due to 70% hematite and magnetite composition. The other minerals are either iron-bearing minerals or contain the inclusion of hematite, and magnetite. Hence, attracted to some extent to the magnet.

SEM-EDS analysis of both ores studied in this research reveals compounds such as iron silicide, ferrosilicon ( $\text{Fe}_2\text{Si}_3$ ), silicon carbide (SiC), Silica ( $\text{SiO}_2$ ), and iron (II/III) oxide. XRD analysis of the crushed and reduced Ores showed hematite, and graphite 2H, a hexagonal crystal structure, indicating the presence of graphitic carbon in the ore after microwave reduction.

The carbonaceous material (ELTs) used in this research work exhibit an effective reaction to produce well-developed iron metals after microwave reduction. Therefore, this carbonaceous material is a suitable reductant for Gangra iron ores.

## 5.2 Recommendations

The following recommendations are based on the findings of this research work:

- i. Evaluating the impact of different polymers on the reduction of the Gangra Iron Ore, such as HDPE, coconut shell, sawdust, etc.;
- ii. Optimizing the use of End-of-Life Tyres (ELTs) to reduce iron ore;
- iii. To establish the economic viability of manufacturing iron using a microwave, a cost study should be done;
- iv. Further research is required to determine the optimal pellet size for microwave reduction;
- v. The SEM-EDS equipment of the University of Mines and Technology (UMaT) Environmental Monitoring Laboratory needs to be calibrated to obtain better (SEM-EDS) results.



## REFERENCES

- Aakyiir, M. N. and Dankwah, J. R., (2017), "Recycling Blends of Waste Groundnut Shells and High-Density Polyethylene as Reductants in the Microwave Production of Iron Nuggets from the Pudo Iron Ore", *Ghana Journal of Technology*, Vol. 1, No. 2, pp. 45 - 50.
- Abotar, E., Dankwah, J. B., Koshy, P. and Dankwah, J. R. (2020), "Production of Metallic Iron from the Pudo Magnetite Ore using End-of-Life Rubber Tyre as Reductant: The Role of an Underlying Ankerite Ore as a Fluxing Agent on Productivity", *Ghana Mining Journal*, Vol. 20, No. 2, pp. 36-42.
- Aguilar, J. A. and Gomez, I., (1997), "Microwaves applied to Carbothermic Reduction of Iron Ore Pellets", *Journal of Microwave Power and Electromagnetic Energy*, No. 32, pp. 67-73.
- Adeleke, R., (2014), "Getting rid of the unwanted: highlights of developments and challenges of Biobeneficiation of iron ore minerals, a Review" *Society for Industrial Microbiology and Biotechnology*, pp.12
- Agrawal, R.K, and Pandey, P.K., (2005), "Productive Recycling of Basic Oxygen Furnace Sludge in Integrated Steel Plant", *Journal of Scientific and Industrial Research*, vol. 64, pp. 703-706
- Akihiro, S., and Mitamoto, T., (2010), "Overview of the market for direct reduced iron, *Kobelco Technology Review* 29, pp. 47-49.
- Akinbomi, J.G., Ogunwumi, O.T., Daniel, R.O., Eweje, O.O., Oluwajobi, S.A., Elegbede, S.O., Ajao A., and Oladeji, O., (2022), "Influence of waste sorting on the effectiveness of polymeric waste pyrolysis", *Global Journal of Technology and Engineering Advances*, Vol. 10, Issue 3, pp. 79-84
- Amikiya, C.A., (2014), "Characterisation of Iron Ore-A Case Study of Mount Tokadeh, Western Nimba Area, Liberia", *A Graduate School Thesis, Kwame Nkrumah University of Science and Technology, Kumasi, Ghana*, pp. 1-119.

- Anon. (2010), "Terrain, and Soil Baseline, ArcelorMittal Liberia Limited Western Range DSO Iron Ore Project", *URS Scott Wilson*, Scott House, Alencon Link, Basingstoke, Hampshire, United Kingdom, Vol. 3, Part 1.1, pp. 1-112, [edepot.wur.nl/483310](http://edepot.wur.nl/483310). Accessed: September 4, 2023.
- Anon. (2010), "Western Range DSO Iron Ore Project, Environmental Impact Assessment Overview, ArcelorMittal Liberia Limited", *Scott Wilson*, Vol. 1, pp. 1-8, ([PDF](#)) [Western Range DSO Iron Ore Project - ArcelorMittal - DOKUMEN.TIPS](#). Accessed: September 4, 2023.
- Anon. (2017), "Steel Statistical Yearbook", [Steel-Statistical-Yearbook-2017.pdf](#) ([worldsteel.org](#)). Accessed: May 16, 2023.
- Anon. (2019), "World Direct Reduction Statistic", [Midrex-STATSbook2019Final.pdf](#)  
Accessed: September 10, 2023
- Anon. (2020), "What does Iron Ore look like?" [www.ftmsino.com](http://www.ftmsino.com). Accessed: June 20, 2023.
- Anon. (2020), "Iron and Steel Technology Roadmap, IEA, Paris, <https://www.iea.org/reports/iron-and-steel-technology-roadmap>. Accessed: March 14, 2023.
- Anon. (2022), "Special Sample Results", *ArcelorMittal Liberia Limited, Yekepa, Liberia*
- Anon. (2023), "World Steel Association", [production totals - worldsteel.org](#). Accessed: July 5, 2023.
- Barbosa, M.G., Siboni, G., Vasconcelos, Corrêa de Araujo, A., Sylow T., and Venturini, M.J., (2016), "Overview of ArcelorMittal Mining Operations and Research & Development Function," *ArcelorMittal Maizières Mining and Mineral Processing Research Center of ArcelorMittal Maizières*, pp. 8-14
- Barbosa M.G., Siboni G., Venturini, M.J., and Correa de Araujo, A., (2017), "The use of Drill Core Blends to Predict Sintering Performance", *Iron Ore Conference / Perth, Australia*, pp.1-6.
- Basdag, A., and Arol, A.I., (2002), "Coating of Iron Oxide Pellet for Direct Reduction" *Scandinavian Journal of Metallurgy*, Vol. 31, Issue 3, pp. 229-233.

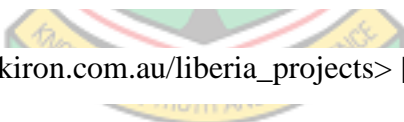
- Berge, J.W., (1974), “Geology, Geochemistry and Origin of the Nimba Itabirite and Associated Rocks, Nimba County, Liberia”, *Econ. Geol.* Vol. 69, pp. 80–92.
- Berge, J.W., Johansson, K., and Jack, J. (1977), “Geology and Origin of the Hematite Ores of the Nimba Range, Liberia”, *Econ. Geol.* Vol. 72, pp. 582–607
- Bhaskar, A., Assadi, M., and Somehsaraei, H.N., (2020), “Decarbonisation of the Iron and Steel Industry with Direct Reduction of Iron Ore with Green Hydrogen”, *Energies*, Vol. 13, Issue 758, pp. 1-23
- Chandio, A.D., Channa, I.A., Madad, A.A.S.S., Rizvi, S.B.H., Shah, A.A., Shar, J.A.M.A., and Alhazaa, A., (2023), “Beneficiation of Low-Grade Dilband Iron Ore by Reduction Roasting”. *Metals*, Vol. 13, Issue.296, pp. 1-16
- Coakley, J.G., (2004), “*The Mineral Industry of Liberia, US Geological Survey Minerals*”, *Yearbook 2004*, <https://bit.ly/3rarpWB>. Accessed: May 10, 2023.
- Costa, S.M.R, Fowler D, Carreira, G.A., Portugal I, and Silva C.M., (2022), “Production and Upgrading of Recovered Carbon Black from the Pyrolysis of End-of-Life Tires” *Material Review*, Vol. 15, Issue 2030, pp. 1-19
- Dankwah, J. R., Koshy, P., O’Kane, P., and Sahajwalla, V., (2012), “Reduction of FeO in EAF Steelmaking Slag by Blends of Metallurgical Coke and End-of-Life Tyre”, *Steel Research International*, Vol.83, Issue 8, pp. 766-774.
- Dankwah, J.R., and Koshy, P., (2013), "Production of Metallic Iron from Iron Oxide ( $\text{Fe}_2\text{O}_3$ ) using End-of-Life Rubber Tyre and its Blends with Metallurgical Coke as Reductants," *In International Journal of Engineering Research in Africa, Trans Tech Publications Ltd*, Vol. 10, pp. 1-12
- Dankwah, J. R., Baawuah, E., Dankwah, J. and Koshy, P., (2015a), “Recycling Mixed Plastic Waste and its Blend with Sawdust as Reductant in Ironmaking,” *Proceedings of 24th International Mining Congress and Exhibition of Turkey (IMCET 2015), April 14-17, Antalya, Turkey*, pp. 1387-1394.

- Dankwah, J. R., Fosu, A.Y., Fosu, N. and Koshy, P., (2015b), “Carbothermal Upgrading of the Awaso Bauxite Ore using Waste Pure Water Sachets as Reductant”, *Ghana Mining Journal*, Vol. 15, No. 1, pp. 64-72.
- Dankwah, J. R. (2018), “Laboratory Studies on the Effect of End-of-Life Rubber Tyre Blending with Metallurgical Coke on Slag Foaming in Electric Arc Furnace Steelmaking”, *Ghana Journal of Technology*, Vol. 3, No. 1, pp. 48 -57.
- Dankwah, J.R., (2022), Ferrous Metallurgy MSc Lecture Note, Mineral Engineering Department, Faculty of Mining, and Minerals Technology, University of Mines and Technology (UMaT), Tarkwa, Ghana
- Dawkins, M., Saal, D., Marco, J.F., Reynolds, J., and Dann, S., (2023), “An iron ore-based catalyst for producing hydrogen and metallurgical carbon via catalytic methane pyrolysis for decarbonisation of the steel industry”, *International Journal of Hydrogen, Energy*, pp.1-13.
- Dering, D., Swartz, C., and Dogan, N., (2020), “Dynamic Modeling and Simulation of Basic Oxygen Furnace (BOF) Operation” *Processes*, Vol.8, No.483, pp.1-23
- Dutta, S.K., and Sah R., (2016), “Direct Reduced Iron: Production”, *Encyclopedia of Iron, Steel, and Their Alloys*. Taylor and Francis: New York, 1st Edition, pp. 1082-1108.
- European Tyre & Rubber Manufacturers’ Association, Statistic report. <https://www.etrma.org/wp-content/uploads/2021/12/20211215-Statistics-booklet2021VF.pdf>, 2021. Accessed: May 5, 2023.
- Forsmo, S.P.E., Apelqvist, A.J., Björkman, B.M.T., and Sam skog, P.O., (2006), “Binding Mechanisms in Wet iron Ore Green pellets with a Bentonite binder”, *Powder Technol.*, Vol. 169, 147–158.
- Ganjian, E., Khorami, M., and Maghsoudi, A.A., (2009), “Scrap-Tyre-Rubber Replacement for Aggregate and filler in concrete”, *Construct. Build. Mater*, Vol. 23, pp. 1828-1836.



- Gamisch, B., Huber, L., Gaderer, M., and Dawoud, B., (2022). “On the Kinetic Mechanisms of the Reduction and Oxidation Reactions of Iron Oxide/Iron Pellets for a Hydrogen Storage Process”, *Energies* 2022, Vol.15, Issue 21, pp. 1-29
- Gines, M.J.L., William, F.J., Graziutti, A., and Ajargo, F., (2016), “Characterization of the Steam-CO<sub>2</sub> Reforming Catalyst Employed in the Midrex Direct Reduction Process”, *6<sup>th</sup> IAS Ironmaking Conference, 2007, Rasario, Argentina*, pp. 49-58
- Gulhane, A., (2017), “Overview of ITmk3 Process”, *International Journal of Industrial Engineering Research and Development*, vol.8, Issue 2, pp. 01–04.
- Gunn, A.G., Dorbor, J.K., Mankelow, J.M., Lusty, P.A.J., Deady, E.A., Shaw, R.A., and Goodenough, K.M., (2018), “A review of the mineral potential of Liberia”, *Ore Geology Reviews*, Vol.101, pp.413-431.
- Heneghan, J., (2010), “Pre-feasibility study, Liberia western range iron ore project”, *Technical version*. A report prepared for ArcelorMittal Liberia. 3rd Revision, 6th January 2010. pp. 32-34
- Holappa, L., (2020), “A General Vision for Reduction of Energy Consumption and CO<sub>2</sub> Emissions from the Steel Industry”, *Metals* 10, Vol.10, pp. 1-21.
- Howard, L.H., (1987), “Society for Mining, Metallurgy and Exploration, Mining Engineering Handbook”, 2nd edition, *American Institute of Mining, Metallurgical and Petroleum Engineers*, New York, Vol. 1., pp. 212
- Hu, Q., He, Y., Wang, F., Wu, J., Ci, Z., Chen, L., Xu, R., Yang, M., Lin, J., Han, J., and Zhang, D (2021), “Microwave technology: a novel approach to the transformation of natural metabolites”, *Chin Med*, vol.16, No. 87, pp.1-22
- Jahirul, M.I., Hossain, F.M., Rasul, M.G., and Chowdhury, A.A, (2021), “A Review on the Thermochemical Recycling of Waste Tyres to Oil for Automobile Engine Application” *Energies*, Vol. 14, Issue 13, pp. 1-18
- Kannan, D., Diabat, A., and Shankar, K.M., (2014), “Analysing the Drivers of End-of-Life Tire Management using Interpretive Structural Modeling (ISM)”, *The International Journal of Advanced Manufacturing Technology*, Vol.72, pp.1603-1614.

- Kikuchi, S., Shuzo I, Kobayashi, I. Dr., Osamu T., and Koji T., (2010), "ITmk3 Process" *Kobelco Technology Review*, Vol. 29, pp. 77-84.
- Madias, J. (2014), "Electric Furnace Steelmaking", In *Treatise on Process Metallurgy, Elsevier Ltd*, Vol. 3, Chapter 1.5, pp. 271-300.
- Madias, J., (2016), "Ironmaking and Steelmaking Processes - Greenhouse Emissions, Control, and Reduction, *Electric Arc Furnace Chapter*, Chapter 10, pp. 1-15
- Masaaki, A., Uemura, H., and Sakaguchi, T., (2010), "MIDREX Processes," *Kobelco Technology Review*, Vol. 29, pp. 50-57.
- Mondol, S.S., (2016), "A Review of Steelmaking Technologies", *Article in International Journal of Science and Research (IJSR)*, Vol. 5. pp. 283-286.
- Moraes, S.L. de, Lima, J.R.B. De, and Neto, J.B.F., (2018), "Effect of Colloidal Agents in Iron Ore Pelletising", *Mineral Processing, and Extractive Metallurgy, Review*, Vol 39, Issue 10, pp. 1-6
- Nakhaeinejad, M., and Zarei, F., (2020) "Analysis of the Factors Affecting the Iron Ore Pellet FeO Index using Data Mining Technique", *Journal System Dan Manajemen Industri*, Vol. 4, No. 2, pp. 83-92.
- Odenthal, H.J., (2017), "An Insight into Steelmaking Process by Computational Fluid Dynamics", Conference Paper, XVIII international UTE-Congress, *Electro-technologies for Material Processing*, Hannover, Germany, June 6-9, 2017, pp.9-19.
- Pal, J., Ammasi, A., Bandyopadhyay, B.S., Dwarapudi, S., and Paul, I., (2022), An Innovative Approach to Replace bentonite in Hematite Ore Pelletizing with Organic Binder, "*Mineral Processing and Extractive Metallurgy Review*" Vol. 44, No. 6, pp. 1-13.
- Patisson, F., and Mirgaux, O., (2020), "Hydrogen ironmaking": How it works, *Metals*, Vol. 10, Issue. 922, pp. 1-15.
- Petruk, W., (2000), "Applied Mineralogy in the Mining Industry", *1st Ed., Elsevier Science B.V.* Amsterdam, The Netherlands, 151 pp.

- Pineau, A., Kanari, N., Gaballah, I., (2006), “Kinetics of Reduction of Iron Oxides by H<sub>2</sub>”: Part I: Low-Temperature Reduction of Hematite, *Termochimica Acta*, Vol., 447, pp. 89–100.
- Ramakgala, C., and Danha, G., (2019), “A review of ironmaking by direct reduction Processes: Quality requirements and sustainability”. *Procedia Manufacturing*, Vol. 35, pp. 242–245.
- Sani, H.F., (2021), “Iron Ore Shipping Review” pp.1-25. Online from [\(2\) \(PDF\) Iron Ore Shipping Review \(researchgate.net\)](#) [Accessed: June 13, 2023]
- Siddiqui M.D. I.H, (2023), “Innovative Green Steelmaking Process for Sustainable Steel Production” *VW Applied Sciences*, Vol. 5, Issue 1, 171-176
- Spreitzer, D., Schenk, J., (2019), “Reduction of Iron Oxides with Hydrogen” A Review, *Steel Research International*, Vol.90, Issue 10, pp.1-17
- Strezov, V., (2006), “Iron ore reduction using sawdust: Experimental analysis and kinetic modeling”, *Renewable Energy*, Vol.31, pp. 1892–1905.
- Tomlinson, S., (2004), “Liberia projects” Available Online from:  
  
[http://www.westpeakiron.com.au/liberia\\_projects](http://www.westpeakiron.com.au/liberia_projects) [Accessed: May 12, 2023]
- Tuck C, Virta R., (2011), Minerals yearbook: Iron ore. USGS [Internet]. 2013. Available from: [http://minerals.usgs.gov/minerals/pubs/commodity/iron\\_ore/myb1-2011-feore.pdf](http://minerals.usgs.gov/minerals/pubs/commodity/iron_ore/myb1-2011-feore.pdf) [Accessed: April 2023].
- Ueda, S., Watanabe, K., Yanagiya, K., Inoue, I., and Ariyama, T., (2009), “Improvement of Reactivity of Carbon Iron Ore Composite with Biomass Char for Blast Furnace”, *ISIJ Int.*, Vol., 49, pp. 1505–1512.
- United States Geological Survey (USGS), (1993-2006), “Slag-iron and steel,” Annual Review, *Mineral Industry Surveys*, U.S. Geological Survey, Minerals Yearbook, Reston, Va., USA,

- US Environmental Protection Agency, EPA., (1994), “Technical Resource Document”, *Extraction and Beneficiation of Ores, and Minerals*, Vol. 3, August 1994 Office of Solid Waste, Special Waste Branch 401 M Street, SW Washington, DC 20460, 530-R-94-030
- Van Der Kraaij F.P.M., (2001), “*Iron Ore*”, <https://bit.ly/466XKfW>. Accessed: May 16, 2023.
- Vishwakarma, S.K., (2016), “Blast Furnace” *Tata Steel Limited*, Jamshedpur Division, Mechanical Engineering Department, DIT University, Dehradun, India, pp. 1-41
- Wei, D. Cang, Y. Bai, D. Huang and Liu, X., (2016), “Reduction characteristics and kinetics of iron oxide by carbon in biomass”, *Ironmaking & Steelmaking*, Vol. 43, Issue 2, pp. 144-152
- World Steel Association, (2020), Total production of crude steel. Available at: <https://www.worldsteel.org/steel-by-topic/statistics/steel>. Accessed: May 10, 2023.
- Yildirim, I.Z., and Prezzi, M., (2011), “Chemical, Mineralogical, and Morphological Properties of Steel Slag”, *Advances in Civil Engineering*, Vol. 2011, pp.1-14
- Zandi, M., Martinez-M.P., and Fray, T.A, (2010), “Biomass for iron ore sintering”, *Minerals Engineering*, Vol. 23, Issue 14, pp. 1139–1145.
- Zhang, (2005), “Systematic Energy Saving in Ironmaking: The Priority to be Paid in Technological Process of China’s Steel Industry in the 21st Century”, *Iron Steel*, Vol. 40, pp. 1–4.
- Zhao, H., Zhou, F., Zhao, H., Ma, C., and Zhou, Y., (2022a), “A Review on the Effect of the Mechanism of Organic Polymers on Pellet Properties for Iron Ore Beneficiation” *Polymers*, Vol. 14, Issue 22, pp. 1-21.
- Zhao, H., Zhou F., Ma C., Wei Z., and Long W. (2022b) “Bonding Mechanism and Process Characteristics of Special Polymers Applied in Pelletising Binders” *Coating*, Vol. 12, Issue 11, pp. 1-21.

## APPENDICES

### APPENDIX A PHOTOMICROGRAPHS OF POLISHED SECTION SHOWING GANGRA FRESH ROCK, OXIDE, TRANSITION LOW-GRADE, AND TRANSITION HIGH-GRADE

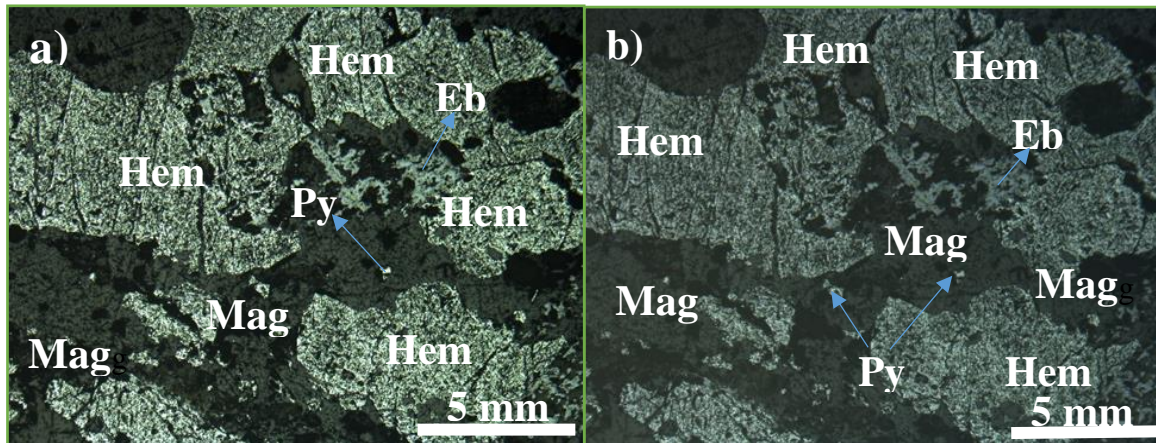


Figure A1 Photomicrographs of Polished Sections under PPL (a) and XPL (b) of Gangra Iron Ore Showing Fresh ((Mag = Magnetite; Hem = Hematite; Py = Pyrite; and Ebn = Erskebornite)

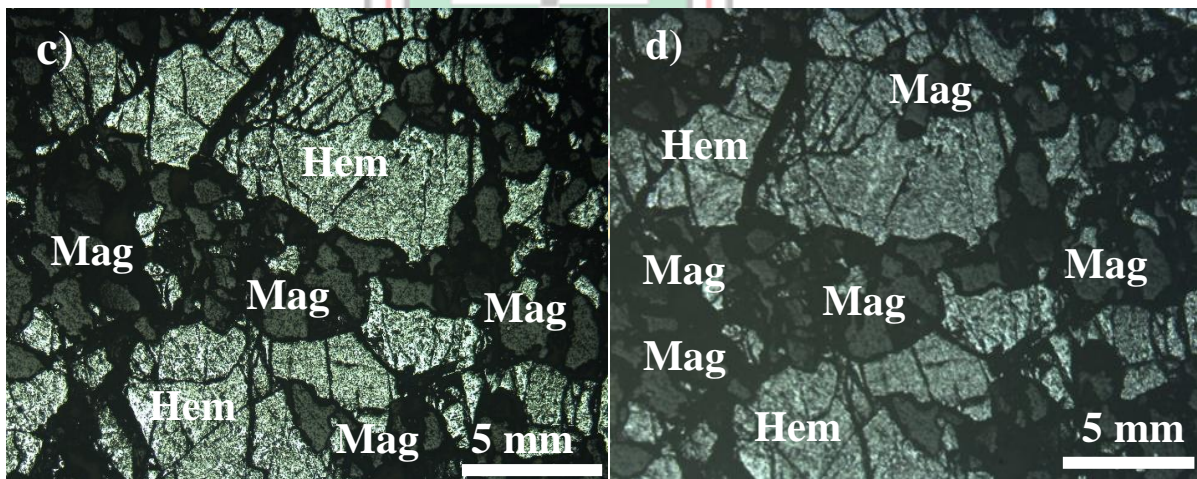
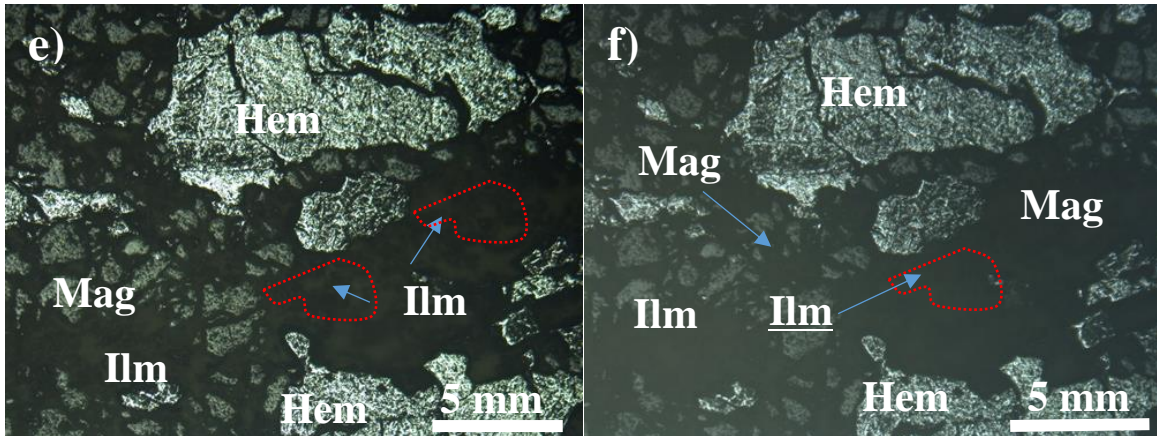
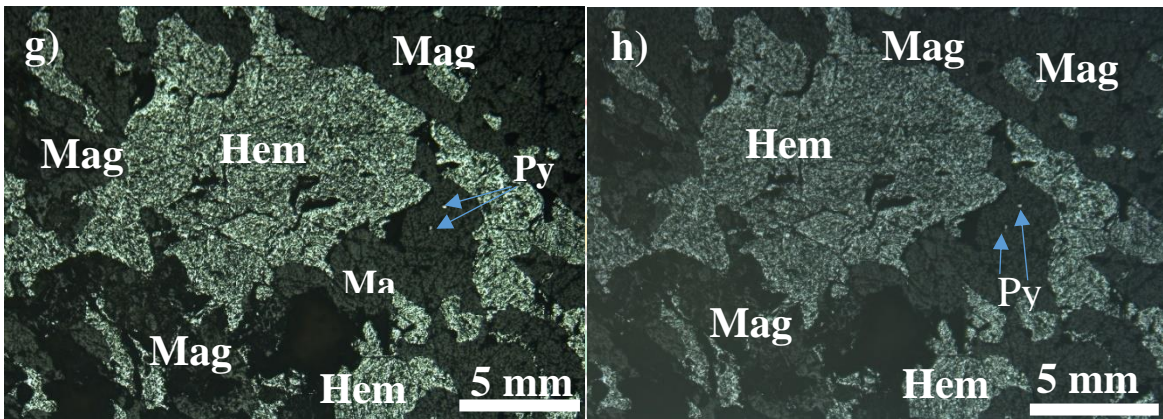


Figure A2 Photomicrographs of Polished Sections under PPL (c) and XPL (d) of Gangra Iron Ore Showing Oxide (Mag = Magnetite; Hem = Hematite)



**Figure A3 Photomicrographs of Polished Sections under PPL (e) and XPL (f) of Gangra Iron Ore Showing (b) Transition Low-grade (Mag = Magnetite; Hem = Hematite; Ilm= Ilminate)**



**Figure A4 Photomicrographs of Polished Sections under PPL (g) and XPL (h) of Gangra Iron Ore Showing Transition High-grade (Mag = Magnetite; Hem = Hematite; Py = Pyrite)**

**APPENDIX B TABLE OF VALUES FOR MICROWAVE REDUCTION OF  
GANGRA LOWGRADE ORE**

**Table B1 Reduction of Gangra Lowgrade Ore at 70 Wt% Ore**

| <b>Pellet ID</b> | <b>Time(Min)</b> | <b>Initial Mass</b> | <b>Mass after Reduction</b> | <b>Weight Loss</b> | <b>% Weight Lost</b> |
|------------------|------------------|---------------------|-----------------------------|--------------------|----------------------|
| A1               | 5                | 29.50               | 26.15                       | 3.35               | 11.36                |
| A2               | 10               | 29.72               | 24.97                       | 4.75               | 15.98                |
| A3               | 15               | 29.72               | 22.81                       | 6.91               | 23.25                |
| A4               | 20               | 28.99               | 20.88                       | 8.11               | 27.98                |
| A5               | 25               | 29.78               | 22.64                       | 7.14               | 23.98                |
| A6               | 30               | 29.90               | 20.31                       | 9.59               | 32.07                |
| A7               | 35               | 29.33               | 20.17                       | 7.16               | 24.41                |
| A8               | 40               | 29.40               | 22.06                       | 7.34               | 24.97                |

**Table B2 Reduction of Gangra Lowgrade Ore by 75 Wt% Ore**

| <b>Pellet ID</b> | <b>Time(Min)</b> | <b>Initial Mass</b> | <b>Mass after Reduction</b> | <b>Weight Loss</b> | <b>% Weight Lost</b> |
|------------------|------------------|---------------------|-----------------------------|--------------------|----------------------|
| A1               | 5                | 28.82               | 27.45                       | 1.37               | 4.75                 |
| A2               | 10               | 29.67               | 24.93                       | 4.74               | 15.98                |
| A3               | 15               | 28.89               | 23.67                       | 5.22               | 18.07                |
| A4               | 20               | 28.60               | 23.13                       | 5.47               | 19.13                |
| A5               | 25               | 28.60               | 17.55                       | 11.41              | 39.40                |
| A6               | 30               | 29.97               | 19.26                       | 10.71              | 35.74                |
| A7               | 35               | 29.59               | 20.69                       | 8.90               | 30.08                |
| A8               | 40               | 28.68               | 22.30                       | 6.38               | 22.25                |

**APPENDIX C TABLE OF VALUES FOR MICROWAVE REDUCTION OF  
GANGRA LOWGRADE ORE**

**Table C1 Reduction of Gangra Transition Ore by 70 Wt% Ore**

| <b>Pellet ID</b> | <b>Time(Min)</b> | <b>Initial Mass</b> | <b>Mass after Reduction</b> | <b>Weight Loss</b> | <b>% Weight Lost</b> |
|------------------|------------------|---------------------|-----------------------------|--------------------|----------------------|
| A1               | 5                | 29.43               | 26.43                       | 3.00               | 10.19                |
| A2               | 10               | 28.45               | 21.72                       | 6.72               | 23.62                |
| A3               | 15               | 29.43               | 20.33                       | 9.10               | 30.92                |
| A4               | 20               | 28.67               | 21.70                       | 6.97               | 24.31                |
| A5               | 25               | 28.72               | 22.99                       | 5.73               | 19.95                |
| A6               | 30               | 29.11               | 19.98                       | 9.13               | 31.36                |
| A7               | 35               | 29.29               | 16.52                       | 12.77              | 43.60                |
| A8               | 40               | 28.58               | 21.51                       | 7.07               | 24.74                |

**Table C2 Reduction of Gangra Transition Ore by 75 Wt% Ratio Ore**

| <b>Pellet ID</b> | <b>Time(Min)</b> | <b>Initial Mass</b> | <b>Mass after Reduction</b> | <b>Weight Loss</b> | <b>% Weight Lost</b> |
|------------------|------------------|---------------------|-----------------------------|--------------------|----------------------|
| A1               | 5                | 29.71               | 25.98                       | 3.73               | 12.55                |
| A2               | 10               | 29.01               | 23.07                       | 5.94               | 20.48                |
| A3               | 15               | 29.60               | 23.22                       | 6.38               | 21.55                |
| A4               | 20               | 29.70               | 19.55                       | 10.15              | 34.18                |
| A5               | 25               | 28.75               | 19.05                       | 9.70               | 33.74                |
| A6               | 30               | 29.61               | 18.90                       | 10.71              | 36.17                |
| A7               | 35               | 29.19               | 16.53                       | 12.66              | 43.37                |
| A8               | 40               | 29.77               | 17.54                       | 12.23              | 41.08                |

Vital Formulas

The initial weight of the pellet before reduction = X

The final weight of the pellet after reduction = Y

Reduce materials = weight of pellet after reduction

Weight lost = Initial weight of pellet – Final weight of pellet

$$\text{Percent weight lost} = \frac{X - Y}{X} \times 100$$



**APPENDIX D MOUNT GANGRA LOWGRADE STOCKPILES**

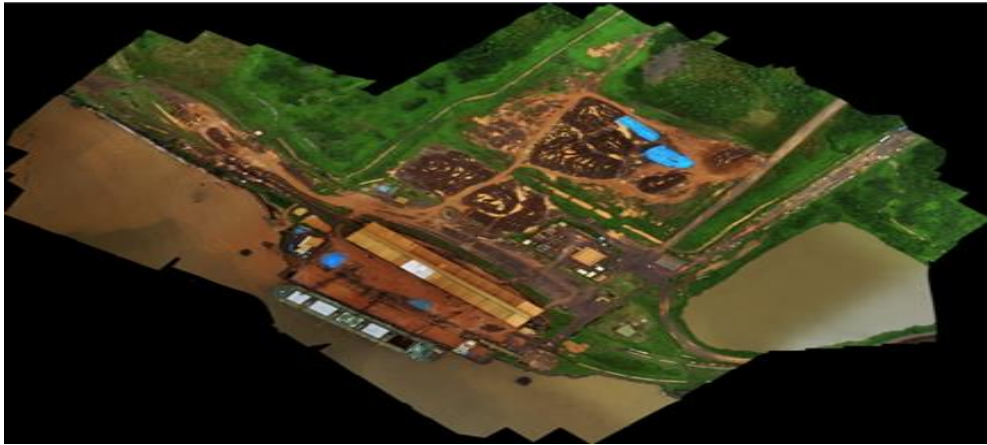


**Figure D1 Buchanan Port Lowgrade Stockpile, Liberia**



**Figure D2 Gangra Lowgrade Stockpile 2B, Liberia**

## Index

### A

Aakyiir, 35, 38, 87 Aakyiir  
and Dankwah, 38 Abotar,  
1–2, 42–43, 47, 87  
agent, reducing, 21–22, 24, 47, 49, 51, 77  
Agrawal, 32–33, 87  
Akihiro, 24–25, 87  
Alternative Ironmaking Processes  
    DR PROCESS, 24  
Aluminium, 60–62  
Amikiya, 6, 10, 12, 14–20, 87  
amphibole, 18, 78–85  
applications, 34, 38, 65  
arsenopyrite, 78, 83–85  
Atomic, 57, 59, 62–73

### B

ball mill, 20, 47–48  
Banded Iron Formation, 10, 14  
banded iron formations (BIF), 14,  
16 Barbosa, 4, 88  
basic oxygen furnace. *See* BOF  
basic oxygen furnace charge, 33  
Berge, 16, 89  
BF (blasting furnaces), 22, 27, 29–  
30 binders, 35–37, 49–50  
    iron ore pelletising, 37  
biomass, 44–45, 94  
blast furnace and basic oxygen converter  
    process routes accounting, 22  
blast furnace route, 21  
blast furnaces, 14–15, 21–24, 27–31,  
    33, 44–45, 93–94  
blasting furnaces. *See* BF  
blend, 48, 89  
BOF (basic oxygen furnace), 30–31, 33, 90

### C

carbon, 2, 29, 31–33, 39–40, 45, 61–66,  
    68–70, 73–74, 77–78, 83, 94  
carbonaceous material, 1–2, 13, 35, 47,  
    51, 86  
carbon monoxide, 22, 32–33, 45  
Chemical Analysis of Gangra Transition  
    Ore, 68–70, 72–73

chemical composition, 35, 52–53, 55–56,  
    83 chlorite, 78, 82, 84–85  
coal, 21, 23–25, 29, 45  
    non-coking, 24, 28  
coke, 21–22, 44–45  
combination of silicon and iron sources,  
    60 compositions, elemental, 52–53, 83–84  
compounds, 58, 63, 65, 67, 69–70, 72, 85  
cone crusher, 47–48  
content, 12, 55, 85  
countries, 1, 7–8, 10–12  
Cross Polarised Light, 82  
crude steel, 8, 22, 30, 94  
Crude Steel Production by Region,  
    11 crystals, 29

### D

Dankwah, 1–2, 22–23, 35, 38–39, 42, 87,  
    89–90  
Dankwah and Koshy,  
    39 deposits, 4, 9–10, 13  
diffraction peaks, 53  
direct reduced iron. *See* DRI  
direct reduction, 4, 22, 25, 88–89  
direct reduction ironmaking, 24  
Direct Reduction of Iron in Electric Arc  
    Furnace, 31  
direct reduction Processes, 25, 43,  
    93 Direct Shipping Ore. *See* DSO  
DRI (direct reduced iron), 23–26,  
    87 DR process, 23  
DSO (Direct Shipping Ore), 4–6, 13, 52

### E

EAFs (electric arc furnaces), 25, 30–31, 33–  
    34  
electric arc furnaces. *See* EAFs electric  
    arc furnace steelmaking, 34, 90  
electron beam, 52  
Element, 15, 21, 31, 53, 57–73, 78, 83  
elemental silicon, 68, 70  
elevation, 5, 48  
ELTs (End-of-Life Tyres), 1–3, 38–40, 42,  
    51, 68, 77, 86, 89  
End-of-Life Tyres. *See* ELTs

energy, 21, 28–29, 38, 44–45, 52–53, 57–59, 61–62, 64, 66, 68, 70–72  
energy storage density (ESD), 44  
erskebornite, 78, 82–85, 95  
ESD (energy storage density), 44

## F

ferrosilicon, 60, 63–65, 67–68, 70–72, 78, 83, 85  
fireclay, 51  
fluxes, 15, 21, 32–34  
foliation, 78–79, 84  
fresh rock, 79, 82, 84–85  
furnace, 21–23, 27, 32–33, 41  
  basic oxide, 31–32

## G

Gangra, 1–2, 4–6, 47, 63, 82, 84–85  
Gangra Fresh Rock, 54, 78, 82, 84, 95  
Gangra Iron Ore Deposit, 1  
Gangra iron ores, 1–3, 54–56, 77, 86  
Gangra Lowgrade Ore, 57, 59, 66, 73, 76, 97–98  
Gangra Lowgrade Pulverised Ore for Region, 59–60  
Gangra Oxide, 54, 81–82, 84  
Gangra Pulverised Transition Ore, 61–62  
Gangra Transition, 60, 68, 70–71, 74, 80, 82–84  
Gangra Transition High-grade, 54, 79–80, 84  
Gangra Transition Ore, 62, 67–75, 98  
gangue minerals, 10, 13–15, 82–83, 85  
garnet, 78–85  
  high-temperature amandine, 84  
goethite, 4, 12–14, 18  
Graphite 2H, 75–76  
gravity, 10, 12, 19–20  
Gulhane, 27–28, 91  
Gunn, 1, 15, 17, 91

## H

heat, 14, 23, 37–38, 41, 44  
hematite, 4, 10, 12–14, 16, 18, 55–56, 68, 71, 73–74, 78, 82–85, 93, 95–96  
  inclusion of, 78, 85  
hematite ores, 14, 89  
hot metal, 21, 32–33  
hydrocyclone, 19–20  
hydrogen, 39–40, 44–45, 90, 93  
hydrogen ironmaking, 45, 92

## I

ilmenite, 10, 12, 78, 82–85  
intensities, 53  
Intensity, 73–76  
iron, 7, 9, 12, 14–16, 18, 21–24, 29–32, 43–44, 52–53, 55–66, 68–73, 78, 83, 85, 89–90  
  scrap, 25, 32–33  
  sponge, 23–24  
iron and oxygen, 15  
iron and steel, 43, 58  
iron and steel-making processes, 2  
Iron and Steel Technology, 31  
iron-bearing minerals, 10, 13, 78, 85  
iron-bearing minerals segregate by gravity, 10  
iron carbonate, 14  
iron content, 9, 14, 43, 78  
  high, 13, 59  
Ironmaking Processes, 28  
  iron metals, 3, 77  
  well-developed, 77, 86  
iron minerals, 10, 13–14, 55  
iron mineral Sedimentation, 10  
iron nuggets, 28, 87  
iron ore, 1, 3–4, 7–10, 12–17, 21, 25, 28–32, 34, 36, 43–47, 49–50, 53–55, 74, 77, 93–94  
iron ore deposits, 1, 9, 17  
  geological processes form, 10  
iron ore fines, 27–28  
Iron Ore Formation Processes, 10  
Iron Ore Grade Specification Material Types, 52  
iron ore minerals, 15, 87

iron ore mining, 4, 17  
 iron ore pellets, 37, 87  
 iron ore reduction, 38, 93  
 iron ore resources, 16, 55  
 iron ore rocks, 54, 83  
 iron ore samples, 3, 48, 53,  
   84 powdered, 53  
 iron ore's mineral makeup, 53  
 iron oxide, reducing, 43  
 iron oxide by carbon, 44, 94  
 iron oxide mineral, 59  
 iron oxides, 2, 4, 23, 33, 39, 43–45, 51,  
   74, 83, 89, 93–94  
 iron pelletising plant, 35  
 iron production, 21, 25, 44–  
 45 iron scrap, 33  
 Iron silicates, 10  
 iron silicide, 60, 62, 83, 85  
 iron smelting and reduction,  
 31 iron sources, 60  
 itabirite-type iron reserves, 15

## J

Jahirul, 40–42, 91

## K

Kikuchi, 27–29, 92  
 Koshy, 39, 87, 89–90

## L

layers, low-carbonate iron oxide, 16  
 Liberia, 1–2, 15–17, 47, 55, 85, 87, 89, 91,  
   99  
 Liberian iron ore, 5  
 limonite, 10, 12–14, 18  
 Loss on Ignition (LOI), 55–56  
 low-grade ore, 43, 55, 85  
 Low-Intensity Magnetic Separator  
 (LIMS), 19  
 low iron content, 43  
 lumps, 23, 25, 48

## M

Madias, 33–34, 92  
 magnet, 14, 78, 85  
 magnetic separator, tertiary, 20  
 magnetite, 4, 10, 12–14, 16, 18, 20, 55, 59,  
   78, 82–85, 95–96  
 Major Iron Minerals, 12  
 Market Share, 8–9  
 martite, 12–14, 16, 18  
 Masaaki, 25–27, 92  
 masses, 35, 48–49, 51, 59  
 Mass Norm, 57–73  
 materials, 18, 29–30, 48–53, 55, 78, 85,  
   98 reduced, 51  
   valuable, 65  
 medium-grained quartz, 78–79, 84 metals,  
 10, 21, 29–30, 40, 52, 77–78, 89,  
   91–92  
 microwave reduction, 51, 77, 85–  
 86 microwaves, 38, 86–87  
 microwave technology, 37–38,  
 91 Midrex, 24–25, 27  
 Million Tonnes, 11–12  
 minerals, 7, 9, 12, 14–15, 53, 55, 58, 78–83,  
   85, 91, 93–94  
 mini blast furnaces (MBF),  
 22 mining, 4, 13–14, 17, 90–  
 91 Mitamoto, 24–25, 87  
 moisture, 42, 55–56  
 molten iron, 21, 28–29, 31, 33,  
 44 Multi-Elements, 56

## N

Nimba Mountains, 4, 15–17



## O

opaque minerals, 78–82,  
84 fine, 78, 84 medium-  
grained, 78, 80  
Operational Region of  
Ironmaking Processes, 28  
ore, 15–16, 18, 50, 53–56, 60, 63, 65,  
67, 71, 73, 77, 85, 94, 97  
high-grade, 43, 85  
lowgrade iron, 1  
oxide, 18, 85  
pelletising iron, 36  
reducing iron, 23  
transition hematite iron, 1  
transition iron, 55, 85  
ore minerals, 18, 85  
ore samples  
boulder Iron, 51  
pulverised Iron, 51  
reduced, 53  
oxide, 18, 45, 47, 51, 54, 56, 59, 81–82,  
85, 95  
oxygen, 15, 21, 23–24, 32–33, 40, 42,  
57–73, 83  
oxygen steel, producing, 30

## P

Pandey, 32–33, 87  
particles, 18–20, 33  
Patisson, 43, 45, 92  
Pelletising Binder, 37, 94  
pelletising process, 35–36  
pellets, 23–25, 35–36, 45, 49–51, 77,  
98 green, 36  
phosphorus, 13–15, 29, 31,  
55 pig iron, 21, 28–29, 32  
carbon-saturated, 27  
Plane Polarised Light. *See* PPL  
Polished Sections, 82–83, 95–  
96 Position, 53, 73–76  
PPL (Plane Polarised Light), 79–82, 95–96  
Precambrian rocks, 15  
Principal Iron Ore Deposits in Liberia, 17  
processes, 9, 14, 16, 21–24, 27–29, 31–32,  
34–37, 40, 44, 50, 90  
direct reduction ironmaking, 24

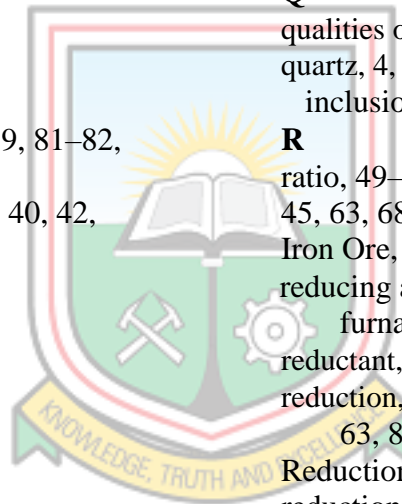
energy-intensive, 29, 44  
steam ironing, 44  
worldwide Direct Reduced Iron  
production, 24  
processing, 13, 48  
process of pelletising iron ore, 36  
Producing Iron Ore Pellets, 35, 37  
products, 4–5, 20, 30, 41, 48  
Properties of Major Iron Minerals, 12  
Pulverised, 56–57, 59–60, 62, 71, 73–  
74 pulverised iron Ores, 49  
pyritic magnetite, 82–  
84 pyrolysis, 40, 89  
pyroxene, 79–80, 82–83,  
85 pyrrhotite, 78, 82–85

## Q

qualities of iron and steel, 58  
quartz, 4, 13–15, 18, 60, 78–85  
inclusion of, 78–79, 84

## R

ratio, 49–50 reaction,  
45, 63, 68 Reduced  
Iron Ore, 77  
reducing agent and energy source in blast  
furnaces, 22  
reductant, 3, 23, 35, 45, 86–87, 89–90  
reduction, 2–3, 31, 43–45, 50–51, 56, 60,  
63, 86, 92–93, 97–98  
Reduction of Iron Oxide by Carbon, 44  
reduction process, 51, 71  
region, 11, 56–73  
lighter, 65, 67  
representation, schematic, 34–35, 40–41  
reservoir, process water, 20  
results in ferrosilicon, 60 rocks,  
10, 13, 15, 54, 58, 78–84  
metamorphic, 84  
rock samples, 54, 83–85  
rolling, 34–35



**S**

Sani, 7–9, 93  
 scrap, 29, 31, 34  
 siderite, 10, 12–14  
 silica, 1, 10, 13–14, 29, 31–32, 37, 55, 57–73, 77–78, 83, 85  
 silica contents, 55,  
 71 silicates, 18, 57  
 silicon and iron sources, 60  
 silicon carbide, 60, 62–65, 67–69, 72, 78, 83, 85  
 silicon dioxide, 55, 58, 65, 67, 72  
 specification, 18, 52–53  
 steel, 11, 14, 21, 23, 29–34, 43, 45, 58, 64, 70, 90  
   high-quality, 32, 34, 64  
 steel companies, 31, 44  
 steel grades, 21, 31, 34  
 steel industry, 1, 21, 34, 38, 44, 65, 89–91  
 steelmaking, 21, 30, 58  
 steelmaking processes, 21, 24, 29–30, 34–35, 44–45, 92  
 steel mills, integrated, 32–33  
 steel production, 7, 14, 27, 29–31, 59, 65, 67  
 steel properties, 34, 64, 70  
 steel scrap, 30–31,  
 33 steel sector, 4, 45

**T**

Technology, 43, 54, 87, 90  
 temperatures, 27, 33, 38, 40  
 texture, granular, 80, 82–84  
 Thin Sections, 78–81  
 time, 17, 22, 27, 34, 40–41  
 Tokadeh, 4–5, 18  
 tonne of steel, 23, 43 tonnes, 10–11, 18, 31, 35, 43  
 Total, 11, 57, 59, 82–83  
 transition, 1, 52, 54–55, 80, 82, 85  
 Transition Low-grade, 80, 95–96  
 transition ores, 50, 55, 73, 77  
 types, 5, 13–15, 24

**U**

usage of iron and steel, 43

**W**

weight, 39, 44, 48–49, 51, 55, 97–98  
 Western Area, 4, 16  
 world, 1, 4, 7–8, 14–15, 17, 21, 25, 29–30, 33, 44  
 Worldwide Direct Reduced Iron Production by Process, 24

**X**

X-ray diffraction. *See* XRD  
 X-ray Fluorescence. *See* XRF  
 XRD (X-ray diffraction), 3, 48, 51, 53, 73–74  
 XRD Spectrum of Gangra Transition Ore, 74–75  
 XRF (X-ray Fluorescence), 3, 48, 51–52, 56

**Y**

Yuelliton, 4–5

**Z**

Zhao, 37, 94

